Doctoral Thesis

Exact Throughput Capacity Studies for Mobile Ad Hoc Networks

by

Yin Chen

Graduate School of Systems Information Science

Future University Hakodate

March 2014

Abstract

The rapid development of wireless communication technology has made mobile ad hoc networks (MANETs) an increasingly appealing option for a lot of critical applications, such as daily information exchange, disaster relief, vehicular networks and military communication. A major obstacle, however, stunting the application of MANETs is the lack of understanding on the throughput capacity, i.e., the maximum achievable throughput between node pairs, of these networks.

By now, a great deal of research activity has been conducted for throughput capacity in MANETs, most of which focused on exploring the scaling behaviors of the throughput capacity as the network size increases. Despite the insights provided by the scaling law results, they tell us little about the actual achievable throughput of a MANET, which is of great interest for network designers. Although there are some preliminary efforts towards the exact studies, the exact throughput capacity remains unknown for many important MANET scenarios.

In this thesis, we study the exact throughput capacity for three important networking scenarios. At first, we study an intermittently connected mobile network (ICMN), a special class of sparse MANETs, where no medium access control (MAC) scheme is adopted and a pair of nodes can communicate whenever they come into the transmission range of each other. For the concerned ICMN, we explore its exact throughput capacity and inherent delay-throughput tradeoff under any routing algorithm. Then, we proceed to study the exact throughput capacity in a continues MANET with a simple ALOHA MAC protocol, where each node independently decides to conduct transmission with a given probability. For the considered A-MANET, we first reveal how its throughput capacity is determined by the successful transmission probability (STP) therein and then develop a theoretical framework that enables efficient and closed-form approximations to be connected for its STP and hence throughput capacity under two popular local transmission schemes, based on which the corresponding capacity optimization issue can also be explored. Finally, we study a cell-partitioned MANET with group-based MAC scheduling. For the concerned MANET, we investigate the impact of directional antenna on its maximum achievable throughput and also explore the corresponding throughput optimization problem therein. For the developed theoretical results, extensive simulations are conducted to demonstrate the efficiency of these theoretical models.

Thesis Supervisor: Xiaohong Jiang
Title: Professor

Acknowledgments

It is undoubted that the Ph.D. studying in Future University Hakodate is one of the most important stages that I will never forget in the rest of my life. Throughout this period, I got a lot of help from so many people. Without their help and encouragement, this work would not and could not have been done.

First and foremost, I would like to my adviser, Professor Xiaohong Jiang, for his continuous guidance, supervision and general support in my academic research. Prof. Jiang not only provides me an excellent research environment for my Ph.D. study, he and his wife, Miss Li, also gave me countless help and precious advices during these time of my living in Hakodate. To me, they are both mentors and close friends, and I would like to thank them in advance for all of their future help and advice.

I would like to give a special thanks to Professor Yulong Shen of Xidian University, China, who introduced me to Prof. Jiang and that is how I can get such a valuable study opportunity. I want to thank Dr. Jiajia Liu, who gave me specific and valuable comments when I started my Ph.D study. I am also very grateful to Professor Osamu Takahashi and Professor Norio Shiratori for their generous support.

I would also like to acknowledge my thesis committee members, Professor Xiaohong Jiang, Professor Osamu Takahashi, Professor Yuichi Fujino and Professor Norio Shiratori, for their interests and for their constructive comments that help to improve this thesis. I would like to give my sincere thanks to other members of the Jiang Lab, the staffs of Future University, Japan-China Friendship Association and Japanese Teaching Society in Hakodate, who has helped me a lot in the past three years. Without your help, the time of my living in Hakodate would never become so joyful and memorable.

Finally, I would thank all my family members for support and love.

THIS PAGE INTENTIONALLY LEFT BLANK

Contents

List of Figures

List of Tables

THIS PAGE INTENTIONALLY LEFT BLANK

Chapter 1

Introduction

1.1 Background

The rapid development of wireless communication technology has made mobile ad hoc networks (MANETs) an increasingly appealing option for a lot of critical applications such as daily information exchange, disaster relief, military communication and vehicular networks. A MANET is a collection of self-autonomous mobile devices that communicate with each other via peer-to-peer wireless links without any support from pre-existing infrastructure. Due to nodel mobility, the network topology always dynamically evolves in MANETs. Hence, the required network management and packet routing are often performed through dynamic distributed algorithms that implement the cooperation among network nodes. In particular, *store-carry-forward* routing, whereby network nodes help each other to carry and relay data toward the final destinations, is typically adopted to increase network performance and throughput as well as the distances over which network source and destination nodes can communicate.

Compared with existing wireless network architectures, such as satellite network, cellular network and Wi-Fi network, MANETs provide many appealing features, making them highly promising for both the academic and industrial communities. First, they can be rapidly deployed and reconfigured. MANETs do not rely on the existence of infrastructures like base station or access point, which not only require unavoidable

initial investment, but also lead to complexity in operation and maintenance. Second, they are of high robustness and can tolerate severe node failure problem, due to their distributed nature and redundancy of nodes. The robustness of MANETs makes them extremely suitable for harsh environments like military communications, where communication devices are vulnerable to enemy attack. Finally, the MANETs make it possible to provide low-cost Internet service for remote communities in developing areas.

1.2 Related Works

Motivated by the these promising applications potentials of MANETs, a great deal of research activity has been dedicated towards a thorough understanding on the fundamental performance limits of the MANETs in the last decade, such as throughput capacity [1–3], transmission capacity [4, 5], packet delay[6, 7] and propagation speed [8–13]. It is expected that such a thorough understanding on these fundamental performance limits of MANETs will provide profound insights to the design and performance optimization of future networks [14, 15], as the theory of Shannon capacity has done for point-to-point and multiuser channels. In this thesis, we focus on the throughput capacity study in MANETs However, the important metric of the exact throughput capacity remains an largely unexplored issue and dedicated studies are still needed for many practical MANET scenarios.

1.2.1 Scaling Law and Order Sense Studies

Since the seminal work of Grossglauser and Tse [2], the throughput capacity and delay-throughput tradeoff have been extensively studied for MANETs under various mobility models, most of which focus on deriving order sense results and scaling laws. It was demonstrated in [2] that a $\Theta(1)$ per flow throughput is achievable in MANETs under the independent and identically distributed (i.i.d.) mobility model[1], where the

[1]In this thesis, for two functions $f(n)$ and $g(n)$, we denote $f(n) = O(g(n))$ iff there exist positive constants c and n_0, such that for all $n \geq n_0$, the inequality $0 \leq f(n) \leq cg(n)$ is satisfied; $f(n) =$

positions of all nodes are reshuffled in each time slot. The result of [2] indicates that the long-term per flow throughput can be kept constant even as the number of network nodes n tends to infinity. Gamal et al. [16, 17] studied a cell-partitioned MANET divided evenly into $n \times n$ cells, on which the nodes move independently according to a symmetric random walk. For the considered MANET, the authors of [16, 17] investigated its optimal scaling behavior of the delay-throughput tradeoff and discovered that the $\Theta(1)$ per flow throughput is achievable at the cost of an average delay of order $\Theta(n \log n)$. A similar delay-throughput tradeoff was shown to also exist in MANETs under restricted mobility model [18]. In the work of [19], Li et al. proposed a controllable mobility model for cell-partitioned MANETs and derived upper and lower bounds on the scaling laws of the achievable throughput and expected delay for the considered networks. The results of [19] showed that such a MANET enables a smooth tradeoff between the throughput and delay to be conducted by properly configuring the mobility parameters. Besides, the scaling laws of the throughput capacity and related delay-throughput tradeoff have also been explored under other mobility models, such as Brownian mobility model [20, 21], hybrid mobility model [22] and correlated mobility model [23].

1.2.2 Exact Studies

It is notable that although the study on order sense results and scaling laws can help us to understand the asymptotic behavior of the throughput capacity and delay-throughput tradeoff as the network size increases, they provide little insight on the actual achievable performance of these MANETs, which is of more interest from the view of network designers. Noting the limitation of scaling law results, some preliminary work has been conducted for the exact study [3, 24–26]. In particular, Neely and Modiano [3] computed the exact throughput capacity and delay-throughput tradeoff in a cell-partitioned MANET under i.i.d. mobility model, where the location of each network node in steady-state is uniformly distributed over all cells. Following

$\Omega(g(n))$ iff $g(n) = O(f(n))$; $f(n) = \Theta(g(n))$ iff both $f(n) = O(g(n))$ and $f(n) = \Omega(g(n))$ are satisfied.

the MANET model of [3], Urgaonkar and Neely investigated the relationship between throughput capacity and energy consumption in [24], and Gao et al. [25] extended the work of [3] to that with adopting a group-based scheduling scheme for medium access control (MAC).

1.3 Main Work and Contributions

Although the available studies discussed in Section 1.2 are helpful for us to have a preliminary understanding on the exact throughput capacity in MANETs, we notice that new dedicated studies are still needed for many important MANET scenarios. In this thesis, we conduct the exact studies for the throughput capacity in MANETs under three typical MAC schemes. The first MANET under study is an intermittently connected mobile network (ICMN), which models a sparse MANET under a simple MAC scheme such that nodes conduct communication whenever they come into the transmission range of each other. The second MANET model considered in this thesis is a continues MANET with an ALOHA protocol (A-MANET), where each node independently tries to conduct transmission towards its intended receiver with a fixed probability at each time slot. The third studied MANET is a cell-partitioned MANET with group-based scheduling scheme for MAC and directional antenna for transmission. The main contributions of the this thesis are summarized as follows.

- At first, we study the exact throughput capacity and related delay-throughput tradeoff in an ICMN under a general mobility model that follows the Poisson meeting process. For the concerned ICMN, we first derive its exact throughput capacity based on the pairwise meeting rate therein and also provide analysis on the expected end-to-end packet delay in the network under a capacity achieving routing algorithm. We then explore the inherent tradeoff between delay and throughput in the network and establish a necessary condition for such tradeoff that holds under any routing algorithm. Case studies are further conducted under the random waypoint and random direction models, two typical mobility models that follow the Poisson meeting process.

- Then, we proceed to study the exact throughput capacity for an A-MANET. We first determine the exact throughput capacity for an A-MANET based on the successful transmission probability (STP) and also derive the expected end-to-end packet delay under a capacity achieving routing algorithm. Notice that the exact modeling of STP is highly cumbersome, we then develop very efficient and closed-form approximations to both the STP and exact throughput capacity in the concerned network under two popular local transmission schemes, based on which the corresponding capacity optimization issue is explored.

- Finally, we analyze the maximum achievable throughput of a cell-partitioned MANET with two hop relay routing algorithm and directional antennas. Based on the Markov chain and automatic feedback theory, we explore a general theoretical framework that enables the achievable throughput analysis to be conducted for a directional antenna-based MANET. Based on the results of the achievable per node throughput, we further explore the throughput optimization problem for a fixed beamwidth θ and determine the corresponding optimal setting of f to achieve the optimal throughput.

1.4 Definition of Performance Metrics

The performance metrics under study in this thesis are defined as follows.

Definition 1. ***End-to-end delay****: The* end-to-end delay *of a packet is the time it takes for the packet to reach its destination after it arrives at its source.*

Definition 2. ***Stability of a network****: For an MANET under a routing algorithm, if the packet arrival rate to each node is λ, the network is called* stable *under this rate if the average number of packets waiting at each node, i.e., the average queue length, does not grow to infinity with time and thus the average end-to-end packet delay is bounded.*

Definition 3. ***Throughput capacity****: The* throughput capacity *of the network is defined as the maximum value of packet arrival rate λ that the network can stably*

support over any possible routing algorithm.

1.5 Thesis Outline

The remainder of this thesis is outlined as follows: In Chapter 2, we study the exact throughput capacity and related delay-throughput tradeoff in ICMNs. Chapter 3 investigates the exact throughput capacity for A-MANET. The maximum throughput of cell-partitioned MANETs with two hop relay routing and directional antenna is studied in Chapter 4. Finally, we conclude this thesis and discuss the future works in Chapter 5.

Chapter 2

Capacity and Delay-Throughput Tradeoff in ICMNs

2.1 Introduction

Intermittently connected mobile networks (ICMNs) represent a class of sparse MANETs, where complete end-to-end path(s) between a node-pair may never exist so nodes mainly rely on mobility as well as basic packet storing, carrying, and forwarding operations to implement end-to-end communication (see e.g., [27] for a survey). ICMNs are highly flexible, robust and can be rapidly deployed and reconfigured, so they serve as an important model for many critical applications such as wildlife tracking and monitoring, battlefield communication, vehicular networks, low-cost Internet service for remote communities.

2.1.1 Available Studies on ICMN

By now, much academic activity has been devoted to the performance study for ICMNs. Subramanian et al. explored the achievable throughput of ICMNs under two-hop routing [28, 29] as well as under multi-hop routing [30]. Their results indicate that for ICMNs with finite buffer size at each node, multi-hop routing usually outperforms its two-hop counterpart in terms of the achievable throughput performance.

Recently, the packet delivery delay performance, i.e., the time it takes for a packet to reach its destination node after it departures from its source node, was extensively studied under various ICMN scenarios [31–35]. For an ICMN with the Poisson meeting process, Groenevelt et al. [31] conducted the Markov chain-based analysis to evaluate its delivery delay performance under both two-hop routing and epidemic routing. Although the Markov chain-based analysis enables the distribution of delivery delay to be calculated, such analysis quickly becomes cumbersome and computationally impractical as network size increases. Based on this observation, Zhang et al. [32] developed a theoretical framework based on ordinary differential equations to significantly reduce the complexity involved in the delivery delay analysis for large scale ICMNs. For ICMNs with two-hop routing and packet life time constraint and ICMNs with spray and wait routing, the corresponding delivery delay performance was reported in [33] and [34, 35], respectively.

2.1.2 Limitations of Available Studies

While the above works are helpful for us to have a preliminary understanding on the performance of ICMNs, further deliberate studies are needed to reveal the fundamental performance limits of such networks. First, the available throughput studies only focus on the achievable throughput of ICMNs under a specified routing algorithm, the fundamental throughput capacity of an ICMN, i.e., its maximum possible throughput over any routing algorithm, is still unknown by now. Second, the studies on delivery delay, which constitutes only a part of the fundamental end-to-end packet delay, can not be directly applied to investigate the inherent tradeoff between the end-to-end delay and achievable throughput in ICMNs.

2.1.3 Chapter Outline

The rest of the chapter is outlined as follows. Section 2.2 presents the system models. The main theoretical results on throughput capacity and delay-throughput tradeoff are derived in Section 2.3. Section 2.4 provides simulation/numerical results and the

corresponding discussions. Finally, we summarize this chapter in Section 2.5.

2.2 System Models

In this section, we introduce the network model, mobility model and traffic model of the considered ICMN.

2.2.1 Network Model

The network under study consists of n identical mobile nodes randomly moving within a continuous square of side-length L. Each node has a maximum transmission distance d. We call that two nodes "meet" when their distance is less than d and thus they can conduct communication. At the beginning of each meeting, either of the two nodes is randomly selected as the transmitter of this meeting with equal probability. Transmission is assumed to be instantaneous and the total number of bits transmitted during a meeting is fixed and normalized to one packet.

2.2.2 Mobility Model

We consider a general mobility model introduced in [31]. Under this mobility model, the meeting process between each pair of nodes can be modeled as mutually independent and homogeneous Poisson processes with rate $\beta > 0$. Equivalently stated, the pairwise inter-meeting times, i.e., the time that elapses between two consecutive meetings of a given pair of nodes, are mutually independent and exponentially distributed with mean $1/\beta$.

It has been demonstrated in a number of studies, e.g., [31–33], that this mobility model can serve as an efficient modeling for ICMNs under a lot of typical mobility models like random waypoint, random direction and random walk models. Specifically, the following lemma (Lemma 4, [31]) provides accurate estimations to the pairwise meeting rates β under the random waypoint and random direction models (see Section 2.4 for the detailed definition of these mobility models).

Lemma 1. *For an ICMN of side-length L and maximum transmission distance d, when $d \ll L$, its pairwise meeting rates β_{RW} under the random waypoint model (RW) and β_{RD} under the random direction model (RD) can be efficiently approximated as*

$$\beta_{RW} \approx \frac{2c_1\, d\, \mathbb{E}[V^*]}{L^2}, \quad \textit{and} \quad \beta_{RD} \approx \frac{2d\, \mathbb{E}[V^*]}{L^2}, \tag{2.1}$$

respectively, where $c_1 = 1.3683$ is a constant and $\mathbb{E}[V^*]$ is the average relative speed between two nodes (see [6] for the numerical calculation of $\mathbb{E}[V^*]$). In the special case that each node travels at a constant speed v, we have $\beta_{RW} \approx \frac{8c_1 dv}{\pi L^2}$ and $\beta_{RD} \approx \frac{8dv}{L^2}$.

2.2.3 Traffic Model

Regarding traffic pattern, we consider the permutation traffic model [2]. Under this model, there are n unicast traffic flows in the network. Each node is the source of the traffic flow generated at itself, and meanwhile, it is also the destination of the traffic flow from some other node. To simplify the analysis, the packet arrival process at each node is assumed to be a Poisson arrival process with rate $\lambda > 0$. This is justified since the arrival model does not affect the throughput capacity that the network can support (see Corollary 5 in [36]). For throughput capacity analysis, we consider that there is no constraint on packet life time and the buffer size in each node is sufficiently large such that packet loss due to buffer overflow will never happen.

2.3 Throughput Capacity and Delay-Throughput Tradeoff

In this section, we first establish a theorem regarding the throughput capacity result in the considered ICMN based on the pairwise meeting rate therein, and provide necessity and sufficiency proofs of the theorem. Then, we proceed to explore the tradeoff between the end-to-end delay under any routing algorithm. Finally, specific case studies are further conducted for MANETs under the random waypoint and random direction mobility models.

2.3.1 Throughput Capacity

Theorem 1. *For the concerned ICMN with n mobile nodes and pairwise meeting rate β, its throughput capacity can be determined as*

$$\mu = \frac{n}{4}\beta. \tag{2.2}$$

Similar to [3], the proof of the capacity μ in Theorem 1 consists of proving that the $\lambda \leq \mu$ is necessary and $\lambda < \mu$ is sufficient to ensure network stability. We establish the necessity in Section 2.3.1 by showing that μ is an upper bound on the achievable throughput under any possible routing algorithm in the considered ICMN. Then, we prove the sufficiency in Section 2.3.1, where a routing algorithm is presented and it is shown that the network is stable under this routing algorithm for any input rate $\lambda < \mu$.

Proof of Necessity

Lemma 2. *For the concerned ICMN with n mobile nodes and pairwise meeting rate β, its throughput under any possible routing algorithm is upper bounded by*

$$\mu = \frac{n}{4}\beta. \tag{2.3}$$

Proof. Consider any possible routing algorithm. Let $X_h(T)$ denote the total number of packets transferred through h hops from their sources to destinations in time interval $[0, T]$. Notice that to ensure network stability, the overall arrival rate of all traffic flows should be not greater than the overall throughput, since otherwise the amount of packets waiting in the network will grow to infinity as time tends to infinity. Formally, it is necessary that for any given $\epsilon > 0$, there must exist an arbitrarily large T such that the following inequality holds

$$\lambda n - \epsilon \leq \frac{1}{T}\sum_{h=1}^{\infty} X_h(T), \tag{2.4}$$

where λ denotes the packet arrival rate at each node.

Notice the fact that during the time interval $[0, T]$, the total number of packet transmissions is lower bounded by $\sum_{h=1}^{\infty} hX_h(T)$ and upper bounded by the total number of meetings between all node pairs during this time interval, denoted by $Y(T)$ in the following. Thus, we have from the transitivity that

$$\sum_{h=1}^{\infty} hX_h(T) \leq Y(T). \tag{2.5}$$

From (2.4) and (2.5), we have

$$\begin{aligned} \frac{1}{T}Y(T) &\geq \frac{1}{T}X_1(T) + \frac{2}{T}\sum_{h=2}^{\infty} X_h(T) \\ &\geq \frac{1}{T}X_1(T) + 2\left[(\lambda n - \epsilon) - \frac{1}{T}X_1(T)\right], \end{aligned} \tag{2.6}$$

and thus

$$\lambda \leq \frac{1}{2n}\left[\frac{1}{T}Y(T) + \frac{1}{T}X_1(T) + 2\epsilon\right]. \tag{2.7}$$

Since a packet can be transferred from its source to destination through one hop only when the source conducts a transmission directly to the destination, the term $X_1(T)$ in (2.7), i.e., the number of packets transferred within one hop during $[0, T]$, is upper bounded by $Y_{sd}(T)$, i.e., the number of transmissions from each source to its destination during the time interval $[0, T]$. From the law of large number, it follows that as $T \to \infty$

$$\frac{1}{T}Y(T) \xrightarrow{\text{a.s.}} \frac{(n-1)n}{2}\beta, \tag{2.8}$$

$$\frac{1}{T}Y_{sd}(T) \xrightarrow{\text{a.s.}} \frac{n}{2}\beta. \tag{2.9}$$

Using (2.8) and (2.9) into (2.7), it follows that

$$\lambda \leq \frac{n}{4}\beta + \frac{\epsilon}{n}, \text{ as } T \to \infty. \tag{2.10}$$

Since ϵ can be arbitrarily small, the result then follows. □

Proof of Sufficiency

For the proof of sufficiency, we present a routing algorithm in Algorithm 1 and derive the average end-to-end packet delay in the considered ICMN under this routing algorithm in Lemma 3. It is shown that the average end-to-end delay is bounded and hence the network is stable for all packet arrival rate $\lambda < \mu$.

Lemma 3. *For the concerned ICMN with n mobile nodes and pairwise meeting rate β, if the packet arrival process at each node is a Poisson arrival process with rate $\lambda < \mu$, where μ is the upper bound determined in Lemma 2, and Algorithm 1 is adopted for*

Algorithm 1 Routing Algorithm.

Suppose that there is a meeting between two nodes, where Tx and Rx are the transmitter and receiver, respectively.
if Rx is the destination of the traffic generated from Tx **then**
  Tx conducts a *source-to-destination* transmission:
  if Tx has a new packet destined for Rx **then**
    Tx transmits the packet to Rx.
  else
    Tx remains idle.
  end if
else
  Tx flips an unbiased coin;
  if it is the head **then**
    Tx conducts a *source-to-relay* transmission:
    if Tx has a new packet (i.e., a packet that has never been transmitted before) **then**
      Tx transmits the packet to Rx.
    else
      Tx remains idle.
    end if
  else
    Tx conducts a *relay-to-destination* transmission:
    if Tx has a packet destined for Rx **then**
      Tx transmits the packet to Rx.
    else
      Tx remains idle.
    end if
  end if
end if

packet routing, the corresponding expected end-to-end delay $\mathbb{E}\{D\}$ *is determined as*

$$\mathbb{E}\{D\} = \frac{n-1}{\mu - \lambda}. \tag{2.11}$$

Proof. Notice that under Algorithm 1, there are three types of transmissions, i.e., *source-to-destination* transmission, *source-to-relay* transmission and *relay-to-destination* transmission. It takes a packet at most two hops to reach its destination and the packet delivery processes of the n traffic flows are independent from each other. Due to this property, we can model the packet delivery process in the considered ICMN under Algorithm 1 as a queuing system that consists of n i.i.d. two-stage queues.

Without loss of generality, we focus on a traffic flow illustrated in Fig. 2-1. From Fig. 2-1 we can see that packets of this flow experience a two-stage queuing process, i.e., the queuing process at the source node (first stage) and the queue process at one of the $n-2$ relay nodes (second stage).

Consider first the source queue. The input to this queue is a Poisson arrival process with rate λ. According to Algorithm 1, a "service" comes when either the source node conducts a *source-to-destination* transmission or a *source-to-relay* transmission. Based on Algorithm 1, we see that the service arrival process at the source node is a Poisson process with rate $\mu = \frac{n}{4}\beta$. Then, it follows that the source queue is an $M/M/1$ queue. Based on the result from queuing theory, the mean queuing delay $\mathbb{E}\{D_s\}$ at the source queue is given by

$$\mathbb{E}\{D_s\} = \frac{1}{\mu - \lambda}. \tag{2.12}$$

Moreover, due to Burke's theorem [37], the departure process from the source queue is also a Poisson process with rate λ.

Consider now the queuing process at one of the $n-2$ relay nodes. Notice that with probability $\frac{1}{n}$ a packet departure from the source node will enter this relay node, so the input to this relay queue is a Poisson process with rate $\frac{\lambda}{n}$. In this relay queue, a "service" arises when this relay node conducts a *relay-to-destination* transmission to the destination node of the concerned traffic flow, so the service process of the

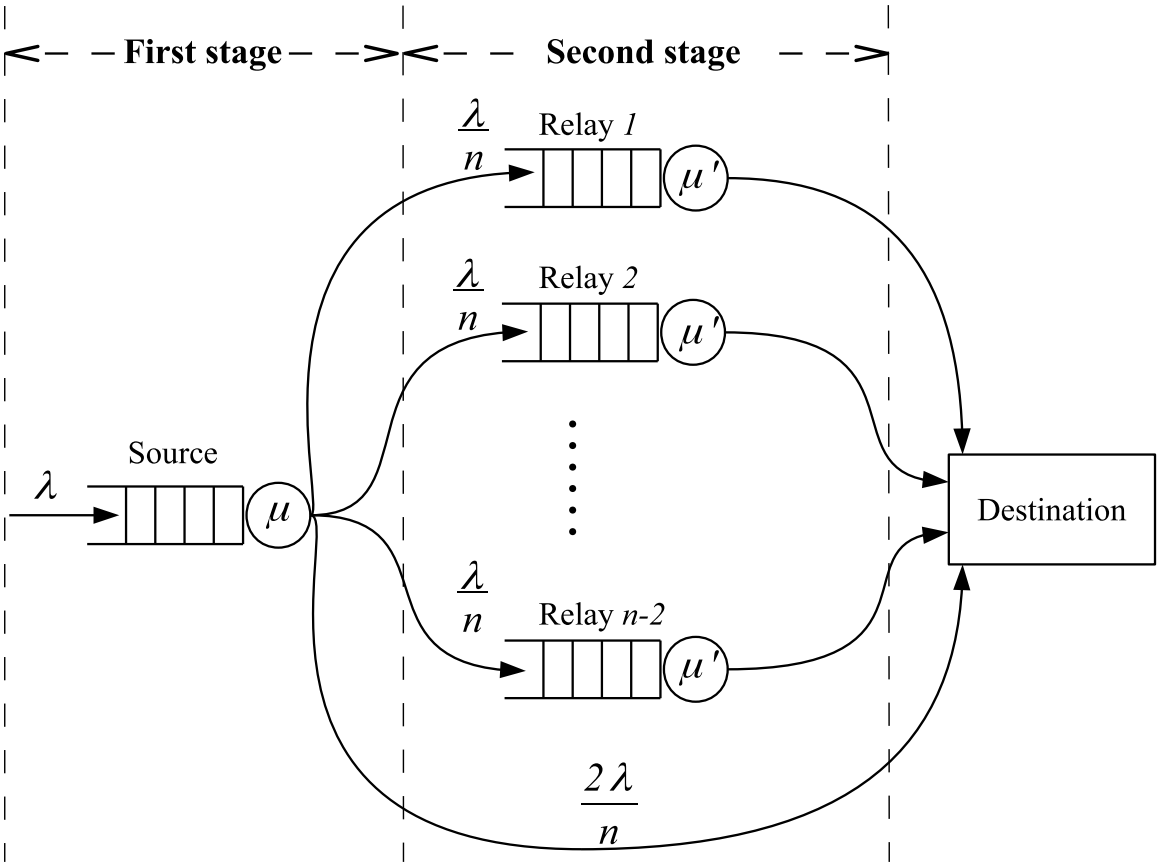

Figure 2-1: Two-stage queuing process under Algorithm 1.
In the figure, the inter-service times in the source node and relay nodes are exponentially distributed with rate $\mu = \frac{n}{4}\beta$ and rate $\mu' = \frac{\beta}{4}$, respectively.

relay nodes is a Poisson process with rate $\mu' = \frac{\beta}{4}$. We can see that the relay queue is again an $M/M/1$ queue. The mean queuing delay $\mathbb{E}\{D_r\}$ at a relay node is given by

$$\mathbb{E}\{D_r\} = \frac{1}{\mu' - \lambda/n}. \tag{2.13}$$

Summing up the above results, we have that the mean end-to-end packet delay is

$$\mathbb{E}\{D\} = \mathbb{E}\{D_s\} + \frac{n-2}{n}\,\mathbb{E}\{D_r\} = \frac{n-1}{\mu - \lambda}, \tag{2.14}$$

which proved the lemma. □

2.3.2 Delay-Throughput Tradeoff

In the following theorem, we establish a necessary condition on the tradeoff between the end-to-end packet delay and achievable throughput under any routing algorithm that stabilizes the network.

Theorem 2. *Consider an ICMN with n mobile nodes and pairwise meeting rate β and the packet arrival rate at each node is λ. A necessary condition for any routing algorithm that can stabilize the network with rate λ while maintaining a bounded expected end-to-end delay $\mathbb{E}\{D\}$ is given by*

$$\frac{\mathbb{E}\{D\}}{\lambda} \geq \frac{2}{(n-1)\beta^2}. \tag{2.15}$$

Proof. Assume that the packet arrival rate to each node is λ and that there is a general routing algorithm that can stabilize the network under this rate. We focus, without loss of generality, on the packet delivery process of traffic flow i.

Let random variable D_i denote the end-to-end delay of a packet in flow i under the routing algorithm and $\mathbb{E}\{D_i\}$ represent its expectation. We can see that the expected end-to-end packet delay of the whole network can be calculated by

$$\mathbb{E}\{D\} = \frac{1}{n}\sum_{i=1}^{n}\mathbb{E}\{D_i\}. \tag{2.16}$$

Let random variable R_i denote the redundancy of a packet in flow i, i.e., this packet is distributed into R_i different nodes (including the destination) in the network, and $\mathbb{E}\{R_i\}$ be its expectation. Notice that the overall generating rate of packet redundancy in the network is

$$\lambda n \cdot \frac{1}{n}\sum_{i=1}^{n}\mathbb{E}\{R_i\} = \lambda\sum_{i}^{n}\mathbb{E}\{R_i\}. \tag{2.17}$$

This quantity is upper bounded by the rate of transmissions in the network, due to the fact that during each transmission at most one copy of a packet is transmitted to

one node. Formally, it is expressed as

$$\lambda \sum_{i}^{n} \mathbb{E}\{R_i\} \leq \binom{n}{2}\beta = \frac{(n-1)n}{2}\beta. \tag{2.18}$$

Now, we consider a virtual network, in which there are n nodes and R_i^* of them initially process copies of a packet destined for some node, where R_i^* has the same distribution with R_i. These R_i^* nodes only transmit the packet to the destination node. We use D_i^* to denote the time taken for the destination node to receive a copy of the packet from one of the R_i^* nodes. We can see that the destination node can receive the packet when a meeting occurs between itself and one of the R_i^* nodes. Hence, conditioned on the event $\{R_i^* = r\}$ the D_i^* is exponentially distributed with parameter $r\beta$, and therefore the expectation of D_i^* is determined as

$$\mathbb{E}\{D_i^*\} = \mathbb{E}\{\mathbb{E}\{D_i^*|R_i^*\}\} \tag{2.19}$$

$$= \mathbb{E}\{\frac{1}{R_i^* \cdot \beta}\} \tag{2.20}$$

$$= \frac{1}{\beta}\,\mathbb{E}\{\frac{1}{R_i}\}, \tag{2.21}$$

where (2.21) results from that R_i^* and R_i are equal in distribution.

Notice that D_i is *stochastically greater* than D_i^*. To prove this, we need to show that for all u,

$$\Pr\{D_i > u\} \geq \Pr\{D_i^* > u\}. \tag{2.22}$$

For $u \leq 0$, (2.22) holds trivially. Consider any $u > 0$, we have

$$\Pr\{D_i > u\} = \sum_{r} \Pr\{D_i > u|R_i = r\} \Pr\{R_i = r\}. \tag{2.23}$$

Let $u_k \geq 0$ denote the time taken by the number of copies of a packet to increase from k to $k+1$. We can see that for any possible combination of $\{u_k\}_{k\in\{1,2,\ldots,r\}}$ such that $\sum_{k=1}^{r} u_k = u$, we have

$$\Pr\{D_i > u | R_i = r\} \geq \exp\left\{-\sum_{k=1}^{r} k\beta u_k\right\} \tag{2.24}$$

$$\geq \exp\{-r\beta u\} \tag{2.25}$$

$$= \Pr\{D_i^* > u | R_i^* = r\}, \tag{2.26}$$

where (2.24) results from that in the considered network, in which there are k nodes holding copies of a packet, the rate that the destination node receives a copy of the packet from those k nodes is at most $k\beta$. Combing (2.26) and (2.23), we have

$$\Pr\{D_i > u\} \geq \sum_r \Pr\{D_i^* > u | R_i^* = r\} \Pr\{R_i = r\} \tag{2.27}$$

$$= \sum_r \Pr\{D_i^* > u | R_i^* = r\} \Pr\{R_i^* = r\} \tag{2.28}$$

$$= \Pr\{D_i^* > u\}, \tag{2.29}$$

which proves (2.22) for $u > 0$.

Since D_i is *stochastically greater* than D_i^*, so that

$$\mathbb{E}\{D_i\} \geq \mathbb{E}\{D_i^*\}. \tag{2.30}$$

Using (2.30), (2.21) in (2.16) leads to

$$\mathbb{E}\{D\} \geq \frac{1}{n}\sum_{i=1}^{n} \frac{1}{\beta}\,\mathbb{E}\left\{\frac{1}{R_i}\right\} \tag{2.31}$$

$$\geq \frac{1}{\beta} \cdot \frac{1}{n}\sum_{i=1}^{n} \frac{1}{\mathbb{E}\{R_i\}} \tag{2.32}$$

$$\geq \frac{1}{\beta} \cdot \frac{1}{\frac{1}{n}\sum_{i=1}^{n} \mathbb{E}\{R_i\}}, \tag{2.33}$$

where (2.32) and (2.33) both result from Jensen's inequality, since the function

$f(x) = 1/x$ is convex for $x > 0$. Combining (2.18) and (2.33), we have

$$\mathbb{E}\{D\} \geq \frac{1}{\beta} \cdot \frac{2\lambda}{(n-1)\beta} = \frac{2}{(n-1)\beta^2} \cdot \lambda. \tag{2.34}$$

Multiplying $1/\lambda$ on both sides of (2.34) proves the theorem. □

2.3.3 Case Studies under Random Waypoint and Random Direction Models

So far, we have derived the throughput capacity and delay-throughput tradeoff for ICMNs under a general class of mobility models, where the pairwise meeting process between each pair of nodes can be modeled as the Poisson process. In the following, we conduct case studies for the random waypoint and random direction mobility models based on results of Lemma 1 and Theorems 1 and 2.

At first, we provide in Corollary 1 estimations to the throughput capacities in ICMNs under the random waypoint and random direction models, respectively.

Corollary 1. *For an ICMN with n mobile nodes, side-length L and maximum transmission distance d, when $d \ll L$, the throughput capacities μ_{RW} under the random waypoint model and μ_{RD} under the random direction model can be efficiently approximated as*

$$\mu_{RW} \approx \frac{c_1 nd\,\mathbb{E}[V^*]}{2L^2} \quad \textit{and,} \quad \mu_{RD} \approx \frac{nd\,\mathbb{E}[V^*]}{2L^2}, \tag{2.35}$$

respectively, where $c_1 = 1.3683$ is a constant and $\mathbb{E}[V^*]$ is the average relative speed between a pair of nodes. In the special case of constant traveling speed v, we have $\mu_{RW} \approx \frac{2c_1 ndv}{\pi L^2}$ and $\mu_{RD} \approx \frac{2ndv}{L^2}$, respectively.

Then, we provide in Corollary 2 the results on the corresponding delay-throughput tradeoff in MANETs under the random waypoint and random direction models, respectively.

Corollary 2. *For an ICMN with n mobile nodes, side-length L and maximum transmission distance d, when $d \ll L$, a necessary condition for any routing algorithm*

that can stabilize the network with packet arrival rate λ while maintaining a bounded expected end-to-end delay $\mathbb{E}\{D\}$ is given by

1. *for the random waypoint mobility model:*

$$\frac{\mathbb{E}\{D\}}{\lambda} \geq \frac{L^4}{2(n-1)(c_1 d\,\mathbb{E}[V^*])^2}, \tag{2.36}$$

2. *for the random direction mobility model:*

$$\frac{\mathbb{E}\{D\}}{\lambda} \geq \frac{L^4}{2(n-1)(d\,\mathbb{E}[V^*])^2}, \tag{2.37}$$

where $c_1 = 1.3683$ is a constant and $\mathbb{E}[V^*]$ is the average relative speed between a pair of nodes. In the special case of constant traveling speed v, the necessary condition is given by

1. *for the random waypoint mobility model:*

$$\frac{\mathbb{E}\{D\}}{\lambda} \geq \frac{\pi^2 L^4}{32(n-1)(c_1 dv)^2}, \tag{2.38}$$

2. *for the random direction mobility model:*

$$\frac{\mathbb{E}\{D\}}{\lambda} \geq \frac{L^4}{32(n-1)(dv)^2}. \tag{2.39}$$

Remark 1. *Notice that for both the random waypoint and random direction mobility models, if we consider that the L and n increase while the node density $\tau = n/L^2$ remains constant, then we have the following observations from Corollaries 1 and 2.*

- *The results of (2.35) reduce to $\mu_{RW} \approx c_1 \tau d\,\mathbb{E}[V^*]$ and $\mu_{RW} \approx \tau d\,\mathbb{E}[V^*]$, indicating that a constant throughput capacity is still achievable in a large scale ICMN. Meanwhile, the result in (2.11) indicates that the average end-to-end delay under Algorithm 1 will increase linearly with the number of nodes n.*
- *The results in Corollary 2 indicates that the delay-throughput scales as $\mathbb{E}\{D\}/\lambda > O(n)$.*

2.4 Simulation and Numerical Results

In this section, we first provide simulation results to validate the efficiency of the theoretical capacity/delay models developed in Section 2.3, and then apply these models to illustrate the performance of ICMNs under different settings of system parameters.

2.4.1 Model Validation

To validate the efficiency of our analytical models, we provide simulation results under the random waypoint and the random direction mobility models in this section. The simulation results were obtained from a self-developed discrete event simulator that implements the packet delivery process under Algorithm 1 and accepts as an input the random mobility trace generated by the NS-2 code of the random waypoint and random direction mobility models.

Mobility Models

The mobility models considered in the simulation are summarized as follows.

- The random waypoint mobility model [31] is widely adopted in the simulation of MANETs. Under this model, each node is assigned an initial location in a finite square and travels at a random travel speed towards a random destination uniformly chosen in the network area. The travel speed is uniformly selected in $(v_{\min}, v_{\max})$ with $v_{\min} > 0$. After arriving at the destination, the node may pause for a random amount of time and then chooses a new destination and a new travel speed, independently of previous ones. It is notable that the location of a node in steady-state under the random waypoint model is not uniformly distributed. Particularly, it was reported in [38] that the stationary distribution of the location of a node is more concentrated near the center of the network region.

- Under the random direction mobility model [31], at the beginning each node randomly selects a direction, a speed and a finite traveling time. The node travels towards the direction at the given speed for the given duration of time. When the travel time duration has expired, the node could pause for a random time, after which it selects a new set of direction, speed and time duration, independently of all previous ones. When the node reaches a boundary, it is either reflected or the area wraps around so that it appears on the other side. It was shown in [39] that the stationary distribution of locations is uniformly distributed for arbitrary distributions of direction, speed and travel time duration, irrespective of the boundaries being reflecting or wrapped around.

Simulation Setting

In our simulation, we consider a square network of side-length $L = 2000$ m and number of nodes $n = 20$. The travel speed is constant and equals to $v = 40$ m/s. There is no pause time. We consider transmission distances of $d = \{20, 50, 100\}$, where the corresponding pairwise meeting rates are determined as $\beta_{\text{RW}} = \{6.96 \times 10^{-4}, 1.74 \times 10^{-3}, 3.48 \times 10^{-3}\}$ for the random waypoint mobility model and $\beta_{\text{RD}} = \{5.09 \times 10^{-4}, 1.27 \times 10^{-3}, 2.55 \times 10^{-3}\}$ for the random direction mobility model, according to Lemma 1. For the simulation measurements of the throughput and average end-to-end delay under Algorithm 1, we focus on a specific traffic flow and measure its throughput and average packet delay over a long time period of 1.0×10^7 seconds for each system load $\rho = \lambda/\mu$.

Simulation Results

To validate the efficiency of the developed throughput capacity model, we summarize in Fig. 2-2 the simulation results of throughput for different values of system load. In Fig. 2-2, the dots represent the simulation results and the dashed lines are the corresponding theoretical throughput capacities, calculated by Corollary 1. We can observe from Fig. 2-2 that for both the random waypoint and random direction mobility models, the throughput increases linearly as ρ increases from 0 to 1 and approaches

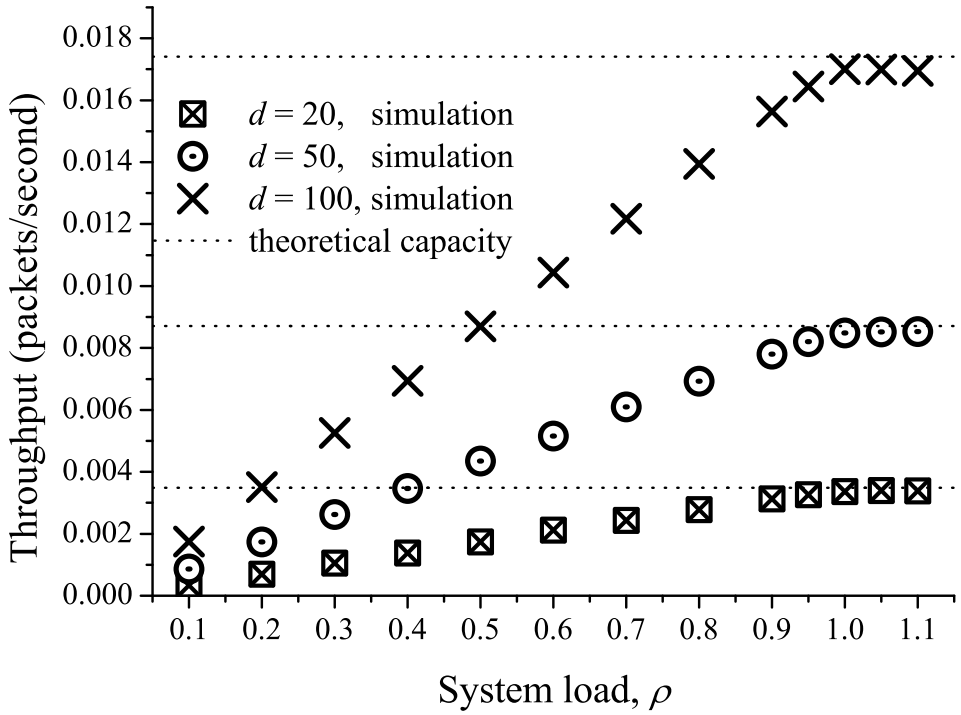

(a) Random waypoint model.

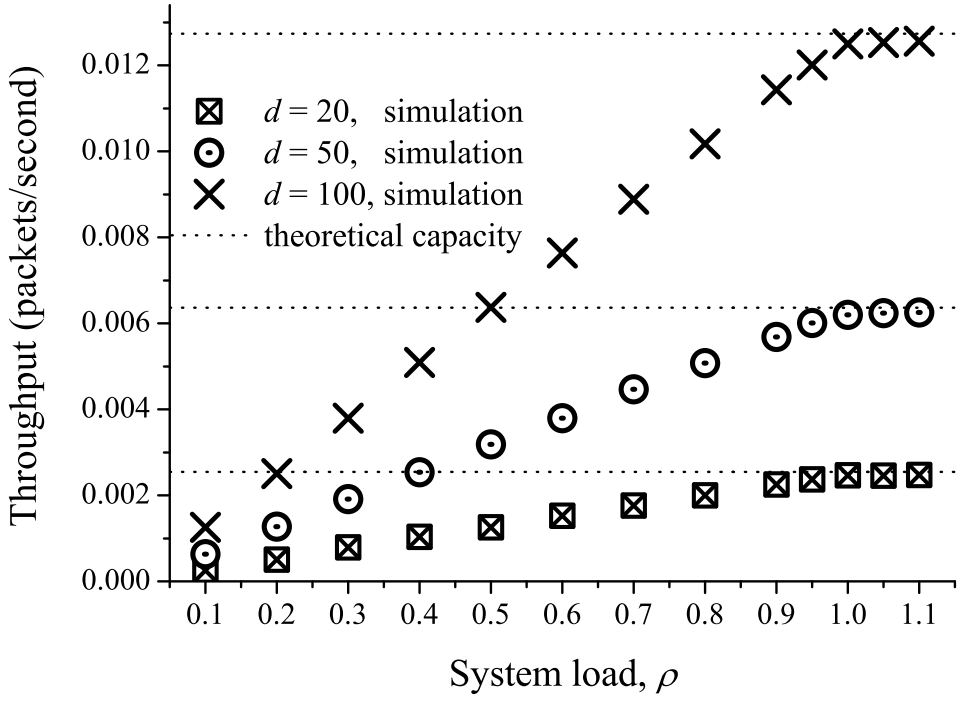

(b) Random direction model.

Figure 2-2: Throughput vs. system load ρ.

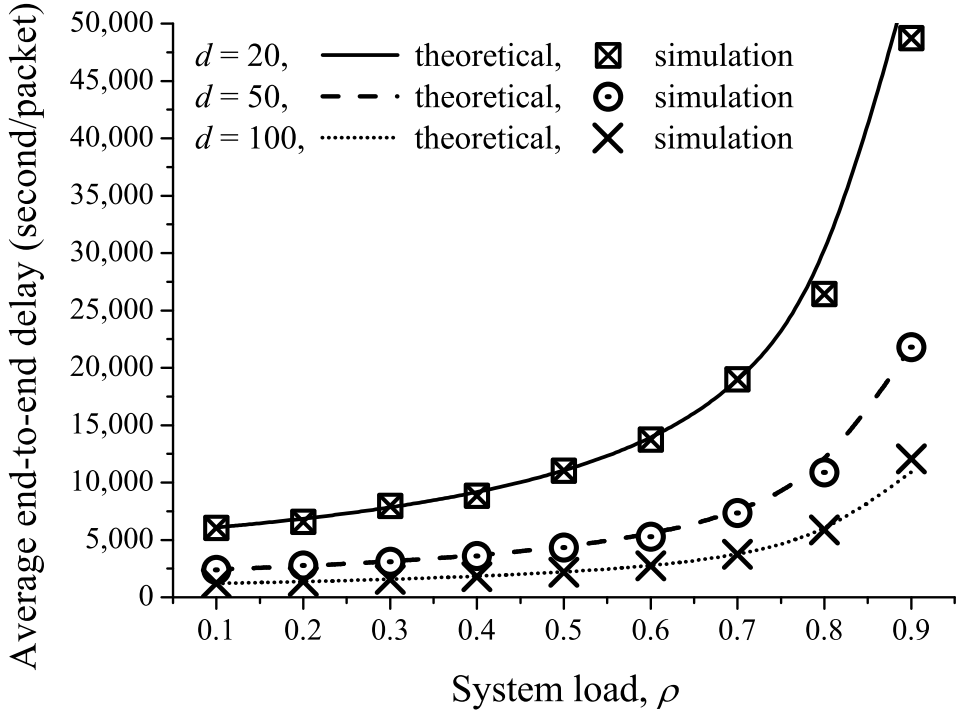

(a) Random waypoint model.

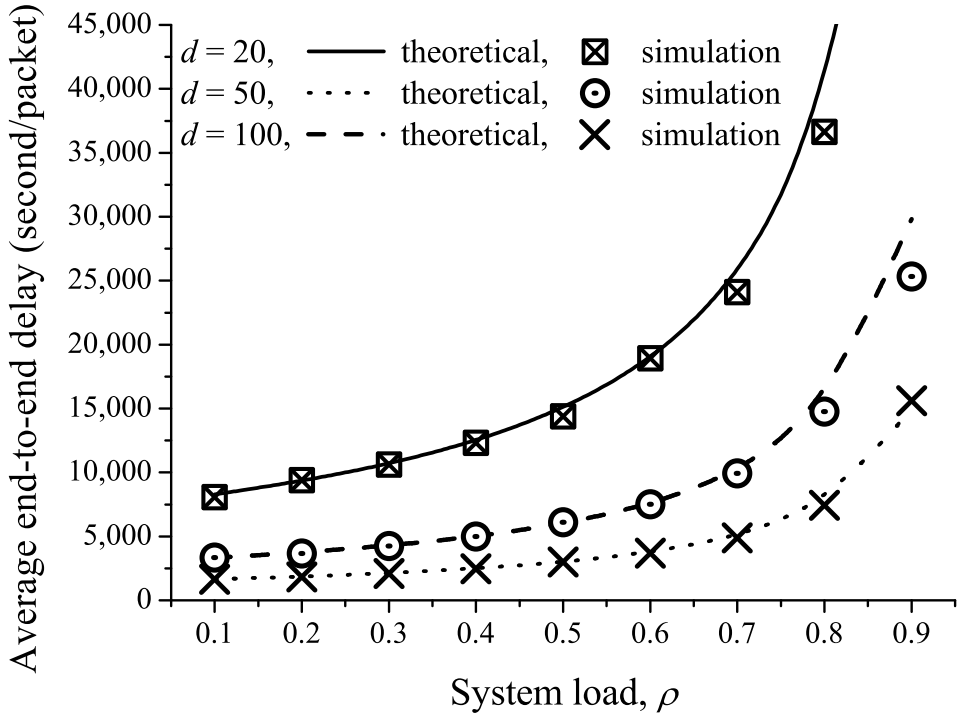

(b) Random direction model.

Figure 2-3: Average end-to-end delay vs. system load ρ.

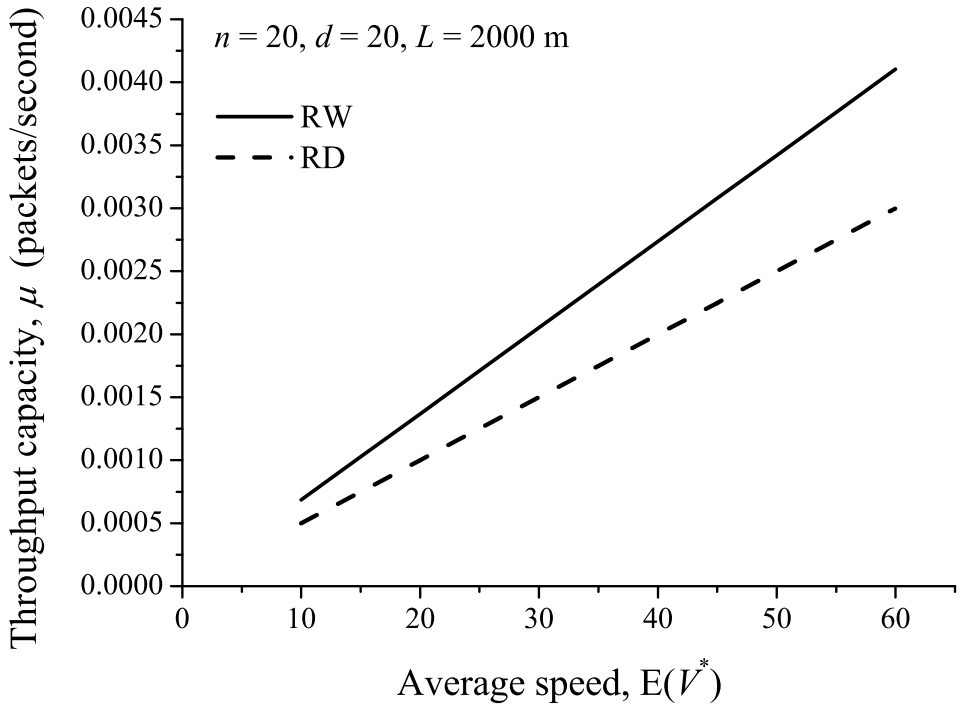

Figure 2-4: Capacity μ vs. average speed $\mathbb{E}\{V^*\}$.

to μ when ρ grows further beyond 1. The results in Fig. 2-2 indicate clearly that our theoretical capacity model of (2.2) can accurately predict the throughput capacity of the considered ICMNs under a general class of mobility models that follows the Poisson meeting process. Moreover, it also indicates that this throughput capacity can be achieved by adopting Algorithm 1 as routing algorithm in the network.

We then proceed to validate the efficiency of our end-to-end delay model. Particularly, we compare in Fig. 2-3 the simulation results of the average end-to-end packet delay to those of theoretical ones calculated by substituting the results in Corollary 1 into (2.11). We can see from Fig. 2-3 that for both the considered mobility models, the theoretical results nicely agree with the simulation ones. This observation indicates that our delay model of (2.11) is accurate and can efficiently capture the delay behavior under Algorithm 1 in the considered network.

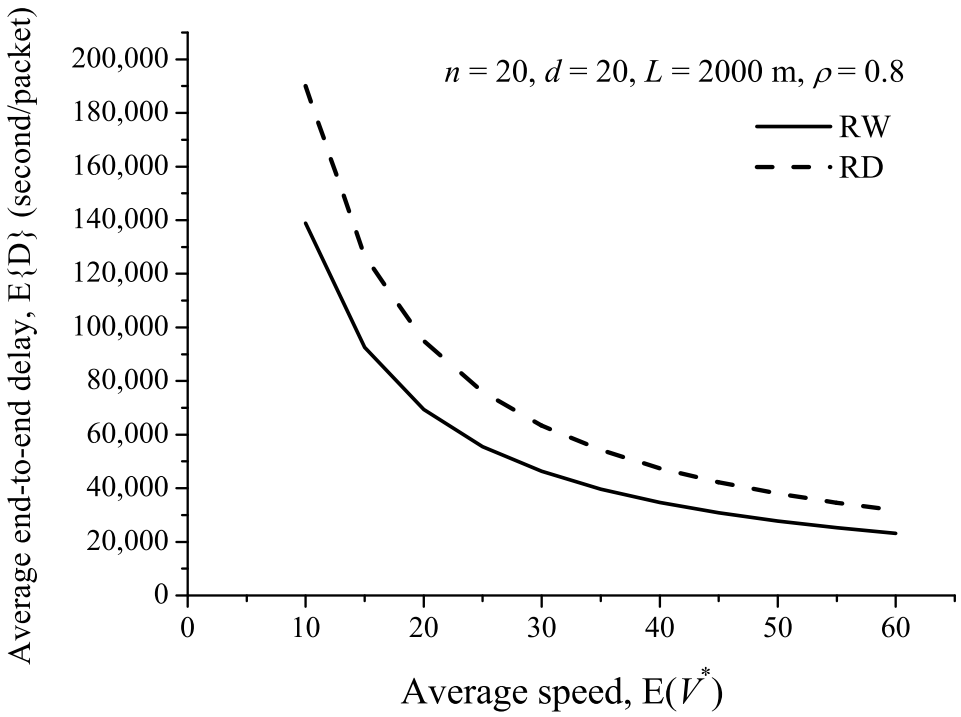

Figure 2-5: Average end-to-end delay $\mathbb{E}\{D\}$ vs. average speed $\mathbb{E}\{V^*\}$.

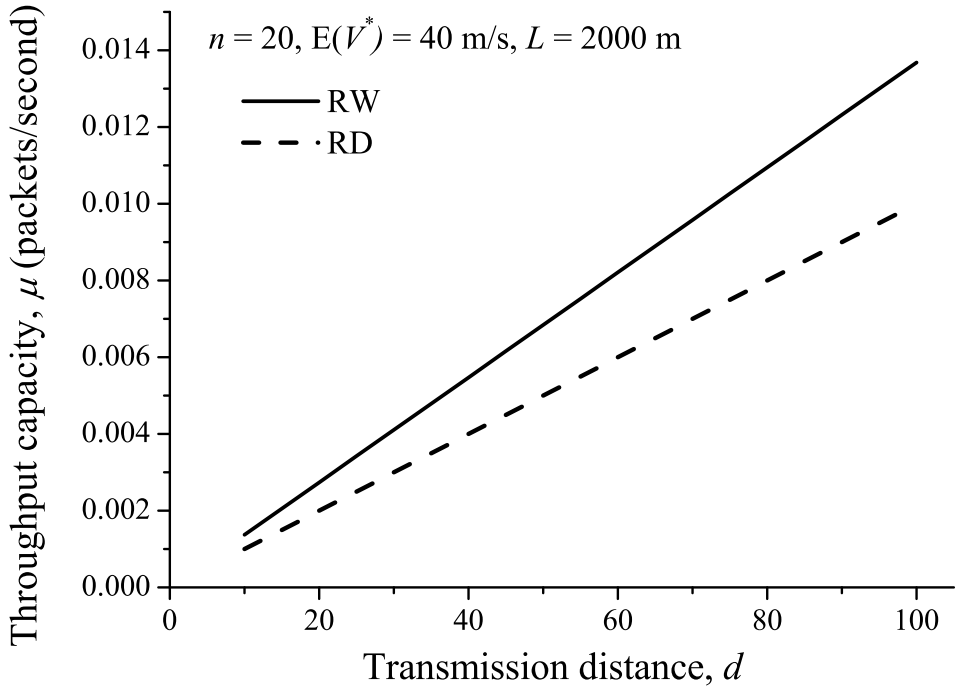

Figure 2-6: Capacity μ vs. transmission distance d.

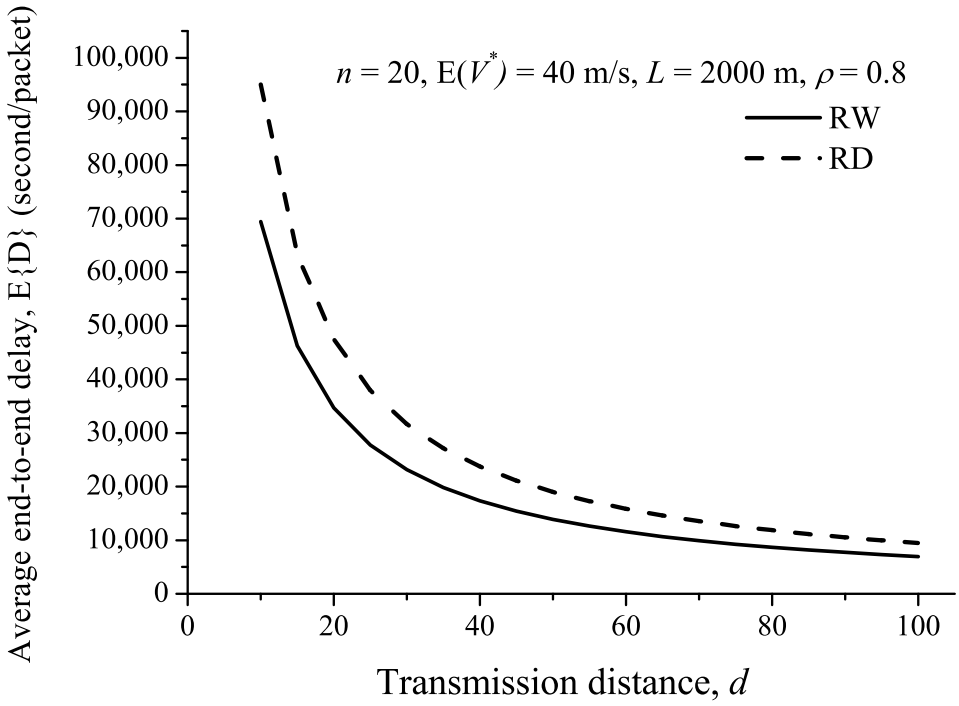

Figure 2-7: Average end-to-end delay $\mathbb{E}\{D\}$ vs. transmission distance d.

2.4.2 Numerical Results and Discussions

Based on our theoretical models, we first explore the impact of nodel traveling speed on the throughput capacity and end-to-end delay. We summarize in Fig. 2-4 how the μ varies with average pairwise relative speed $\mathbb{E}\{V^*\}$ in a network of $n = 20, d = 20$ m and $L = 2000$ m. Fig. 2-4 shows that as the $\mathbb{E}\{V^*\}$ increases, the throughput capacities under both the random waypoint and random direction models increase linearly. This is mainly due to that a higher average travel speed will lead to an increase on the pairwise meeting rate as shown in (2.1), and hence to a higher throughput capacity. For the same network setting, we then present in Fig. 2-5 how the average delay $\mathbb{E}\{D\}$ under Algorithm 1 varies with $\mathbb{E}\{V^*\}$ under system load $\rho = 0.8$. It can be observed in Fig. 2-5 that increasing $\mathbb{E}\{V^*\}$ will cause a lower average delay, which is because the $\mathbb{E}\{D\}$ is inverse proportional to the throughput capacity μ as indicated in (2.11).

We then present in Fig. 2-6 and 2-7 how the throughput capacity μ and average end-to-end packet delay vary with transmission distance d for a network of $n =$

$20, \mathbb{E}\{V^*\} = 40$ m/s, $L = 2000$ m and $\rho = 0.8$ (for delay). It can be seen from in Figs. 2-6 and 2-7 that the impacts of the transmission distance d on the behavior of capacity and delay are similar to those of the $\mathbb{E}\{V^*\}$, for the reason that as shown in (2.1), d is also a factor in the evaluation of β.

It is also interesting to see that from Figs. 2-4-2-7 that the random waypoint mobility model provides a performance better than that of the random direction mobility model for the network settings here. Recall that compared with the random direction model that has a uniform stationary distribution of nodes location, the stationary distribution of the location of a node under the random waypoint mobility model is more concentrated near the center of the network region (see Section 2.4.1). Therefore, the random waypoint mobility model leads to a higher nodel pairwise meeting rate (see (2.1)) and hence a higher throughput capacity, for the same network setting of L, $\mathbb{E}\{V^*\}$ and d.

2.5 Summary

In this chapter, we studied the exact throughput capacity and delay-throughput tradeoff in a general ICMN with a type of mobility models that follow the Poisson meeting process. Based on the pairwise meeting rate in the concerned ICMN, its exact throughput capacity is derived and a necessary condition on the delay-throughput tradeoff is also established to reveal the inherent relationship between the end-to-end packet delay and achievable throughput. We expect that the theoretical analysis developed in this chapter will be also helpful for exploring the throughput capacity and delay-throughput tradeoff in ICMNs under other types of mobility models as well. The results in Corollary 1 indicate that under the random waypoint or random direction mobility, a constant throughput capacity is achievable even in a large scale ICMN as far as the node density is kept constant, but at the cost of a linearly increasing end-to-end delay. Our results also reveal that by increasing the average node traveling speed or transmission range in an ICMN, an improvement on both its throughput and end-to-end delay performance can be expected.

Chapter 3

Throughput Capacity in ALOHA MANETs (A-MANETs)

3.1 Introduction

In this chapter, we focus on a class of MANETs where mobile nodes are deployed in a continuous network area[40], and a slotted ALOHA [41] protocol is adopted for MAC. It is notable that the concerned MANETs with ALOHA protocol and continuous network model serve as an important networking model for practical MANETs. This is because that in comparison with the discrete network model with cell-partition [3, 17], the continuous network model and mobility model defined based on it provide a more realistic characterization of network topology and node mobility in practical MANETs. Also, the ALOHA is a very attractive MAC protocol for practical MANETs since it is simple yet efficient and can be easily implemented in a distributed fashion.

3.1.1 Available Studies on A-MANET

By now, a lot of work has been done to help us understand the basic performance of A-MANETs. Baccelli et al. [41] studied the optimization on transmission progress under Poisson point process model [42–44]. The interference and outage probability were investigated in [45] and [46] under infinite and finite network scenarios, respec-

tively. The work in [47, 48] provided analysis on the asymptotic behavior of packet propagation speed in A-MANETs. The authors of [49] took a game theory approach to explore the power control issue in A-MANETs. Recently, the local delay of A-MANETs, i.e. the time it takes a node to successfully transmit a packet, has been explored in [50–52].

3.1.2 Limitations of Available Studies

Despite the insight provided in available studies discussed above, the exact throughput capacity of A-MANETs remains unexplored in the literature. Although extensive research has been devoted to the study of throughput capacity under various network scenarios, the analysis developed there cannot be applied to study the exact throughput capacity in A-MANETs. This is mainly due to the difficulty in exactly modeling the successful transmission probability (STP) in such networks, which usually involves very complicated geometric calculations and thus prevents a closed-form result on STP (and also exact throughput capacity) from being derived. To address this issue, this chapter develops a novel theoretical framework to enable the efficient and closed-form approximations to both STP and exact throughput capacity to be conduced for A-MANETs.

3.1.3 Chapter Outline

The rest of the chapter is organized as follows. Section 3.2 introduces system models. The analysis on the throughput capacity and expected end-to-end delay of a capacity achieving routing algorithm is presented in Section 3.3. In Section 3.4, we derive approximations to both the STP and throughput capacity under two popular local transmission schemes, conduct analysis on the corresponding approximation errors and also explore the capacity optimization issue. Simulation/numerical studies and the corresponding discussions are provided in Section 3.5. Finally, we summarize this chapter in Section 3.6.

3.2 System Models

In this section, we present the network model, communication model and traffic model under study and also define the successful transmission probability.

3.2.1 Network Model

We consider a time-slotted network of a continuous unit square area. Similar to previous studies [17, 53, 54], the network is assumed to have torus boundaries, so the opposite sides of the network will be identical. There are n mobile nodes in the network, and they randomly move according to the two dimensional i.i.d. mobility model [2]. Under such mobility model, each node independently and uniformly selects a point in the network area at the beginning of each time slot and then stays at it during the time slot.

3.2.2 Communication Model

A half-duplex medium is shared by all the nodes for data communication, and a slotted ALOHA protocol [41] is adopted for MAC. Under this protocol, in each time slot one node tries to conduct a transmission (i.e, to become a transmitter) with probability q and keeps silent as a potential receiver with probability $1 - q$.

We adopt the protocol model defined in [17] to decide if a transmission between a transmitter and its intended receiver is successful in this chapter. Under the protocol model, the transmission from transmitter i to receiver j is successful iff for any other transmitting node l,

$$d_{lj} \geq (1 + \Delta)d_{ij}, \tag{3.1}$$

where d_{lj} denotes the Euclidean distance between node l and node j and $\Delta > 0$ models a guard zone to prevent the transmission from being corrupted by interference from other simultaneous transmissions. During a successful transmission, the total number of bits that can be transmitted is fixed and normalized to one packet.

Previous works from both practice and theoretical analysis indicate that the local transmission provides a better throughput performance, so we consider here the following two popular local transmission schemes for receiver selection [1, 2, 51].

Nearest Neighbor Transmission (NNT): Under NNT, the intended receiver of a transmitter is the node closest to the transmitter among all other nodes.

Nearest Receiver Transmission (NRT): Under NRT, the intended receiver of a transmitter is the silent node closest to the transmitter among all other nodes.

3.2.3 Traffic Model

Regarding traffic pattern, we also consider the permutation traffic model [2]. We assume that the packet arrival process at each node is an i.i.d. Bernoulli process with rate λ packets/slot, such that with probability λ a single packet arrives at the node at the beginning of each time slot. To simplify capacity analysis, we assume that there is no constraint on packet lifetime and the buffer size in each node is sufficiently large so packet loss due to buffer overflow will never happen.

3.2.4 Definition of STP

Definition 4. ***Successful transmission probability (STP)*** *: The* successful transmission probability *is defined as the probability that a node establishes a successful transmission to its intended receiver in a time slot.*

3.3 Throughput Capacity

In this section, we first establish the following theorem regarding the throughput capacity result of an A-MANET, and then provide necessity and sufficiency proofs for this result.

Theorem 3. *For an A-MANET with n mobile nodes and STP P_S, its throughput capacity is determined as*

$$\mu = \frac{n}{2(n-1)} P_S. \tag{3.2}$$

The proof of Theorem 3 involves proving that $\lambda \leq \mu$ is necessary and also $\lambda < \mu$ is sufficient for ensuring network stability. We prove the necessity in Section 3.3.1 by showing that μ serves as an upper bound on the throughput over any routing algorithm in the network. The sufficiency is established in Section 3.3.2, where we provide a routing algorithm and show that the network is stable under this algorithm for any $\lambda < \mu$.

3.3.1 Proof of Necessity

Lemma 4. *(**Necessity**) For an A-MANET with n mobile nodes and STP P_S, its throughput under any routing algorithm is upper bounded by*

$$\mu = \frac{n}{2(n-1)} P_S. \tag{3.3}$$

Proof. The necessity can be proved following a method similar to that of [3]. For any possible routing algorithm, we use $X_h(T)$ to denote the total number of packets transferred through h hops from their sources to destinations in time interval $[0, T]$. Notice that to ensure network stability, the overall arrival rate of all traffic flows should be less than the overall throughput. Formally, it is required that for any given $\epsilon > 0$, there must exist an arbitrarily large T such that the following inequality holds

$$\lambda n - \epsilon \leq \frac{1}{T} \sum_{h=1}^{\infty} X_h(T), \tag{3.4}$$

where λ is the packet arrival rate at each node.

Notice the fact that during time interval $[0, T]$ the total number of packet transmissions is at least $\sum_{h=1}^{\infty} hX_h(T)$, which is upper bounded by the total number of successful transmissions $Y(T)$ in this time interval. Thus, we have

$$\sum_{h=1}^{\infty} hX_h(T) \leq Y(T). \tag{3.5}$$

From (3.4) and (3.5), we have

$$\begin{aligned}\frac{1}{T}Y(T) &\geq \frac{1}{T}X_1(T) + \frac{2}{T}\sum_{h=2}^{\infty}X_h(T) \\ &\geq \frac{1}{T}X_1(T) + 2\left[(\lambda n - \epsilon) - \frac{1}{T}X_1(T)\right], \end{aligned} \tag{3.6}$$

and thus

$$\lambda \leq \frac{1}{2n}\left[\frac{1}{T}Y(T) + \frac{1}{T}X_1(T) + 2\epsilon\right]. \tag{3.7}$$

Since a packet can be transferred from its source to destination through single hop only when the source can conduct a successful transmission to the destination, $X_1(T)$ is upper bounded by the total number of successful source-to-destination transmissions $Y_{sd}(T)$ in time interval $[0, T]$. Based on the law of large number, we know that as $T \to \infty$

$$\frac{1}{T}Y(T) \xrightarrow{\text{a.s.}} nP_{\text{S}}, \tag{3.8}$$

$$\frac{1}{T}Y_{sd}(T) \xrightarrow{\text{a.s.}} \frac{n}{n-1}P_{\text{S}}. \tag{3.9}$$

Hence,

$$\lambda \leq \frac{n}{2(n-1)}P_{\text{S}} + \frac{\epsilon}{n}, \text{ as } T \to \infty. \tag{3.10}$$

Since ϵ can be arbitrarily small, the result then follows. □

3.3.2 Proof of Sufficiency

In this section, we will prove that the upper bound in (3.3) is just the exact throughput capacity for the concerned A-MANET. The basic idea of our proof is to first construct a routing algorithm and then show that the routing algorithm can stabilize the network for any packet arrival rate $\lambda < \mu$. The routing algorithm considered here is summarized in Algorithm 2.

According to Algorithm 2, when a node obtains a transmission opportunity, it can conduct only one of the following three types of transmissions: *source-to-*

Algorithm 2 Routing Algorithm:

1: Suppose that a transmitter Tx can conduct a successful transmission to its receiver Rx in the current time slot.
2: **if** Rx is the destination node of Tx **then**
3: Tx conducts **Procedure 1** with Rx.
4: **else**
5: Tx flips an unbiased coin;
6: **if** it is the head **then**
7: Tx conducts **Procedure 2** with Rx.
8: **else**
9: Tx conducts **Procedure 3** with Rx.
10: **end if**
11: **end if**

Procedure 1 Source-to-destination transmission:

1: **if** Tx has a new packet destined for Rx **then**
2: Tx transmits the packet to Rx.
3: **else**
4: Tx remains idle.
5: **end if**

Procedure 2 Source-to-relay transmission:

1: **if** Tx has a new packet (i.e., a packet that has never been transmitted before) **then**
2: Tx transmits the packet to Rx.
3: **else**
4: Tx remains idle.
5: **end if**

Procedure 3 Relay-to-destination transmission:

1: **if** Tx has a packet destined for Rx **then**
2: Tx transmits the packet to Rx.
3: **else**
4: Tx remains idle.
5: **end if**

destination transmission, *source-to-relay* transmission and *relay-to-destination* transmission. Thus, a packet takes at most two hops to reach its destination.

Now, we show in the following lemma that for any arrival rate $\lambda < \mu$, the expected end-to-end delay under Algorithm 2 is bounded and hence the network stability is ensured.

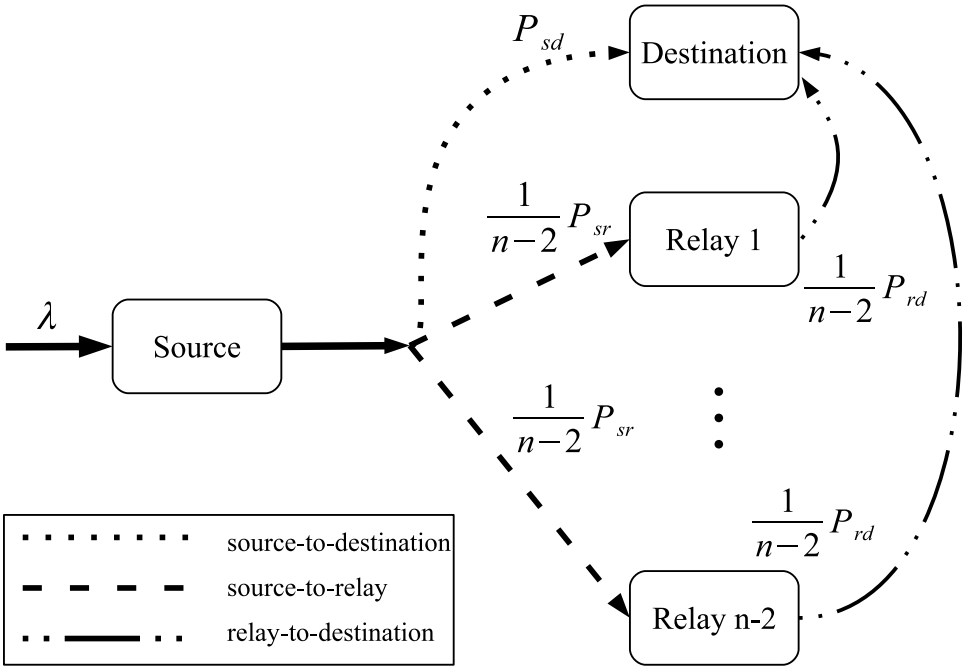

Figure 3-1: The packet routing process under Algorithm 2.

Lemma 5. *(**Sufficiency**) In the concerned A-MANET with n mobile nodes, if the packet arrival process at each node is an i.i.d. Bernoulli stream with rate $\lambda < \mu$ and the Algorithm 2 is adopted for packet routing, the expected end-to-end packet delay $E\{D\}$ is determined as*

$$\mathbb{E}\{D\} = \frac{n - \lambda - 1}{\mu - \lambda} = \frac{n - \rho\mu - 1}{(1 - \rho)\mu}, \tag{3.11}$$

where $\rho = \lambda/\mu$ denotes the system load.

Proof. For a given node and a given time slot, we use P_{sd}, P_{sr} and P_{rd} to denote the probability that it conducts a source-to-destination transmission, the probability that it conducts a source-to-relay transmission and the probability that it conducts

a relay-to-destination transmission, respectively. We can easily see that

$$\begin{aligned} P_{sd} &= \frac{1}{n-1} P_{\mathrm{S}}, \\ P_{sr} &= \frac{n-2}{2(n-1)} P_{\mathrm{S}}, \\ P_{rd} &= \frac{n-2}{2(n-1)} P_{\mathrm{S}}. \end{aligned} \tag{3.12}$$

With the help of P_{sd}, P_{sr} and P_{rd}, the packet routing process under Algorithm 2 is illustrated in Fig. 3-1, where the source node conducts a source-to-destination transmission with probability P_{sd} and conducts a source-to-relay transmission to one relay node with probability $\frac{P_{sr}}{n-2}$, and a relay node conducts a relay-to-destination transmission to the destination node with probability $\frac{P_{rd}}{n-2}$. We can see from Fig. 3-1 that the packet routing process of each traffic involves a two-stage queuing process. The first stage is the queuing process at the source node, while the second stage is the queuing process at one of the $n-2$ relay nodes.

First, for the queuing process at the source node, we can see that its packet arrival rate is λ and its service rate is $P_{sd} + P_{sr} = \mu$. Such a queue is termed as a state independent Bernoulli server in [55]. Let l denote the queue length of the source queue, its stationary distribution $\pi(l)$ is given by

$$\begin{aligned} \pi(l) &= \left(1 - \frac{\lambda}{\mu}\right) \left(\frac{\lambda(1-\mu)}{\mu(1-\lambda)}\right)^{l} \left(\frac{1}{1-\mu}\right) \text{ for } l \geq 1, \\ \pi(0) &= \left(1 - \frac{\lambda}{\mu}\right). \end{aligned}$$

Thus, the expected queue length $\mathbb{E}\{L_s\}$ at the source is determined as

$$\mathbb{E}\{L_s\} = \sum_{l=1}^{\infty} l\pi(l) = \frac{\lambda^2 - \lambda}{\lambda - \mu}. \tag{3.13}$$

Notice that the queue at the source is reversible, so its output is also a Bernoulli stream with rate λ.

Second, consider the queuing process at one of the $n-2$ relay nodes. A packet

transmitted from the source will be delivered to this relay node with probability $\frac{P_{sr}}{(n-2)\mu} = \frac{1}{n}$, so the arrival rate at the relay queue is determined as $\lambda' = \frac{\lambda}{n}$. Regarding the service rate of the relay queue, we can easily see that it is given by $\mu' = \frac{1}{n-2}P_{rd}$, i.e., the probability that the relay conducts a relay-to-destination transmission with the destination node. Since the arrival and departure at a relay node are mutually exclusive, this queue can be regarded as a birth-death chain. Let l' denote the relay queue length, its stationary distribution $\pi'(l')$ is given by

$$\pi'(l') = \left(1 - \frac{\lambda'}{\mu'}\right)\left(\frac{\lambda'}{\mu'}\right)^{l'}, \; l' \geq 0. \tag{3.14}$$

Thus, the expected queue length $\mathbb{E}\{L_r\}$ at a relay node is determined as

$$\mathbb{E}\{L_r\} = \sum_{l'=1}^{\infty} l'\pi'(l') = \frac{\lambda'}{\mu' - \lambda'}. \tag{3.15}$$

From Little's Theorem, the expected end-to-end delay $E\{D\}$ is then evaluated as

$$\begin{aligned} \mathbb{E}\{D\} &= \left[\mathbb{E}\{L_s\} + (n-2)\,\mathbb{E}\{L_r\}\right]/\lambda \\ &= \frac{n - \lambda - 1}{\mu - \lambda}. \end{aligned} \tag{3.16}$$

□

3.4 Approximations of STP and Capacity

The result in Theorem 3 indicates that the throughput capacity of an A-MANET is mainly determined by the STP in such network. In this section, we will show that the exactly modeling of STP is highly cumbersome, and then develop efficient closed-form approximations to both STP and exact throughput capacity in the concerned network under the NNT and NRT schemes, respectively. The related issues of approximation error analysis and capacity optimization will be also explored.

3.4.1 Node Distance Analysis

For the analysis of STP and thus throughput capacity under the NNT and NRT schemes, where the node (or silent node) closest to the transmitter will be selected as the receiver, we first need to determine the distance distribution between a node and its neighbor nodes.

Lemma 6. *For an A-MANET with n mobile nodes, we use R_k $(0 < k \leq n-1)$ to denote the distance between a node and its k-th nearest neighbor at a time slot, then the probability density function $f_{R_k}(r)$ of R_k is determined as*

$$f_{R_k}(r) = \frac{\omega'(r)\left(\omega(r)\right)^{k-1}\left(1-\omega(r)\right)^{n-k-1}}{B(k, n-k)}, \tag{3.17}$$

where

$$\omega(r) = \begin{cases} \pi r^2 & 0 \leq r \leq \frac{1}{2} \\ \pi r^2 - 4r^2 \operatorname{arcsec}(2r) & \\ \quad + \sqrt{4r^2 - 1} & \frac{1}{2} < r \leq \frac{\sqrt{2}}{2} \end{cases}, \tag{3.18}$$

$\omega'(r)$ is the derivative of $\omega(r)$ determined as

$$\omega'(r) = \begin{cases} 2\pi r & 0 < r < \frac{1}{2} \\ 2\pi r - 8r \operatorname{arcsec}(2r) & \frac{1}{2} < r < \frac{\sqrt{2}}{2} \end{cases}, \tag{3.19}$$

and $B(x, y)$ is the beta function that can be expressed in terms of gamma functions as $B(x, y) = \frac{\Gamma(x)\Gamma(y)}{\Gamma(x+y)}$.

Proof. Without loss of generality, we consider a node in the center of the network at the current time slot, and use $\omega(r)$ to denote the intersection between the circular region centered at the node with radius r and the network region[1]. Since the network region is an unit square, it is easy to see that $\omega(r)$ can be easily determined as (3.18) by considering the cases $0 \leq r \leq \frac{1}{2}$ and $\frac{1}{2} < r \leq \frac{\sqrt{2}}{2}$, respectively.

[1]For simplicity, we use $\omega(r)$ to denote both the intersection and area of this intersection here.

Let N_r denote the number of nodes (excluding the concerned node) that fall within $\omega(r)$ in the current time slot, we can see that N_r follows the binomial distribution with parameters $n-1$ and $\omega(r)$. Notice that a node falls within $\omega(r)$ iff its distance to the concerned node is no larger than r. Thus, the cumulative density function $F_{R_k}(r)$ of R_k is given by

$$\begin{aligned} F_{R_k}(r) &= \Pr\{R_k \leq r\} \\ &= \Pr\{N_r \geq k\} \\ &= \sum_{t=k}^{n-1} \binom{n-1}{t} (\omega(r))^t (1-\omega(r))^{n-1-t} \\ &= I_{\omega(r)}(k, n-k), \end{aligned} \tag{3.20}$$

where $I_x(a,b)$ is the regularized incomplete beta function [56]. Taking derivative with respect to r in both sides of (3.20), the formula (3.17) then follows. □

3.4.2 STP and Capacity under NNT

In this section, we analyze the STP and throughput capacity under the NNT scheme. Without loss of generality, we focus on a node i and its nearest neighbor node j in a time slot. The node i can successfully establish a transmission to node j in the time slot iff the following three events happen simultaneously: (i) Node i is transmitting; (ii) Node j is silent; (iii) The successful transmission condition specified by the protocol model in (3.1) holds.

We use indicator function $\delta_{i,j} = 1$ to denote that the condition in (3.1) is true for the transmission from i to j ($\delta_{i,j} = 0$, otherwise). Since above three events are mutually independent, we can see that the STP P_{S} under the NNT scheme is determined as

$$\begin{aligned} P_{\mathrm{S}} &= q(1-q)\Pr\{\delta_{i,j} = 1\} \\ &= q(1-q)\,\mathbb{E}\{\delta_{i,j}\}. \end{aligned} \tag{3.21}$$

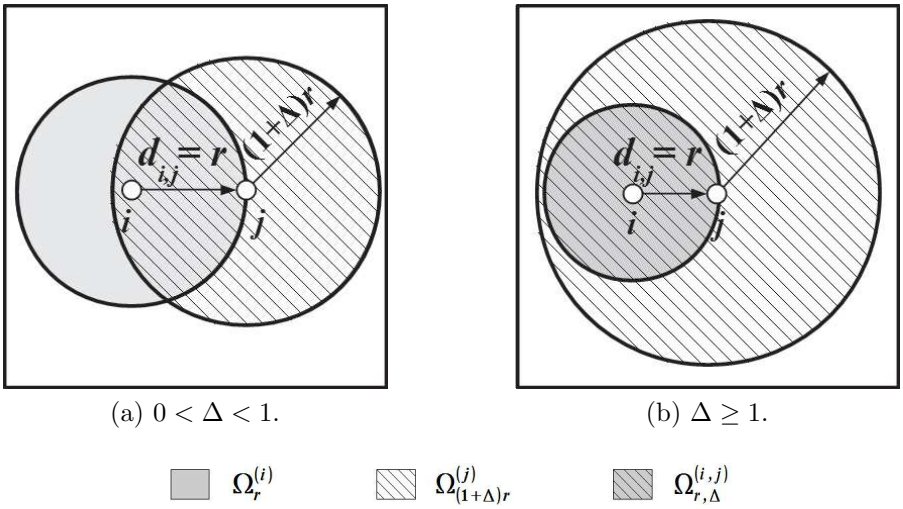

(a) $0 < \Delta < 1$. (b) $\Delta \geq 1$.

Figure 3-2: Illustration of $\Omega_r^{(i)}$, $\Omega_{(1+\Delta)r}^{(j)}$ and $\Omega_{r,\Delta}^{(i,j)}$.

Let $\mathbb{E}\{\delta_{i,j}|d_{ij} = r\}$ denote the expectation of $\delta_{i,j}$ conditioned on $d_{ij} = r$, we have

$$\mathbb{E}\{\delta_{i,j}\} = \int_0^{\frac{\sqrt{2}}{2}} \mathbb{E}\{\delta_{i,j}|d_{ij} = r\} f_{R_1}(r)\, \mathrm{d}r, \tag{3.22}$$

where $f_{R_1}(r)$ is just the probability density function of distance between a node and its nearest neighbor, which can be evaluated based on (3.17).

Formulas (3.21) and (3.22) indicate that we need to determine $\mathbb{E}\{\delta_{i,j}|d_{ij} = r\}$ for the evaluation of P_{S}. We use $\Omega_r^{(a)}$ to denote the intersection between the network region and the circular region centered at a node a with radius r, and use $\Omega_{r,\Delta}^{(i,j)}$ to denote the intersection between $\Omega_r^{(i)}$ and $\Omega_{(1+\Delta)r}^{(j)}$.

As illustrated in Fig. 3-2 that $\mathbb{E}\{\delta_{i,j}|d_{ij} = r\}$ actually accounts for the probability that all transmitting nodes other than i are outside of $\Omega_{(1+\Delta)r}^{(j)}$ given that all nodes other than i and j are outside of $\Omega_r^{(i)}$. Let $p_{i,j}$ denote the probability that a node is outside of $\Omega_{(1+\Delta)r}^{(j)}$ given that it is outside of $\Omega_r^{(i)}$, we have

$$\mathbb{E}\{\delta_{i,j}|d_{ij} = r\} = \sum_{k=0}^{n-2} \binom{n-2}{k} (q \cdot p_{i,j})^k (1-q)^{n-2-k}, \tag{3.23}$$

here

$$p_{i,j} = \frac{1 - |\Omega_r^{(i)}| - |\Omega_{(1+\Delta)r}^{(j)}| + |\Omega_{r,\Delta}^{(i,j)}|}{1 - |\Omega_r^{(i)}|}, \tag{3.24}$$

and $|\cdot|$ denotes the area of a region.

Since $|\Omega_r^{(i)}|$ and $|\Omega_{(1+\Delta)r}^{(j)}|$ can be easily determined based on (3.18), the only difficulty in the evaluation of $\mathbb{E}\{\delta_{i,j}|d_{ij} = r\}$ is to determine $|\Omega_{r,\Delta}^{(i,j)}|$. We can see from Fig. 3-2 that the evaluation of $|\Omega_{r,\Delta}^{(i,j)}|$ can be divided into two scenarios of $0 < \Delta < 1$ and $\Delta \geq 1$. We now focus on the scenario of $0 < \Delta < 1$ (the analysis for the scenario of $\Delta \geq 1$ can be conducted similarly).

To evaluate $|\Omega_{r,\Delta}^{(i,j)}|$ under the scenario of $0 < \Delta < 1$, we need to further specify the parameter r. As shown in Fig. 3-2a that for the case $(3 + \Delta)r \leq 1$ (or equivalently $0 < r \leq \frac{1}{3+\Delta}$), $|\Omega_{r,\Delta}^{(i,j)}|$ can be easily evaluated since it just corresponds to the area of the intersection between two disks. We now consider the case $(3 + \Delta)r > 1$ (or equivalently $\frac{1}{3+\Delta} < r \leq \frac{\sqrt{2}}{2}$). As showed in Fig. 3-3 that under the latter case, $\Omega_{r,\Delta}^{(i,j)}$ corresponds to the intersection of multiple disks and it also varies with the direction from transmitter i to receiver j. Thus, evaluation of $|\Omega_{r,\Delta}^{(i,j)}|$ under this case is quite cumbersome.

Based on above discussion, we can see that for the scenario of $0 < \Delta < 1$, $\mathbb{E}\{\delta_{i,j}\}$ can be evaluated as

$$\begin{aligned}\mathbb{E}\{\delta_{i,j}\} = &\underbrace{\int_0^{\frac{1}{3+\Delta}} \mathbb{E}\{\delta_{i,j}|d_{ij} = r\} f_{R_1}(r)\,\mathrm{d}r}_{(a)} \\ &+ \underbrace{\int_{\frac{1}{3+\Delta}}^{\frac{\sqrt{2}}{2}} \mathbb{E}\{\delta_{i,j}|d_{ij} = r\} f_{R_1}(r)\,\mathrm{d}r}_{(b)},\end{aligned} \tag{3.25}$$

in which the integration (a) can be analytically derived while the analysis of integration (b) is highly cumbersome (if not impossible) due to the difficulty in modeling $|\Omega_{r,\Delta}^{(i,j)}|$ there. Fortunately, as to be proved in Appendix A.1 that the integration (b) in (3.25) actually accounts for only a negligible part of $\mathbb{E}\{\delta_{i,j}\}$, which enables an efficient and closed-form approximation to P_{S} to be made.

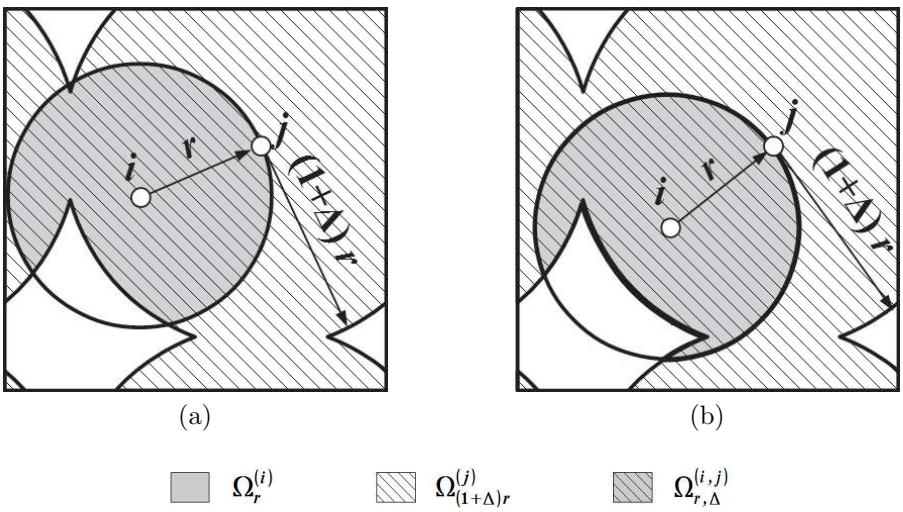

Figure 3-3: Illustration for $\Omega_{r,\Delta}^{(i,j)}$ when $0 < \Delta < 1$ and $\frac{1}{3+\Delta} < r \leq \frac{\sqrt{2}}{2}$.

Lemma 7. *In the considered A-MANET with n mobile nodes, transmission probability q and guard factor $\Delta > 0$, its STP P_S under the NNT scheme can be approximated as*

$$P_S \approx \widehat{P}_S = \begin{cases} \frac{\pi q(1-q)}{\pi + q \cdot \Psi(\Delta)}, & \text{if } 0 < \Delta < 1 \\ \frac{q(1-q)}{1+2\Delta q+\Delta^2 q}, & \text{if } \Delta \geq 1 \end{cases}, \tag{3.26}$$

and the corresponding approximation error $\epsilon_P = P_S - \widehat{P}_S$ is upper and lower bounded as

$$\epsilon^- \leq \epsilon_P \leq \epsilon^+, \tag{3.27}$$

where

$$\Psi(\Delta) = \pi(1+\Delta)^2 - (1+\Delta)^2 \arccos\left(\frac{1+\Delta}{2}\right) - \arccos\left(1 - \frac{(1+\Delta)^2}{2}\right) + (1+\Delta)\sqrt{1 - \frac{(1+\Delta)^2}{4}}, \tag{3.28}$$

$$\epsilon^- = \begin{cases} -\frac{\pi q(1-q)}{\pi+q\cdot\Psi(\Delta)}\left(1-\frac{\pi+q\cdot\Psi(\Delta)}{(3+\Delta)^2}\right)^{n-1}, & \text{if } 0<\Delta<1 \\ -\frac{q(1-q)}{1+2\Delta q+\Delta^2 q}\left(1-\frac{(1+2\Delta q+\Delta^2 q)\pi}{(2+2\Delta)^2}\right)^{n-1}, & \text{if } \Delta\geq 1 \end{cases} \tag{3.29}$$

and

$$\epsilon^+ = \begin{cases} q(1-q)\left[\left(1-q\cdot\frac{\Psi(\Delta)}{(3+\Delta)^2-\pi}\right)^{n-2}\left(1-\frac{\pi}{(3+\Delta)^2}\right)^{n-1}\right. \\ \left.-\frac{\pi}{\pi+q\cdot\Psi(\Delta)}\left(1-\frac{\pi+q\cdot\Psi(\Delta)}{(3+\Delta)^2}\right)^{n-1}\right], & \text{if } 0<\Delta<1 \\ \\ q(1-q)\left[\left(1-q\cdot\frac{\pi(1+\Delta)^2-\pi}{(2+2\Delta)^2-\pi}\right)^{n-2}\left(1-\frac{\pi}{(2+2\Delta)^2}\right)^{n-1}\right. \\ \left.-\frac{1}{1+2\Delta q+\Delta^2 q}\left(1-\frac{(1+2\Delta q+\Delta^2 q)\pi}{(2+2\Delta)^2}\right)^{n-1}\right], & \text{if } \Delta\geq 1 \end{cases} \tag{3.30}$$

Proof. See Appendix A.1. □

Remark 2. *The Lemma 7 indicates that* $\lim_{n\to\infty}\epsilon_P = 0$*, so we have* $\lim_{n\to\infty} P_S = \widehat{P}_S$ *under the NNT scheme. We can see from (3.29) and (3.30) that our approximation in (3.26) is highly efficient in the sense that as n increases both* ϵ^+ *and* ϵ^- *(and thus* ϵ_P*) approach to zero exponentially.*

Based on Theorem 3 and Lemma 7, we now can establish the following result regarding the throughput capacity under the NNT scheme.

Theorem 4. *For the concerned A-MANET with n mobile nodes, transmission probability q and guard factor* $\Delta > 0$*, its throughput capacity* μ_{NNT} *under the NNT scheme can be approximated as*

$$\begin{aligned} \mu_{NNT} \approx \widehat{\mu}_{NNT} &= \frac{n}{2(n-1)}\widehat{P}_S \\ &= \begin{cases} \frac{n\pi q(1-q)}{2(n-1)(\pi+q\cdot\Psi(\Delta))}, & \text{if } 0<\Delta<1 \\ \frac{nq(1-q)}{2(n-1)(1+2\Delta q+\Delta^2 q)}, & \text{if } \Delta\geq 1 \end{cases} \end{aligned} \tag{3.31}$$

and the corresponding approximation error $\epsilon_\mu = \mu_{NNT} - \widehat{\mu}_{NNT}$ *is determined as*

$$\epsilon_\mu = \frac{n}{2(n-1)}\epsilon_P, \tag{3.32}$$

where $\Psi(\Delta)$ *is defined in (3.28) and* ϵ_P *is bounded by* ϵ^+ *and* ϵ^- *as shown in (3.27).*

Remark 3. *From Lemma 7 and Theorem 4 we can easily see that*

$$\lim_{n\to\infty} \mu_{NNT} = \lim_{n\to\infty} \widehat{\mu}_{NNT} = \frac{1}{2}\widehat{P}_S. \tag{3.33}$$

Thus, a constant throughput capacity is achievable under the NNT scheme even when n *grows to infinity. Notice that* $\frac{1}{2} < \frac{n}{2(n-1)} < 1$ *for* $n \geq 2$*, we can see from (3.32) that as* n *increases the approximation error* ϵ_μ *also approaches to zero exponentially.*

Remark 4. *Let* q^*_{NNT} *denote the optimal setting of* q *to achieve the* $\mu^*_{NNT} = \max_{q\in(0,1)} \widehat{\mu}_{NNT}$*. We can see from (3.31) that* q^*_{NNT} *and* μ^*_{NNT} *are determined as*

$$q^*_{NNT} = \begin{cases} \frac{\sqrt{\pi^2+\pi\cdot\Psi(\Delta)}-\pi}{\Psi(\Delta)}, & \text{if } 0 < \Delta < 1 \\ \frac{1}{2+\Delta}, & \text{if } \Delta \geq 1 \end{cases} \tag{3.34}$$

and

$$\mu^*_{NNT} = \begin{cases} \frac{n\pi}{2(n-1)\left[\Psi(\Delta)+2\left(\pi+\sqrt{\pi^2+\pi\cdot\Psi(\Delta)}\right)\right]}, & \text{if } 0 < \Delta < 1 \\ \frac{n}{2(n-1)(2+\Delta)^2}, & \text{if } \Delta \geq 1 \end{cases} \tag{3.35}$$

where $\Psi(\Delta)$ *is defined in (3.28).*

It is worth mentioning that (3.34) indicates that the optimal setting of q for capacity maximization is actually independent of the network size n.

3.4.3 STP and Capacity under NRT

Since the analysis of STP and capacity under the NRT scheme faces the same difficulty as that of the NNT scheme, we also provide here efficient approximations to them.

Following an argument similar to that of Lemma 7, we have the following lemma on the approximation of STP P_S under the NRT scheme.

Lemma 8. *In the considered A-MANET with n mobile nodes, transmission probability q and guard factor $\Delta > 0$, its STP P_S under the NRT scheme can be approximated as*

$$P_S \approx \widehat{P}_S = \frac{q(1-q)}{1+2\Delta q+\Delta^2 q}, \tag{3.36}$$

and the corresponding approximation error $\epsilon_P = P_S - \widehat{P}_S$ is upper and lower bounded as

$$\epsilon^- \leq \epsilon_P \leq \epsilon^+, \tag{3.37}$$

where

$$\epsilon^- = -\frac{q(1-q)}{1+2\Delta q+\Delta^2 q}\left(1-\frac{(1+2\Delta q+\Delta^2 q)\pi}{(2+2\Delta)^2}\right)^{n-1}, \tag{3.38}$$

$$\epsilon^+ = \begin{cases} \frac{q(1-q)}{1-q\left(1+\frac{\Psi(\Delta)}{(3+\Delta)^2-\pi}-\frac{\Psi(\Delta)-(1+\Delta)^2}{\pi}\right)}\left[\left(1-\frac{q\Psi(\Delta)}{(3+\Delta)^2-\pi}\right)^{n-1}\right. \\ \left.-\left(q-q\cdot\frac{\Psi(\Delta)-(1+\Delta)^2}{\pi}\right)^{n-1}\right] \\ -\frac{q(1-q)}{1+2\Delta q+\Delta^2 q}\left(1-\frac{(1+2\Delta q+\Delta^2 q)\pi}{(3+\Delta)^2}\right)^{n-1}, \\ \qquad\qquad\qquad\qquad \text{if } 0<\Delta<1 \\ q(1-q)\left[\left(1-q\cdot\frac{\pi(1+\Delta)^2-\pi}{(2+2\Delta)^2-\pi}\right)^{n-2}\left(1-\frac{\pi}{(2+2\Delta)^2}\right)^{n-1}\right. \\ \left.-\frac{1}{1+2\Delta q+\Delta^2 q}\left(1-\frac{(1+2\Delta q+\Delta^2 q)\pi}{(2+2\Delta)^2}\right)^{n-1}\right], \\ \qquad\qquad\qquad\qquad \text{if } \Delta\geq 1 \end{cases} \tag{3.39}$$

Proof. See Appendix A.2. □

Remark 5. *Lemma 8 indicates that $\lim_{n\to\infty} P_S = \widehat{P}_S$ under the NRT scheme. Similarly to Remark 2, we can see from (3.38) and (3.39) that our approximation in (3.36) is of high efficiency in the sense that as n increases both ϵ^+ and ϵ^- (and thus ϵ_P) approach to zero exponentially. It is also notable that for the scenario of $\Delta \geq 1$ both the NNT and NRT schemes results in the same result of STP. This is because that*

according to the protocol model in (3.1), in the case of $\Delta \geq 1$ *a non-nearest neighbor transmission can not be successfully received.*

Based on Theorem 3 and Lemma 8, we have the following result regarding the throughput capacity under the NRT scheme.

Theorem 5. *For the considered A-MANET with* n *mobile nodes, transmission probability* q *and guard factor* $\Delta > 0$*, its throughput capacity* μ_{NRT} *under the NRT scheme can be approximated as*

$$\mu_{NRT} \approx \widehat{\mu}_{NRT} = \frac{nq(1-q)}{2(n-1)(1+2\Delta q+\Delta^2 q)}, \tag{3.40}$$

and the corresponding approximation error $\epsilon_\mu = \mu_{NRT} - \widehat{\mu}_{NRT}$ *is determined as*

$$\epsilon_\mu = \frac{n}{2(n-1)}\epsilon_P \tag{3.41}$$

where ϵ_P *is bounded by* ϵ^+ *and* ϵ^- *as shown in (3.37).*

Remark 6. *From Lemma 8 and Theorem 5, we can easily see that*

$$\lim_{n\to\infty} \mu_{NRT} = \lim_{n\to\infty} \widehat{\mu}_{NRT} = \frac{1}{2}\widehat{P}_S \tag{3.42}$$

Similar to Remark 3, we can see the approximation error ϵ_μ *in (3.41) will approach to zero exponentially as* n *increases.*

Remark 7. *Let* q^*_{NRT} *denote the optimal setting of* q *to achieve* $\mu^*_{NRT} = \max\limits_{q\in(0,1)} \widehat{\mu}_{NRT}$*, we can see from (3.40) that* q^*_{NRT} *and* μ^*_{NRT} *are determined as*

$$q^*_{NRT} = \frac{1}{2+\Delta} \tag{3.43}$$

and

$$\mu^*_{NRT} = \frac{n}{2(n-1)(2+\Delta)^2}. \tag{3.44}$$

3.5 Numerical Results and Discussions

In this section, we first provide simulation results to validate the theoretical models developed in this chapter, and then apply these models to illustrate the performance of A-MANETs under different settings of system parameters.

3.5.1 Simulation Setting

For model validation, a simulator was developed to simulate the packet delivery process under Algorithm 2 and system models defined in Section 3.2 [57]. A network scenario with transmission probability $q = 0.4$ and guard factor $\Delta = 0.2$ is considered in the simulation[2], where the throughput capacity, throughput and average end-to-end delay are measured as follows. To get the simulation results for throughput capacity, we first simulate $P_{\rm S}$ by focusing on a specified node and calculating the average number of successful transmissions conducted by the node per time slot over a time interval of 1.0×10^6 time slots, and then substitute the simulated $P_{\rm S}$ into (3.2). For the simulation of throughput and average end-to-end delay under Algorithm 2, we focus on a traffic flow and measure its throughput and average packet delay over a period of 1.0×10^7 time slots under a system load $\rho = \lambda/\hat{\mu}_{\rm NNT}$ or $\rho = \lambda/\hat{\mu}_{\rm NRT}$.

3.5.2 Model Validation

To validate the throughput capacity models developed for NNT and NRT schemes, we considered networks of different size n. The corresponding simulation results and theoretical ones are summarized in Fig. 3-4. We can see from Fig. 3-4 that the simulation results match nicely with the theoretical ones for both NNT and NRT schemes, which indicates that our models in (3.31) and (3.40) are highly efficient in approximating the throughput capacities of the concerned A-MANETs. Fig. 3-4 also shows that as n increases both the throughput capacity under the NNT or NRT scheme will converge to constant values, respectively. This observation agrees with

[2]Simulation under other scenarios can be conducted as well via our simulator.

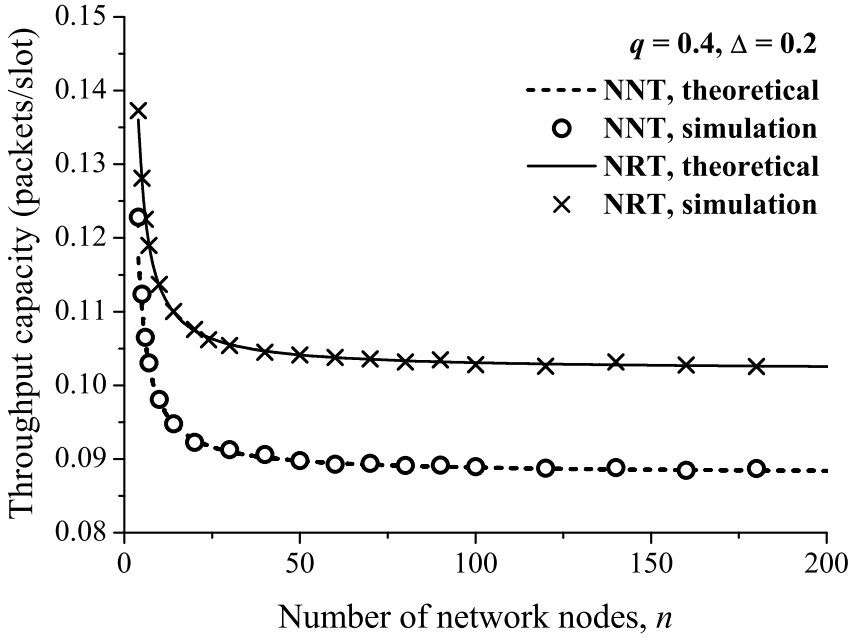

Figure 3-4: Throughput capacity vs. number of network nodes n.

the discussion of Remarks 3 and 6, and it shows that the considered A-MANET can provide a constant throughput capacity even as n grows to infinity.

To further validate the end-to-end delay model (3.11) and also the achievability of the throughput capacities under Algorithm 2, we conducted simulation for a network with $n = 32$ to measure its throughput and end-to-end packet delay under Algorithm 2 and different system load ρ. Fig. 3-5 shows the comparison between simulation and theoretical results on end-to-end packet delay[3], while Fig. 3-6 illustrates the simulation results of throughput and the corresponding theoretical results of throughput capacities $\hat{\mu}_{\mathrm{NNT}}$ and $\hat{\mu}_{\mathrm{NRT}}$. Fig. 3-5 indicates clearly that our theoretical model (3.11) is accurate and can efficiently capture the delay behavior under Algorithm 2. It is interesting to see from Fig. 3-6 that the throughput linearly increases as ρ increases from 0 to 1 and then approaches to $\hat{\mu}_{\mathrm{NNT}}$ or $\hat{\mu}_{\mathrm{NRT}}$ as ρ further increases beyond 1. The results in Fig. 3-6 show that just as proved in Section 3.3.2, the throughput

[3]The theoretical delay results for NNT and NRT schemes are obtained by substituting $\hat{\mu}_{\mathrm{NNT}}$ and $\hat{\mu}_{\mathrm{NRT}}$ into (3.11), respectively.

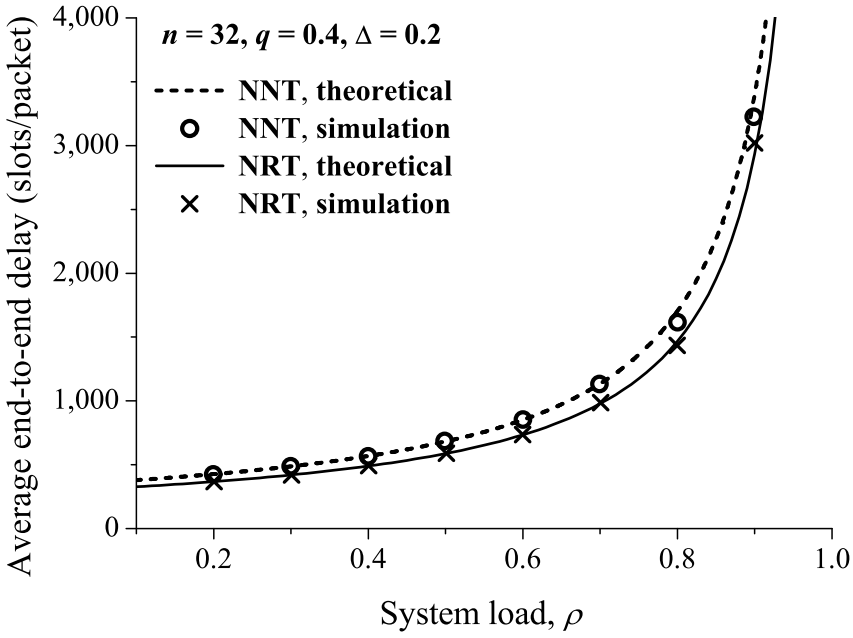

Figure 3-5: Average end-to-end delay vs. system load ρ.

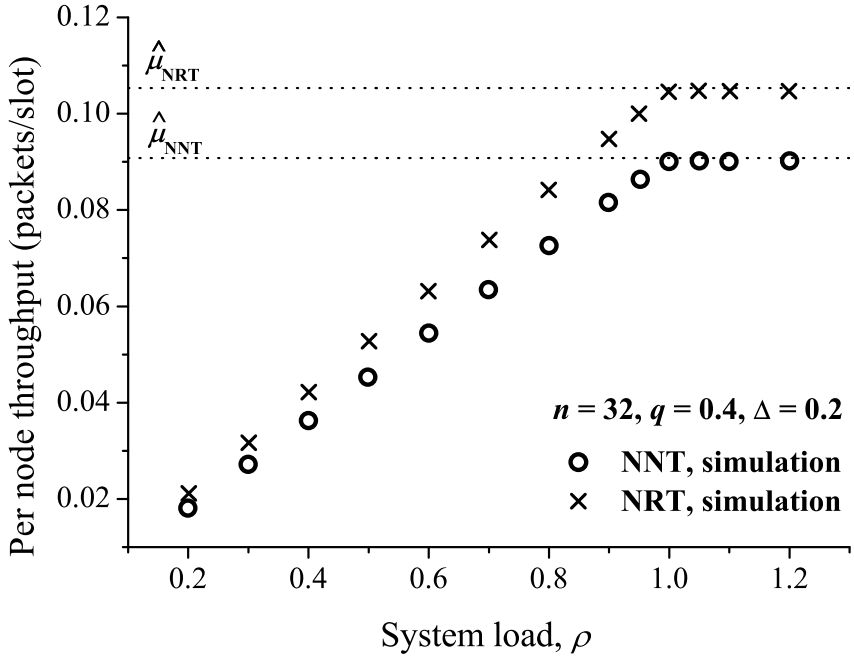

Figure 3-6: Throughput vs. system load ρ.

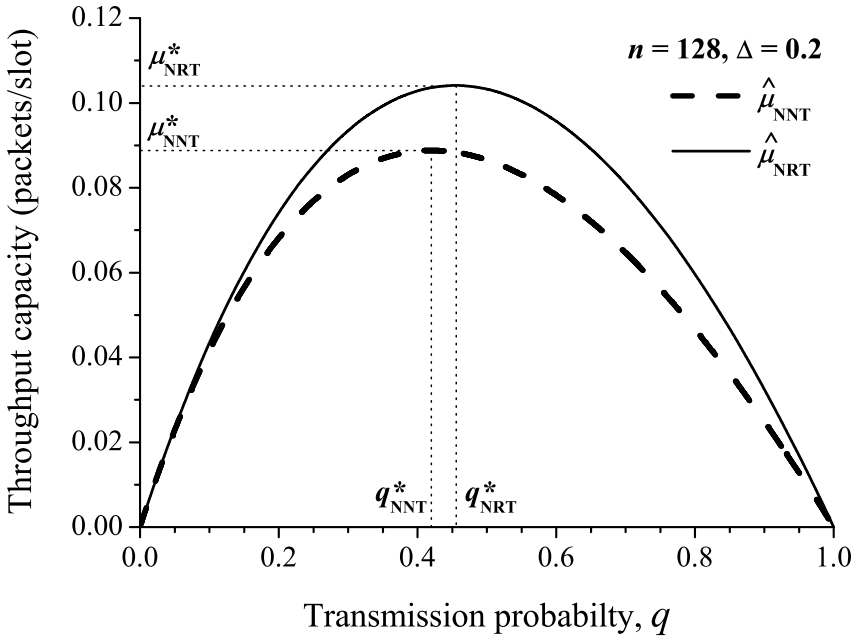

Figure 3-7: Capacity versus transmission probability q.

capacity of an A-MANET is achievable by adopting Algorithm 2 for routing in such a network.

3.5.3 Throughput Capacity

Based on our throughput capacity models, we first explore the impact of transmission probability q on the throughput capacity. We summarize in Fig. 3-7 how $\hat{\mu}_{\rm NNT}$ and $\hat{\mu}_{\rm NRT}$ vary with q in a network with $n = 128$ and $\Delta = 0.2$. It can be observed from Fig. 3-7 that as q increases both $\hat{\mu}_{\rm NNT}$ and $\hat{\mu}_{\rm NRT}$ first increase and then decrease, and just as discussed in Remarks 4 and 7 that there exists an optimal setting of q to achieve the maximum capacity $\mu^*_{\rm NNT}$ or $\mu^*_{\rm NRT}$. This is mainly due to the reason that the effects of transmission probability q on throughput capacity are two folds. In one hand, a higher transmission probability will result in a larger number of simultaneous transmissions, but on the other hand, a higher transmission probability will lead to a lower probability that a transmission is successfully received. It is also interesting

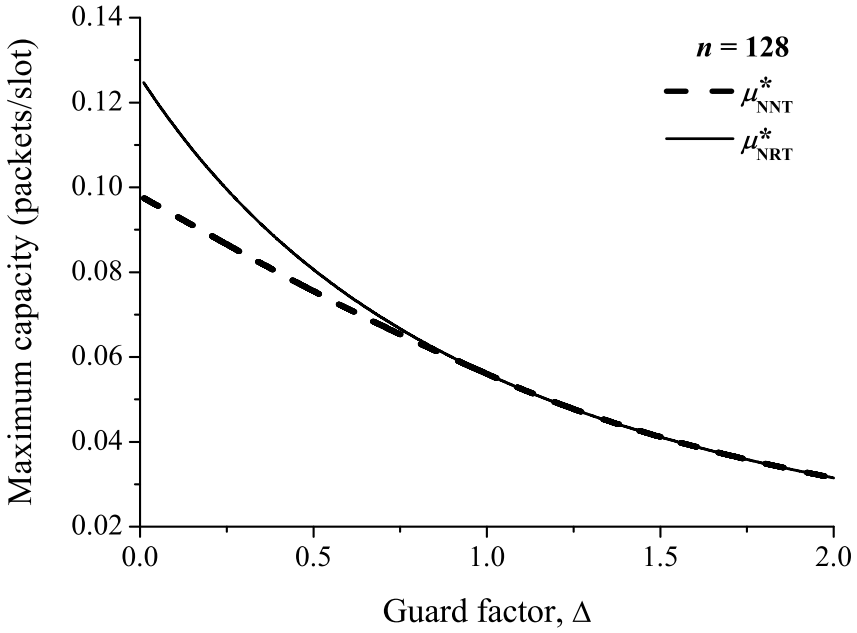

Figure 3-8: Maximum capacity versus guard factor Δ.

to see from Fig. 3-7 that for a given setting of q the throughput capacity under the NRT scheme is always higher than that under the NNT scheme. This is because that under the NRT scheme a transmitter will try to find some other node as its receiver if the nearest neighbor is not available, so in comparison with the NNT scheme more transmission opportunities can be obtained under the NRT scheme.

To understand the impact of Δ on the maximum capacities, we summarize in Fig. 3-8 how $\mu^*_{\rm NNT}$ and $\mu^*_{\rm NRT}$ vary with Δ in a network of $n = 128$. We can see from Fig. 3-8 that as Δ increases both $\mu^*_{\rm NNT}$ and $\mu^*_{\rm NRT}$ monotonously decrease. This is mainly due to the reason that under the protocol model defined in (3.1), a larger value of Δ will lead to a lower probability that a transmission is successfully received and thus a smaller capacity. Another observation of Fig. 3-8 is that as Δ increases the gap between $\mu^*_{\rm NNT}$ and $\mu^*_{\rm NRT}$ quickly vanishes and becomes zero when Δ is larger than 1. This is because that under the NRT scheme, increasing Δ will lead to a decrease in the successful probability of the non-nearest neighbor transmissions and thus a reduction in the capacity improvement $\mu^*_{\rm NRT} - \mu^*_{\rm NNT}$. Specifically, as discussed

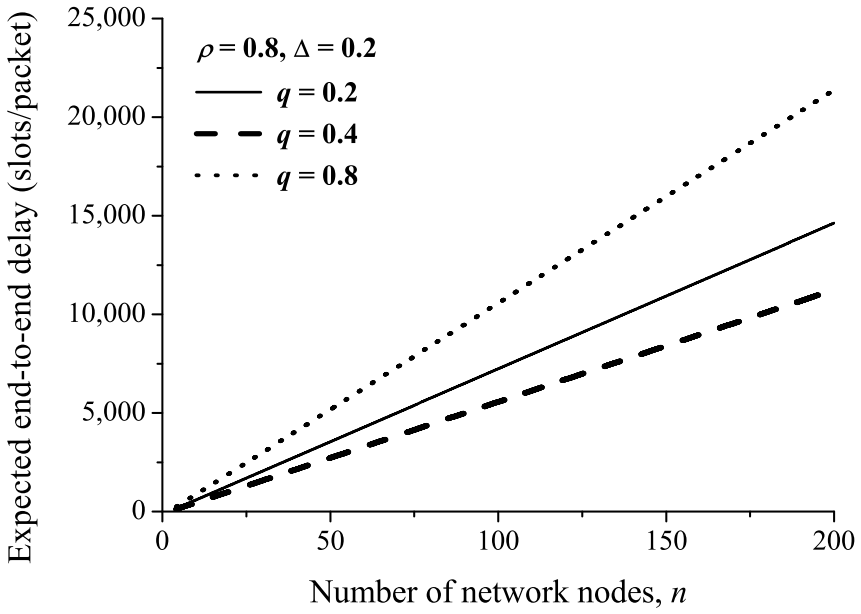

Figure 3-9: Expected end-to-end delay $\mathbb{E}\{D\}$ vs. number of network nodes n under the NNT scheme.

in Remark 5 that when Δ increases beyond 1, the successful probability of non-nearest neighbor transmissions becomes zero and thus no capacity improvement can be obtained by adopting the NRT scheme.

3.5.4 End-to-End Delay

The results in Fig. 3-4 indicate that a constant throughput capacity is achievable even in a large scale A-MANET. To understand the corresponding delay overhead to achieve such a constant capacity, we examine in Fig. 3-9 how the expected end-to-end delay under the NNT scheme varies with network size n for the settings of $\rho = 0.8$, $\Delta = 0.2$ and $q = \{0.2, 0.4, 0.8\}$[4]. We can see from Fig. 3-9 that for a given setting of ρ, Δ and q, the end-to-end delay increase linearly as n increases. The results in Figs. 3-4 and 3-9 indicate that as network size increases a constant throughput capacity can be achieved in an A-MANET at the cost of a linearly increasing end-to-end delay.

[4]The delay performance under the NRT scheme is similar, so we provide here only the result of NNT for illustration.

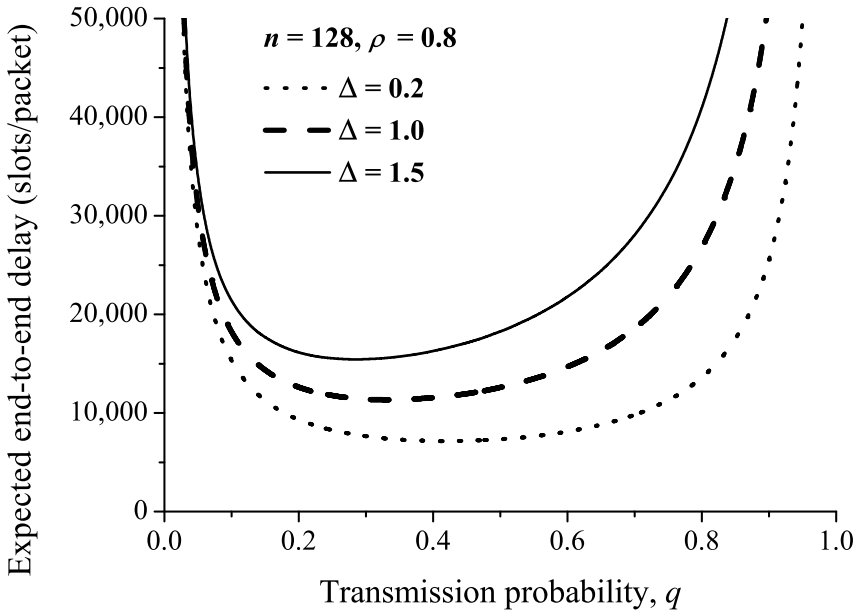

Figure 3-10: Expected end-to-end delay $\mathbb{E}\{D\}$ vs. transmission probability q under the NNT scheme.

Fig. 3-9 also indicates that for a given network size, the delay behavior may dramatically change with the setting of q. To further explore the effect of q on delay performance, we summarize in Fig. 3-10 how the expected end-to-end delay varies with q under the settings of $n = 128$, $\rho = 0.8$ and $\Delta = \{0.2, 1.0, 1.5\}$. Fig. 3-10 shows that for a given setting of n, ρ and Δ, as q increases the delay first decreases and then increases; while for a given setting of n, ρ and q, the delay monotonously increases as Δ increases. The main reason behind these behaviors is that as shown in (3.11) the end-to-end delay is inversely proportional to the capacity, so the relationship between delay and (q, Δ) is just reverse to the the relationship between capacity and (q, Δ) shown in Fig. 3-7 and Fig. 3-8.

3.6 Summary

This chapter first revealed the inherent relationship between the throughput capacity of an A-MANET and per node successful transmission probability in it, and then

developed a theoretical framework for efficient and closed-form approximations of the exact throughput capacity in an A-MANET under the NNT and NRT, two typical local transmission schemes. The expected end-to-end delay under a capacity achieving routing algorithm was also derived. It is expected the theoretical framework developed in this chapter will be helpful for exploring A-MANET throughput capacity under other transmission schemes as well. The results in this chapter indicate that even in large scale A-MANETs a constant throughput capacity can still be guaranteed at the cost of a linearly increasing end-to-end delay with network size. Another interesting finding of this chapter is that for throughput capacity maximization in A-MANETs, the corresponding optimal setting of transmission probability in ALOHA protocol only dependents on guard zone parameter Δ and thus can be fixed for A-MANETs with different network size.

THIS PAGE INTENTIONALLY LEFT BLANK

Chapter 4

Throughput Analysis in MANETs with Directional Antennas

4.1 Introduction

This chapter studies the achievable throughput of a cell-partitioned MANET, where each node is equipped with a directional antenna for transmission and a group-based scheduling is adopted for MAC. A directional antenna is an antenna that transmits/receives radiation power more efficiently in some directions than in others. Due to its merits like high energy efficiency, low interference and long transmission range, it is expected that using directional antennas in MANETs will provide a significant performance improvement.

4.1.1 Available Studies on Achievable Throughput with Directional Antennas

Many research efforts have been made to empirically investigate the throughput for wireless ad hoc networks using directional antennas. Ramanathan [58] simulated a 40 node network and showed that an improvement of up to 118% in throughput can be achieved by adopting directional antennas. Liu *et al.* [59] built a nine node testbed and showed that it is possible to improve the indoor network throughput by

coordinating the orientation of the directional antennas equipped in network nodes.

The achievable throughput of directional antenna-based wireless ad hoc networks has also been analytically studied in the literature. Spyropoulos and Raghavendra investigated the asymptotic throughput scaling behaviors of wireless ad hoc network for various kinds of directional antenna and communication models in [60, 61]. Based on the typical framework developed in [1], Yi *et al.* [62, 63] assumed a *sender-based* protocol model and showed that under the considered network scenario the throughput improvement compared to the omnidirectional network is $2\pi/\sqrt{\alpha\beta}$ in random networks and is $4\pi^2/\alpha\beta$ in arbitrary networks, where α and β are the antenna beamwidths for transmission and reception, respectively. By introducing a new directional protocol model in [64], Li *et al.* provided an upper bound of $O(\sqrt{\log n/n})$ and a lower bound of $\Omega(1/\sqrt{n \log n})$ on the maximum achievable throughput of random networks with multihop relay schemes, where n is the number of nodes randomly distributing in a disk network of unit area. The studies of network throughput improvement by using directional antennas have also been extended to flow networks [65], multi-channel wireless networks [66] and hybrid wireless networks with infrastructures support [67–69].

4.1.2 Limitations of Available Studies

It is notable that the available studies discussed above mainly focus on the throughput analysis in wireless ad hoc network with directional antennas, and to the best of our knowledge, the throughput analysis of MANETs with directional antennas is still an unexplored issue. Another common limitation of the above works is that they only explored the order sense behaviors of achievable throughput. Recently, Liu *et al.* [70, 71] developed a theoretical framework to analyze the achievable throughput in a cell-partitioned MANET with group-based MAC scheduling and omnidirectional antennas. They studied in [70] the achievable throughput of cell-partitioned MANETs under a general two-hop relay algorithm with packet redundancy limit f (2HR-f) for packet routing, and further explored in [71] the impact of transmission power constraint on the achievable throughput therein. In this chapter, we study the achievable throughput of a cell-partitioned MANET in which each mobile node is equipped with

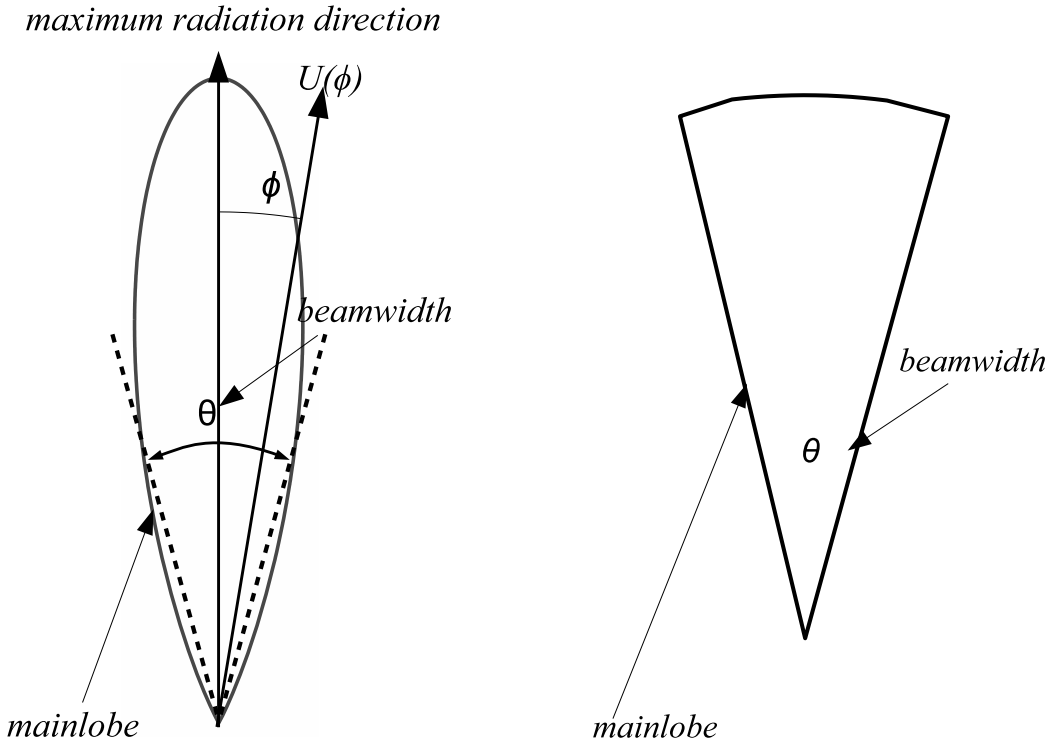

(a) Realistic antenna model (b) Ideal antenna model

Figure 4-1: Directional antenna models.

a directional antenna for transmission and the general 2HR-f algorithm is adopted for packet routing.

4.1.3 Chapter Outline

The rest of the chapter is organized as follows. In Section 4.2 and 4.3, we introduce the system models and the two hop relay routing algorithm under study. Section 4.4 presents the main results on achievable throughput and related throughput optimization problem. The numerical results and associated discussions are provided in Section 4.5. We finally summarize this chapter in Section 4.6.

4.2 System Model

4.2.1 Directional Antenna Model

Directional antennas have the property of radiating electromagnetic waves more effectively in some directions than in others. In this chapter, we consider that the directional antenna consists of a mainlobe which represents the main intended radiation directions. Sidelobes are ignored for the reason that they usually indicate radiation in undesired directions and the antenna gain in them is too small in comparison with that in the mainlobe [66]. *Beamwidth* is an important parameter to character the mainlobe and in this chapter we refer the beamwidth to the half-power beamwidth, which is defined as the angle between the two directions in which the radiation intensity is one-half value of the maximum radiating direction. The antenna gain (in a given direction) is defined as the ratio of the radiation intensity in a given direction to the radiation intensity of an ideal isotropically antenna, whose radiation intensity is given by $\eta P_{rad}/4\pi$, where P_{rad} is the total radiation power over all directions and η is the antenna efficiency which is fixed to be 1 in this chapter. In this chapter, we consider two antenna models: a realistic antenna model and an ideal antenna model.

Realistic antenna model: For the realistic antenna model, we consider that the antenna gain is a function of the radiation angle ϕ with respect to the maximum radiation direction. Formally, the antenna gain $G(\phi)$ in direction ϕ can be expressed as:

$$G(\phi) = \frac{4\pi U(\phi)}{\eta P_{rad}} \tag{4.1}$$

where $U(\phi)$ is the radiation intensity. An example of a directional antenna with realistic radiation pattern is provided in Fig.4-1a.

Ideal antenna model: For the ideal antenna model [62, 66, 72], we consider that the directional antenna is approximated as a circular sector of angle θ by assuming that the radiation power within the beamwidth θ is uniformly distributed and that the radiation outside the beamwidth is neglected, where $0 < \theta \leq 2\pi$. In this model,

the antenna gain G_m is a constant in the mainlobe and can be calculated by taking the average antenna gain over the beamwidth. An example of the ideal antenna model is plotted in Fig. 4-1b.

Since it is difficult to character directional antennas with variable antenna gain in throughput analysis, we use the ideal antenna model in the theoretical study as previous works [62, 63, 66–68] for simplicity. The analysis result with the ideal antenna model will be compared with a more realistic achievable performance obtained from simulation with the realistic antenna model in Section 4.5. The antenna gain G_m of the ideal antenna model can be derived as follows [73]:

Let P_θ be the total radiation power within beamwidth θ, we have

$$P_\theta = \int_0^{2\pi} \int_0^{\frac{\theta}{2}} U(\phi) \sin\phi d\phi d\sigma$$

Therefore, the average radiation intensity U_m in the mainlobe is

$$U_m = \frac{P_\theta}{\int_0^{2\pi} \int_0^{\frac{\theta}{2}} \sin\phi d\phi d\sigma}$$

The antenna gain G_m in the ideal directional antenna model can be derived by substituting U_m into (4.1).

Additionally, we consider a steerable antenna, i.e., each node can beamform its antenna in any desired direction. Therefore, the probability that the mainlobe of a node covers a direction is given by $\theta/2\pi$ [27, 66–68, 74].

4.2.2 Network and Power Propagation Model

Similar to the previous studies [3, 20, 70, 71], we consider a two-dimensional torus network with unit area and n mobile nodes. We assume that the time is slotted and the network is evenly divided into $m \times m$ cells with $1/m^2$ area each,as illustrated in Fig. 4-2. Furthermore, we consider that each node moves independently from one cell to another, following the bi-dimensional i.i.d mobility model [3, 75, 76]. Under the mobility model, each node first independently and uniformly chooses one cell over all

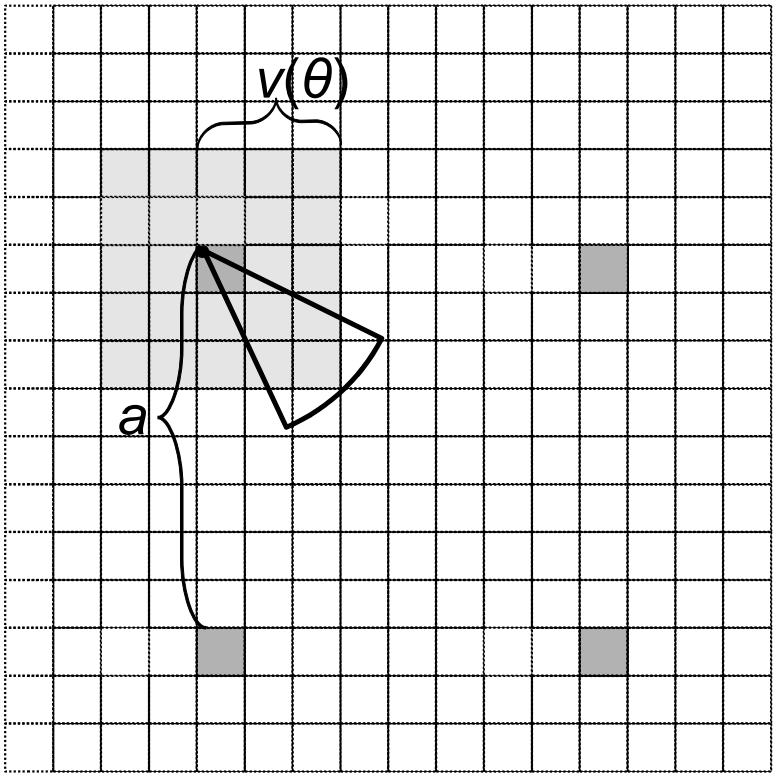

Figure 4-2: Cell-partitioned network model.

m^2 cells at the beginning of every time slot and stays in it for the whole slot. We also assume that during each time slot every node has the knowledge about which cell it is located in based on localization techniques, such as GPS.

To predict the received signal at the receiver, we employ a general power propagation model [77]:

$$P_r = \frac{P_t C G_t G_r}{d^\alpha} \tag{4.2}$$

where P_t and P_r are the transmitted and received power levels, respectively, G_t and G_r are the gain factors for the transmitting and receiving antennas, respectively, C is a constant determined by antenna heights, wave length, and so on, d is the distance between the transmitter and receiver, and α is the path loss exponent which is greater than 2 in most cases.

4.2.3 Communication Model

We assume that all the nodes transmit at the same nominal power and the transmission data rate is uniform for all transmissions such that the total number of bits that can be transmitted per time slot is fixed and normalized to one packet. For the transmission and reception scenario, we consider that the transmission is directional and the reception is omnidirectional [72], since in MANETs receivers usually have no knowledge of which direction the transmission will come from, and therefore they overhear omnidirectionally.

To characterizing interference issue, we consider an interference model [78] in the analysis. Suppose that at some time slot a node T_i is trying to transmit to a node R_i, this transmission can be successful if and only if the following conditions hold:

(1) T_i's mainlobe covers R_i;

(2) $|T_i - R_i| \leq r(\theta)$;

(3) $|T_k - R_i| \geq (1 + \Delta)\, r(\theta)$ for every other node T_k that simultaneously transmits with the node T_i, where $\Delta > 0$ is a specified guard-factor for interference prevention.

We notice that in realistic communication, the *signal-to-interference ratio* (SIR) is the measure usually used to determine whether a transmission is successful. To simplify the analysis, we consider an optimal transmission range $r(\theta)$ within which the transmission is high enough such that the transmission is successful with a high probability, as previous studies [62, 66, 70, 79]. Since we adopt a cell-partitioned network and to simplify the analysis, we will use $v(\theta)$ to approximate $r(\theta)$ as previous study [71] such that each node can cover a set of cells that have a horizontal and vertical distance of no greater than $v(\theta) - 1$ cells away from its current cell as illustrated in Fig. 4-2 and $v(\theta)$ can be determined as

$$v(\theta) = min\left\{\lfloor (m+1)/2 \rfloor, \lfloor m \cdot r(\theta)/\sqrt{2} \rfloor\right\}. \tag{4.3}$$

4.2.4 Traffic Model

We also assume the permutation traffic pattern [2, 3] to model the traffic flows in the network. The traffic originated from each node is assumed to have a average rate λ (packets/slot). Note that each packet arrives at the beginning of time slots and this process is independent of the mobility process. The impact of limitation on packet life time and buffer space is ignored for analysis simplicity.

4.3 Group-Based Transmission Scheduling and Two-hop Relay Routing Algorithm

In this section, we introduce the transmission scheduling and routing schemes considered in this chapter.

4.3.1 Transmission-Group Based Scheduling

To support as many simultaneous transmissions as possible based on the interference model, we adopt a transmission-group based scheduling scheme similar to those in [80–82].

Transmission-Group: A transmission-group (see Fig. 4-2 for an example) is a subset of cells where any two cells have a vertical and horizontal distance of some multiple of a cells such that all the cells there can safely transmit simultaneously. It is clear to see that all the cells can be divided into a^2 transmission groups. By letting all the transmission-groups alternatively be active (i.e., get the transmission opportunity), then each cell can be active in every a^2 time slots. According to the considered communication model, the parameter a must satisfy

$$\frac{1}{m}(a - v(\theta)) \geq (1 + \Delta)r(\theta) \tag{4.4}$$

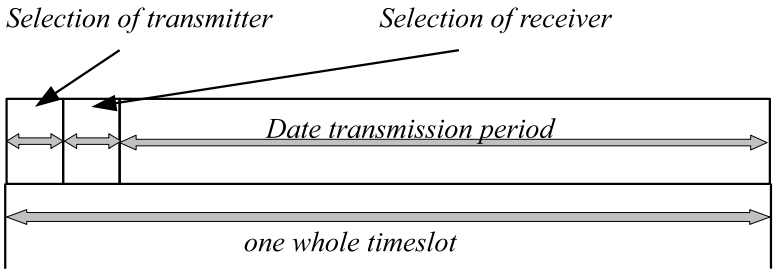

Figure 4-3: Partition of a time slot.

Since a is an integer and $a \leq m$, then we can set a as

$$a = min\{v(\theta) + \lceil m(1+\Delta)r(\theta) \rceil, m\} \tag{4.5}$$

To address the competition of transmission and reception, we consider a transmitter selection and a receiver selection mechanism, which are conducted at the beginning of each time slot as illustrated in Fig. 4-3. The durations of these periods are fixed.

Selection of Transmitter: In order to guarantee that only one transmitter is randomly selected from all the nodes in an active cell, we adopt a mechanism similar to the IEEE 802.11 DCF. The IEEE 802.11 DCF employs a CSMA/CA with a random backoff algorithm and is the fundamental MAC technique used in IEEE 802.11 WLAN standards. We adopt the idea of random backoff counting from the IEEE 802.11 DCF to address the competition issue in our scheduling. Notice that during the competition for transmitting opportunity, all the nodes in an active cell work omnidirectionally to broadcast and overhear until the transmitter is selected. At the beginning of each time slot, each node independently judge weather it is inside an active cell or not. If not, it remains silent during the transmitter selection period. Otherwise, it starts a back-off counter with a seed randomly selected from $[0, CW]$ (where CW represents the contention window), and overhears the channel until its back-off counter becomes 0 or it hears a broadcasting message from a transmitter. If no broadcasting message is heard before the back-off counter approaches 0, the node broadcasts out a message to other nodes denoting itself as the transmitter. Other nodes in the active cell will stop back-off counting and quit transmitting contention after they hear the transmitter's claim. Based on the back-off counting mechanism, each node of an active cell has the

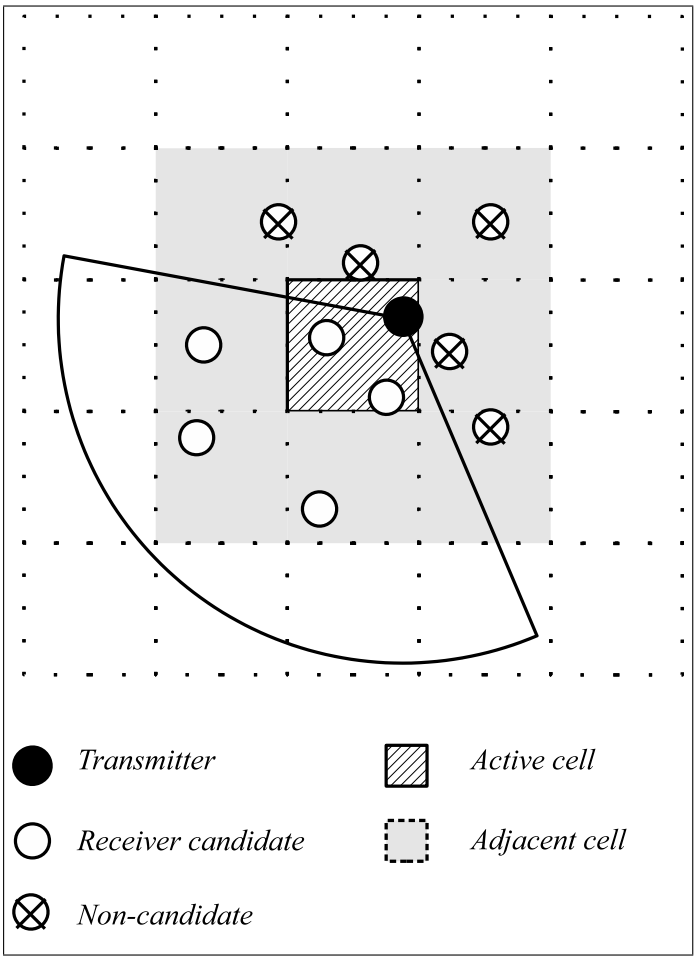

Figure 4-4: Illustration of receiver contention.

same probability to win the transmitting opportunity.

Remark 8. *Please notice that there are two main differences between our scheme and the IEEE 802.11 DCF. First, the conditions to start a random back off counting are different. In the IEEE 802.11 DCF, a node senses the channel before transmitting and starts a random backoff counter if the channel is busy; in our mechanism, a node starts a random backoff counter if it comes into an active cell. Second, the conditions to terminate backoff counting and the behaviors of nodes when its backoff counting ends are different. In the IEEE 802.11 DCF, when the backoff counter of a node becomes* 0*, the node will sense the channel again and starts a new backoff counting if the channel is still busy; in our mechanism, the node will stop backoff if it overhears a claim of being the transmitter from some other node in the same active cell before its counter approaches* 0*, otherwise it will claim itself as the transmitter when its counter reaches* 0*.*

After the selection of transmitter, each transmitter will change to directional mode with a random beamforming direction. The transmitter will directionally broadcast a receiver-request message to start the receiver contention period.

Selection of Receiver: According to the directional antenna model, a node can receive the request from the transmitter if and only if it is covered by the transmitter's directional antenna as illustrated in Fig. 4-4. If the destination node of the transmitter is a receiver candidate, it will respond to the transmitter immediately by sending a message after it. Other candidate receivers will start a back-off counting and overhearing mechanism similar to that of the transmitter selection. The transmitter chooses the one whose reply arrives first as the receiver. Accordingly, if the destination node of the transmitter is a receiver candidate, it will be definitely selected as the receiver; otherwise, each candidate receivers has the same probability to become a receiver.

4.3.2 Routing Algorithm

In this chapter, we employ the two-hop relay algorithm with packet redundancy f (2HR-f) [3] for packet routing, where $1 \leq f \leq n-2$. We briefly summarize the 2HR-f as follows: When the source S wins the transmission opportunity at the current time slot, the S first broadcasts a message to request a receiver.

1. If its destination D can hear this message, then it will reply to S immediately. If the S receives the reply from the D, it selects D as the receiver and transmits to D the packet D is requesting (Source-to-Destination transmission).

2. If no reply from D is received by S, a random receiver (say R) is selected among all the candidate nodes based on the mechanism discussed in Section 4.3.1. With 1/2 probability, the S and R conduct either Source-to-Relay or Relay-to-Destination transmission:

    - Source-to-Relay: Assume that the S is delivering packet P at the current time slot. If R does not have a copy of P, then S transmits a copy of P to R; otherwise, the S remains idle for this time slot.
    - Relay-to-Destination: In this transmission, the S performs as a relay node to help deliver the traffic whose destination is R. The S checks if it has a copy of the packet that R is requesting. If so, the S transmits the packet to R; otherwise, the S remains idle for this time slot.

In this algorithm, the total number of hops from a source to its destination is no more than 2, the number of the overall copies of one packet distributed by the source is no more than $f+1$ (including the original one in S), and the packets of a traffic flow should arrive at its destination in order. According to the permutation traffic model, there are n distinct traffic flows in the network. Without loss of generality, we focus on one traffic flow in our discussion and denote its source node and destination node as S and D, respectively. Other nodes can perform as relay nodes to help the source to deliver the packets to the destination. As a result, the destination D can

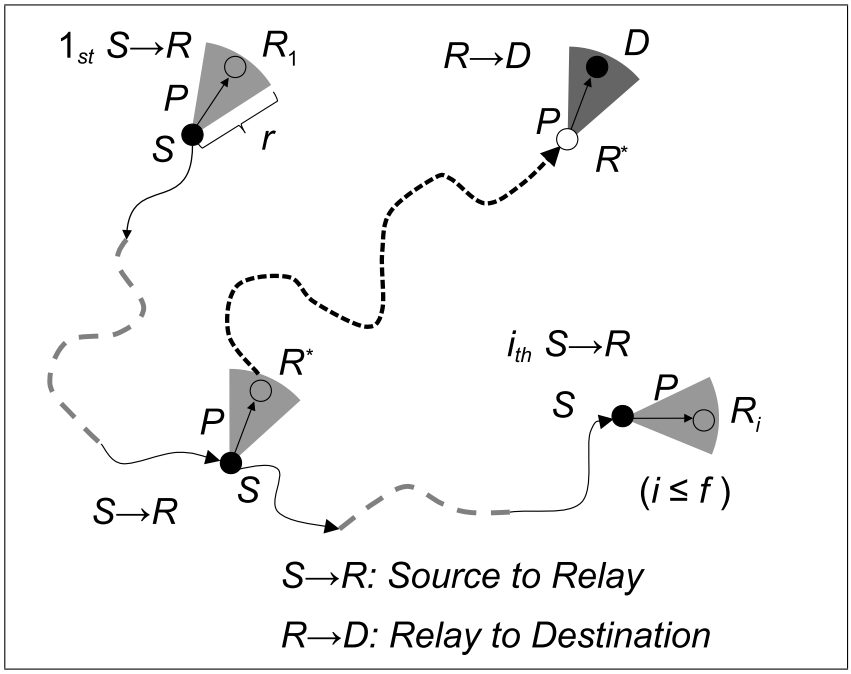

Figure 4-5: Illustration of the 2HR-f relay.
The figure presents the packet delivery process of a given packet P of a tagged flow delivered from the source S to the destination D through a relay node R^*. The dashed lines indicate the movement of nodes.

obtain the packet either from S or from one of the relay nodes. An example of the routing process is illustrated in Fig. 4-5.

4.4 Throughput Analysis

In this section, we first derive the directional transmission range under given transmission power. We then analyze some basic probabilities and establish Markov chains to model the packet distribution and reception processes at the source node and destination node, respected. Based on the expected service time obtained from the Markov chains and automatic feedback theory, the result on the achievable throughput can be derived in our considered networks. Finally, we explore the throughput optimization problem based on the result of the achievable throughput. We establish the following Lemmas and Theorem (please refer to A for proofs).

4.4.1 Communication Range

If we use omnidirectional transmission range $r(2\pi)$ to represent the transmission power level as previous studies [83] and assume that an SNR threshold is required to determine the transmission range, then we have

Lemma 9. *In a MANET where the transmission is directional with beamwidth θ and the reception is omnidirectional, the transmission range $r(\theta)$ under given transmission power can be determined as*

$$r(\theta) = \left(\frac{2\pi}{\theta}\right)^{\frac{1}{\alpha}} r(2\pi) \tag{4.6}$$

where α is the pathloss exponent.

4.4.2 Some Basic Probabilities

We first define the probability that a node is beamformed by the other one as follows:

Definition 5. *For the two nodes, the probability that one node is beamformed by the other is defined as the probability that the line connecting them is covered by the mainlobe of the latter's.*

Based on Lemma 9, the transmission group parameter a can be determined by equation (4.5). In the following lemma, we derive the probabilities for a node to conduct different kinds of transmissions in the considered network based on basic sub-event analysis.

Lemma 10. *For a given time slot and a tagged flow in a MANET the transmission is directional with beamwidth θ and the reception is omnidirectional, we use $p_1(\theta)$ and $p_2(\theta)$ to denote the probability that the S conducts a Source-to-Destination transmission and the probability that the S conducts a Source-to-Relay or Relay-to-Destination*

transmission, respectively. Let $w = (2v(\theta) - 1)^2$, *we have*

$$p_1(\theta) = \frac{\theta}{2\pi a^2}\left\{\frac{wn - m^2}{n^2 - n} + \frac{m^2 - (w-1)n - 1}{n^2 - n}\psi_1^{n-1}\right\} \tag{4.7}$$

$$p_2(\theta) = \frac{1}{a^2}\left\{\frac{m^2}{n} + \frac{(m^2 - wn)\theta}{2\pi(n^2 - n)} - \frac{1}{n}\sum_{i=0}^{n-1}\psi_2^i\psi_3^{n-1-i} + \left(\frac{(wn - n - m^2 + 1)\theta}{2\pi(n^2 - n)} - \frac{m^2 - 1}{n}\right)\psi_1^{n-1}\right\} \tag{4.8}$$

where $\psi_1 = \frac{m^2-1}{m^2}$, $\psi_2 = \frac{2\pi m^2 - 2\pi - (w-1)\theta}{2\pi m^2}$ *and* $\psi_3 = \frac{2\pi m^2 - w\theta}{2\pi m^2}$.

For a given traffic flow, please notice that the probabilities $p_1(\theta)$ and $p_2(\theta)$ are independent of the number of copies of packets. The packet distribution process at the S and the packet reception process at the D for the packet P can be modeled by the Markov chains in Fig. 4-6, where the transition probabilities are formulated in the following lemma based on those obtained by Lemma 10.

Lemma 11. *For a given traffic flow, suppose that in the current time slot the source* S *is delivering copies of the packet* P *and at the same time the destination* D *is also requesting* P, *and there are already* j $(1 \leq j \leq f + 1)$ *copies of* P *in the network (including the one possessed by the* S*). For the next time slot, we use* $P_r(\theta, j)$ *to denote the probability that* D *will receive* P , $P_d(\theta, j)$ *to denote the probability that* S *will deliver a new copy of* P *(if* $j \leq f$*) and* $P_s(\theta, j)$ *to denote the probability that the above two events happen simultaneously. Then, we have*

$$P_r(\theta, j) = p_1(\theta) + \frac{j-1}{2\,(n-2)} \cdot p_2(\theta) \tag{4.9}$$

$$P_d(\theta, j) = \frac{n-j-1}{2\,(n-2)} \cdot p_2(\theta) \tag{4.10}$$

$$P_s(\theta,j)=\frac{(j-1)(n-j-1)(m^2-a^2)}{4m^2a^4}\cdot\left\{\frac{n-4}{n-2}\sum_{k=0}^{n-5}\binom{n-5}{k}f(k)\left[h(k)g(n-4-k)\right.\right.$$
$$\left.\left.+\left(1-\frac{\theta}{2\pi}\right)h(k+1)g(n-5-k)\right]+\frac{2}{n-2}\sum_{k=0}^{n-4}\binom{n-4}{k}f(k)h(k)g(n-4-k)\right\} \tag{4.11}$$

where

$$h(x) = \frac{9\left(\frac{2}{m^2}\right)^{x+1}-8\left(\frac{w-1}{m^2}\right)^{x+1}}{x+2} \tag{4.12}$$

$$f(x) = \frac{1}{x+1}\left[1-\left(1-\frac{\theta}{2\pi}\right)^{x+1}\right] \tag{4.13}$$

$$g(x) = \sum_{t=0}^{x}h(t)f(t)\left(\frac{m^2-2w}{m^2}\right)^{x-t} \tag{4.14}$$

4.4.3 Packet Distribution and Reception Process

Now, we introduce the corresponding definitions of service time as follows:

Definition 6. *For a general packet P of a given flow, its service time at the source S is defined as the time elapsed between the time slot when the S starts to deliver copies for the P and the time slot when the S stops distributing copies for the P; the service time at the destination D is defined as the time elapsed between the time slot when the D starts to request for the P and the time slot when the D receives the P.*

Assume that there are k copies of P in the network when the destination node starts to request for the packet of a given traffic flow, if we denote by $X_S(k)$ and $X_D(k)$ the corresponding service time of the packet at the source S and the destination D, respectively, from the Markov chain theory, we can see that the $X_S(k)$ is the time the Markov chain in Fig. 4-6a takes to become absorbed given that the chain starts from the state 1, and the $X_D(k)$ is the time the Markov chain in Fig. 4-6b takes to become absorbed given that it starts from the state k. Based on the transition probabilities of Lemma 11 and the Markov chains in Fig. 4-6, we have the following lemma on the expected service times at the S and the D.

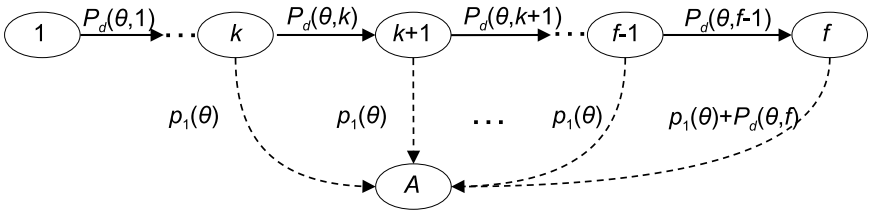

(a) Absorbing Markov chain for the packet distribution process at the source node S.

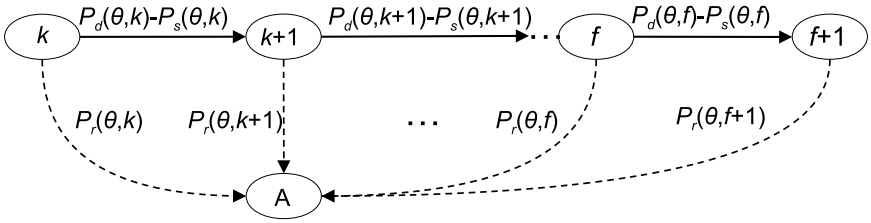

(b) Absorbing Markov chain for the packet reception process at the destination node D.

Figure 4-6: Absorbing Markov chains for a packet P of the tagged flow. Suppose that the destination node D starts to request for P when there are already k copies of P in the network. For each transient state, the transition back to itself is not shown for simplicity.

Lemma 12. *For a packet P of the given traffic flow in a MANET with directional antennas and exploiting 2HR-f routing algorithm, suppose that there are k copies of P in the network when the destination D states to request for the P, $1 \le k \le f+1$, then the expectation of service times $\mathbb{E}\{X_S(k)\}$ and $\mathbb{E}\{X_D(k)\}$ can be determined as*

$$\mathbb{E}\{X_S(k)\} = \begin{cases} \sum_{i=1}^{k-1} \frac{1}{P_d(\theta,i)} + \frac{1}{p_1(\theta)+P_d(\theta,k)} \\ \cdot \left(1 + \sum_{j=1}^{f-k} \varphi_1(k,j)\right) & \text{if } 1 \le k \le f \\ \sum_{i=1}^{k-1} \frac{1}{P_d(\theta,i)} & \text{if } k = f+1 \end{cases} \tag{4.15}$$

$$\mathbb{E}\{X_D(k)\} = \begin{cases} \frac{1}{P_r(\theta,k)+P_d(\theta,k)-P_s(\theta,k)} \big(1 + \sum_{j=1}^{f-k} \varphi_2(k,j) \\ + \frac{P_d(\theta,f)-P_s(\theta,f)}{P_r(\theta,f+1)} \varphi_2(k,f-k)\big) \\ & \text{if } 1 \le k \le f-1 \\ \frac{1+\frac{P_d(\theta,f)-P_s(\theta,f)}{P_r(\theta,f+1)}}{P_r(\theta,f)+P_d(\theta,f)-P_s(\theta,f)} & \text{if } k = f \\ \frac{1}{P_r(\theta,f+1)} & \text{if } k = f+1 \end{cases} \tag{4.16}$$

where

$$\varphi_1(k,j) = \prod_{t=1}^{j} \frac{P_d(\theta, k+t-1)}{p_1(\theta) + P_d(\theta, k+t)}$$
$$\varphi_2(k,j) = \prod_{t=1}^{j} \frac{P_d(\theta, k+t-1) - P_s(\theta, k+t-1)}{P_r(\theta, k+t) + P_d(\theta, k+t) - P_s(\theta, k+t)}$$

4.4.4 Achievable Throughput

For a mobile ad hoc network using directional antennas, we can establish the following theorem on its per node achievable throughput based on the expectations of service times of Lemma 12 and automatic feedback theory.

Theorem 6. *For a cell partitioned MANET, where nodes move under i.i.d. mobility model, each one is equipped with a directional antenna with beam-width θ ($0 \leq \theta \leq 2\pi$) for both transmission and reception, and the 2HR-f relay routing scheme ($1 \leq f \leq n-2$) is exploited. If we denote by $\mu(\theta, f)$ the maximum achievable per node (flow) throughput, i.e., the network can stably support any input rate $\lambda < \mu(\theta, f)$, then we have*

$$\mu(\theta, f) = min \left\{ p_1(\theta) + \frac{f}{2(n-2)} \cdot p_2(\theta) \,, \; \frac{p_1(\theta) + p_2(\theta)/2}{1 + \sum_{j=1}^{f-1} \prod_{t=1}^{j} \frac{(n-t-1)p_2(\theta)}{2(n-2)p_1(\theta) + (n-t-2)p_2(\theta)}} \right\} \tag{4.17}$$

$\mu(\theta, f)$ indicates the maximum per node input rate that the network can stably support. When the input rate is above $\mu(\theta, f)$, the average delay will tend to infinity which means that congestion will occur in somewhere of the network.

Remark 9. *Notice that when $\theta = 2\pi$, our results are reduced to the ones of the omnidirectional networks considered in [71].*

4.4.5 Throughput Optimization

From Theorem 6, we can see that the packet redundancy parameter f determines the per node achievable throughput in a given network. To explore the optimal achievable throughput for a given network, we formulate the following throughput optimization problem and obtain the optimal achievable throughput and corresponding f to achieve it in Lemma 13 based on the result of Theorem 6.

Throughput Optimization Problem: For a MANET using directional antennas with a fixed beamwidth θ for both transmission and reception and exploiting a 2HR-f relay routing scheme, calculate its optimal achievable throughput for any value of f. For a given beamwidth θ, if we denote the corresponding optimal achievable throughput by $\mu^*(\theta)$, it can be formulated as

$$\mu^*(\theta) \;=\; max\Big\{\mu(\theta, f) : 1 \le f \le n-2\Big\} \tag{4.18}$$

Lemma 13. *For any given $\theta \in [0, 2\pi]$, we have*

$$\mu^*(\theta) = max\Bigg\{p_1(\theta) + \frac{f}{2\,(n-2)} \cdot p_2(\theta)\Big|_{f_0}, \frac{p_1(\theta) + p_2(\theta)/2}{1 + \sum_{j=1}^{f-1} \prod_{t=1}^{j} \frac{(n-t-1)p_2(\theta)}{2(n-2)p_1(\theta)+(n-t-2)p_2(\theta)}}\Big|_{f_1}\Bigg\} \tag{4.19}$$

where

$$f_0 = max\Big\{f \Big| \mathbb{E}\{X_S(1)\} \le \mathbb{E}\{X_D(f+1)\}\Big\} \tag{4.20}$$

$$f_1 = min\Big\{f \Big| \mathbb{E}\{X_S(1)\} \ge \mathbb{E}\{X_D(f+1)\}\Big\} \tag{4.21}$$

Lemma 13 indicates that for a MANET with a given beamwidth θ, as the redundancy parameter f increases, the maximum achievable per node throughput $\mu(\theta, f)$ will first increase and then decrease, and therefore there exists an optimal f to achieve the optimal achievable per node throughput $\mu^*(\theta)$.

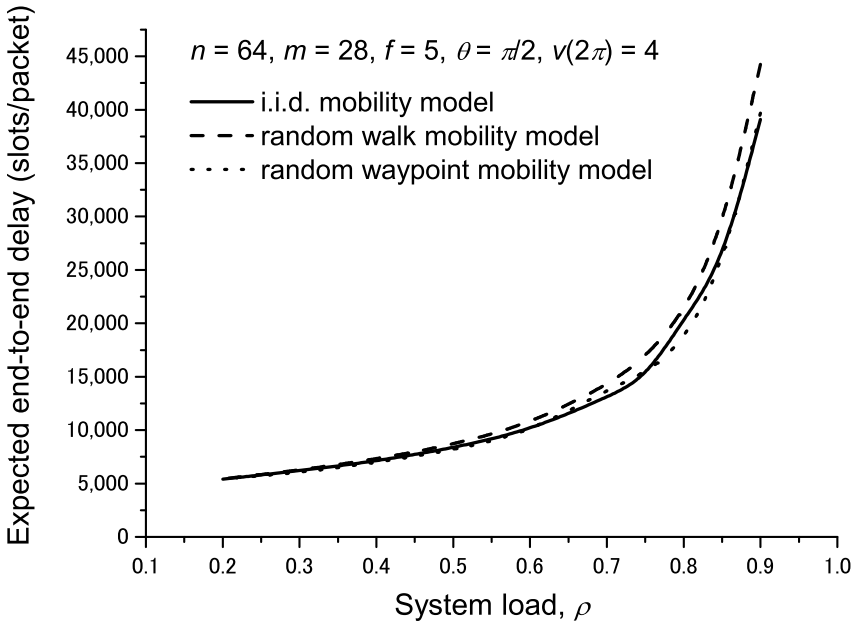

(a) Network scenario 1

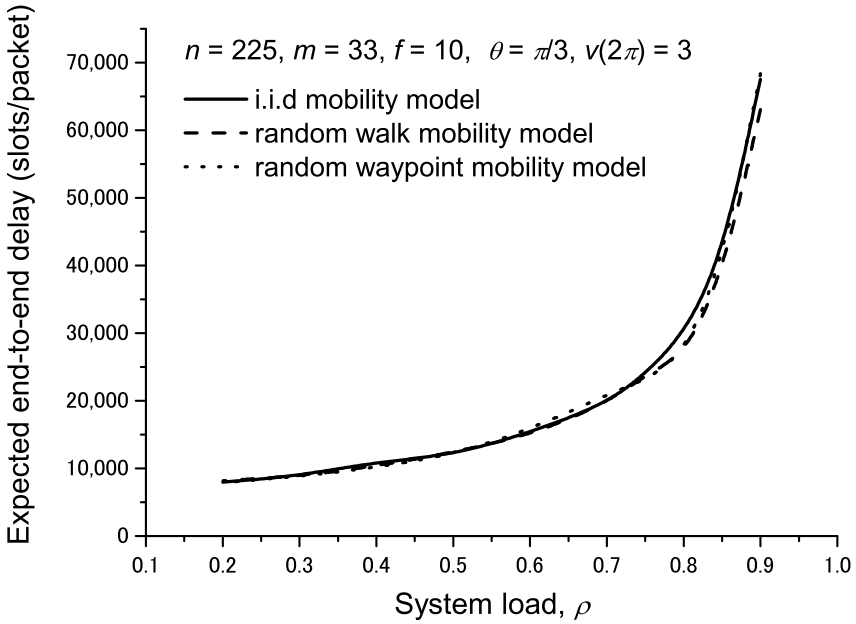

(b) Network scenario 2

Figure 4-7: The expected end-to-end delay vs. system load $\rho = \lambda/\mu(\theta, f)$.

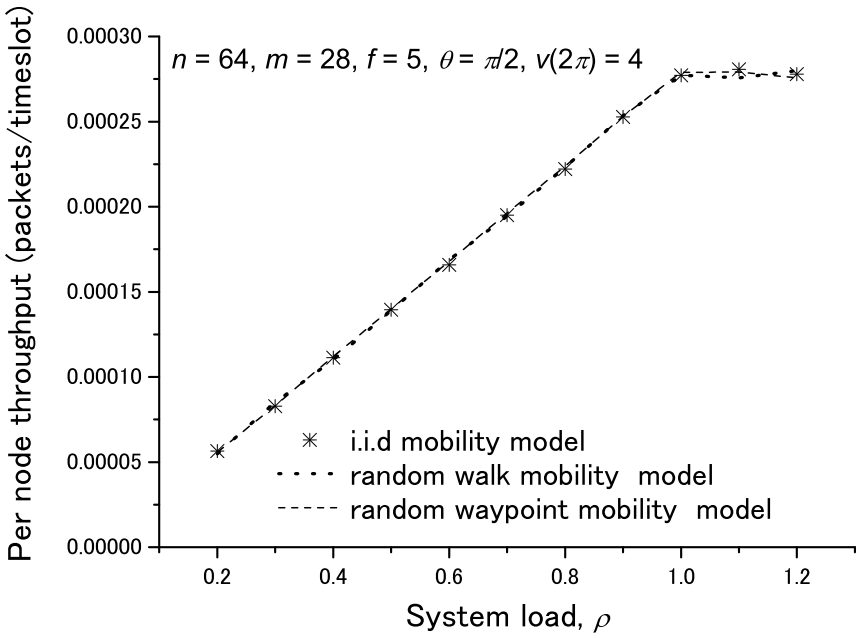

(a) Network scenario 1

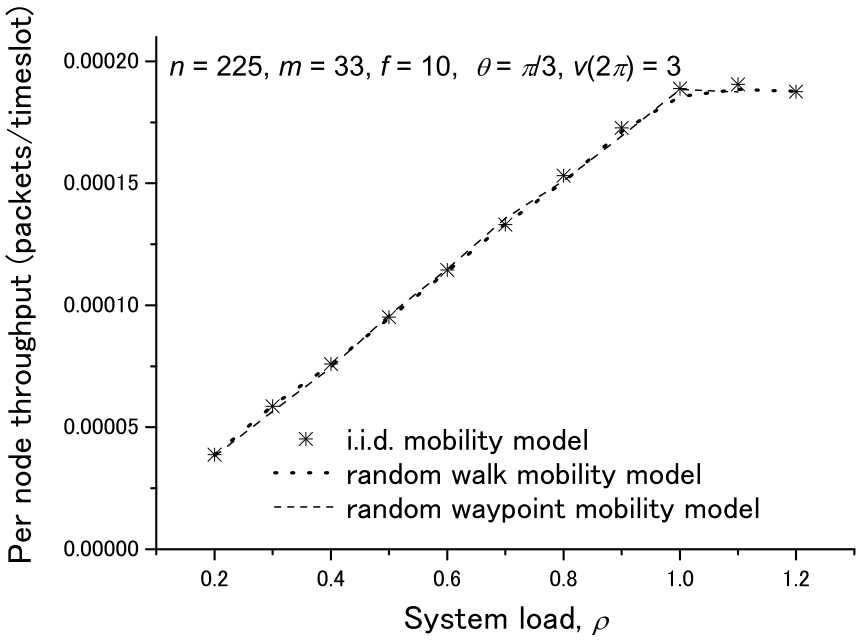

(b) Network scenario 2

Figure 4-8: The per node throughput vs. system load $\rho = \lambda/\mu(\theta, f)$.

	n	m	f	θ	$v(2\pi)$	$v(\theta)$	a	$\mu(\theta, f)$ packets/slot
scenario 1	64	28	5	$\pi/2$	4	5	14	2.8×10^{-4}
scenario 2	225	33	10	$\pi/3$	3	5	11	1.9×10^{-4}

Table 4.1: Simulation scenarios.

4.5 Numerical Results

In this section, we first evaluate the accuracy of our theoretical models with simulations and then proceed to explore the performance analysis.

4.5.1 Model Validation

We develop a simulator in C++ to simulate the packet delivery process for the considered MANETs. In the simulation, we implement a Poisson stream with input rate λ for the traffic flow, a fixed path loss exponent $\alpha = 6$ for the power propagation model and a fixed guard factor $\Delta = 0.2$ for the interference model, respectively. We use $v(2\pi)$ to denote the transmission power in this section. In addition to the i.i.d mobility model, we also implemented simulations for the random walk [17] model and the random waypoint [76] model, respectively.

First, we implement the models considered in the theoretical analysis, where the ideal antenna model with beamwidth θ is considered. The simulations results are presented in Fig. 4-7 and 4-8. The parameters of each network scenario are summarized in Table 4.1. In Fig. 4-7, we plot the expected end-to-end delay when the system load $\rho = \lambda/\mu(\theta, f)$ increases. It is clear to see that as the system load ρ increases, the expected delay also increases. A more careful observation is that when the system load ρ approaches 1, which means that the input rate λ approaches the maximum achievable throughput $\mu(\theta, f)$ determined by our theoretical result, the growth rate of the expected delay tends to infinity. This phenomenon can be explained as that we derived the maximum throughput that the network can stably support and when the input rate is above it, the network will become congested and thus the expected end-to-end delay will tend to infinity. Meanwhile, we plot in Fig. 4-8 the measured per node throughput obtained from the simulations as the system load increases. It

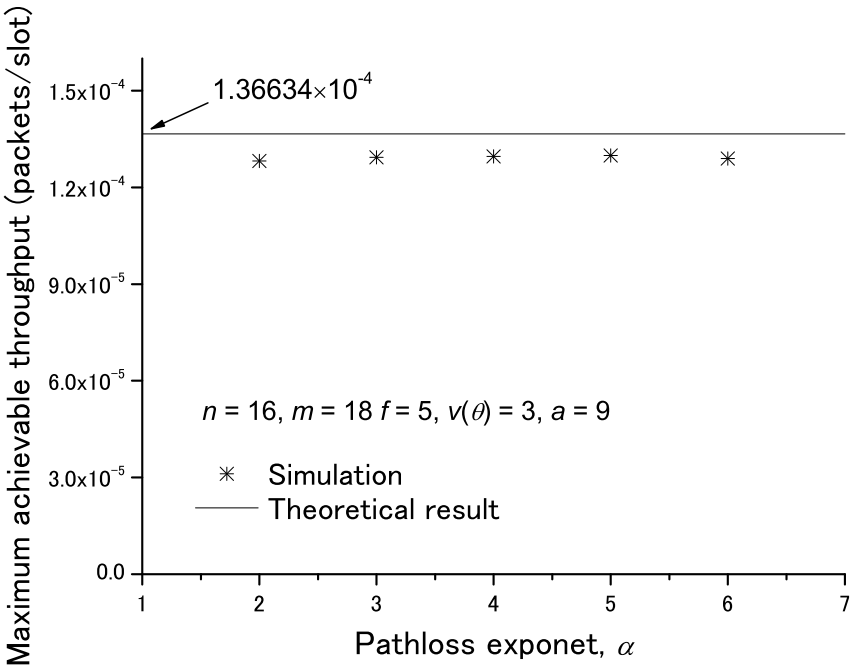

Figure 4-9: The maximum achievable throughputs obtained in the simulation for pathloss exponent $\alpha = 2, 3, 4, 5$ and 6.

can be observed from the figure that the throughput increases as the system load increases when system load is less that 1, while there are only small increases or even reductions in the actual throughput when the system load increases over 1. The simulation results in Fig. 4-8 confirm the validity of the theoretical result in Theorem 6 on the maximum achievable throughput of the network models considered in the analysis. Further, we conduct simulations with considering a realistic antenna model of the normalized radiation intensity [73]:

$$U(\phi) = \cos^2(\phi)\cos^2(3\phi), (0 \leq \phi \leq \frac{\pi}{6}, 0 \leq \sigma \leq 2\pi) \tag{4.22}$$

The beamwidth of the directional antenna $\theta \approx \pi/6$. With Eqn.(4.1), we have that $G(\phi) \approx 52.8259 \times U(\phi)$ for the realistic antenna model. The antenna gain for its counterpart of the ideal antenna model is $G_m \approx 37.5$. The simulation setting is as follows. The setting of network is $n = 16, m = 18, f = 5$ and $a = 9$. We notice that

under the realistic antenna model, the transmission range is no more uniform over all directions within the mainlobe. To make a justifiable comparison, we set that the transmission range $v(\theta) = 3$ for the theoretical result; for the realistic antenna model, we consider that at least the same received power as that of the ideal antenna model at the edge of the transmission range is required for a successful transmission. Formally, it can be expressed as that for the realistic antenna model, a transmission at distance d away from the transmitter is successful iff

$$PCG(\phi)d^{-\alpha} \geq PCG_m(r(\theta))^{-\alpha}$$

where $G(\phi)$ is the antenna gain in the direction from the transmitter to the receiver, d is the transmission distance, G_m is the antenna gain in the ideal antenna model and $r(\theta) = v(\theta) \cdot \frac{\sqrt{2}}{m}$ is the transmission range. By dividing both sides with PC in the inequality above, we have

$$G(\phi)d^{-\alpha} \geq G_m(r(\theta))^{-\alpha} \tag{4.23}$$

Eqn.(4.23) is implemented in the simulation with the realistic antenna model to determine whether a transmission is successful. The maximum achievable throughputs obtained in the simulation for different pathloss exponent α are summarized in Fig. 4-9. In the figure, we can see that the maximum achievable throughput with the realistic antenna model is at most 7% less than theoretical result. The gap between the realistic performance and the theoretical result is because that the analysis is based on an approximate antenna model and the transmission range is over estimated in some directions compared with the realistic antenna model considered in the simulation.

4.5.2 Performance Analysis

Achievable Throughput

Fig. 4-10 illustrates how the maximum achievable throughput $\mu(\theta, f)$ varies as the directional antenna beamwidth θ increases from 0 to π. It indicates that in general the

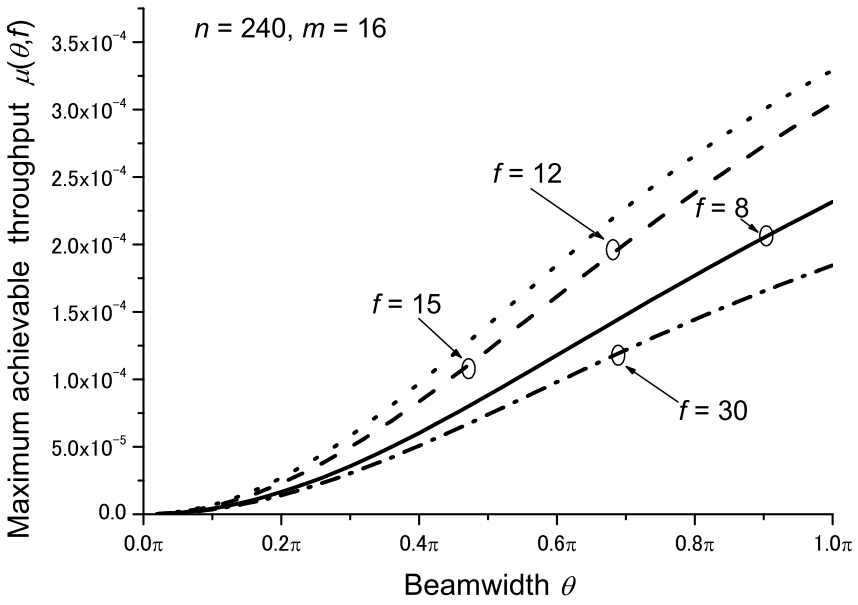

(a) The maximum achievable throughput $\mu(\theta, f)$ vs. θ with $f = 8, 12, 15$ and 30.

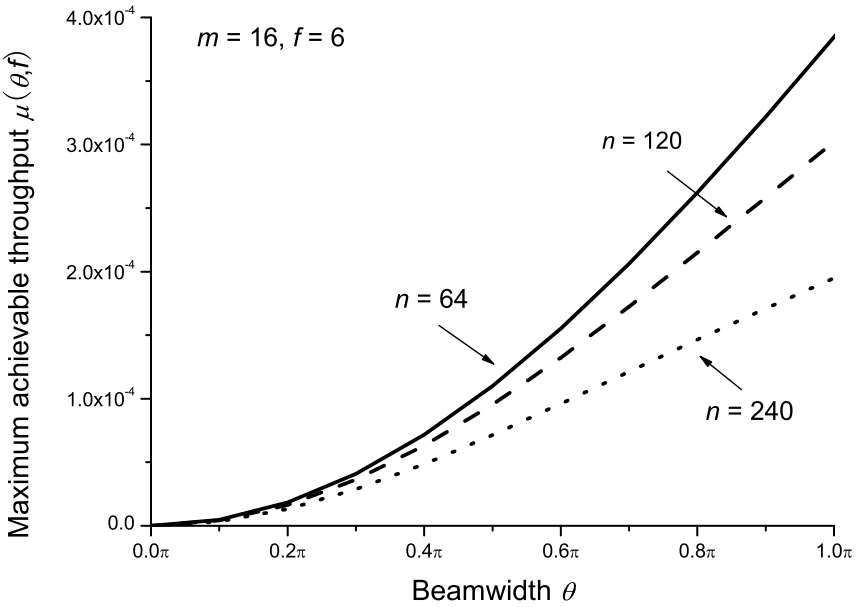

(b) The maximum achievable throughput $\mu(\theta, f)$ vs. θ with $n = 64.120$ and 240.

Figure 4-10: The maximum achievable throughput vs. beamwidth θ varying from 0 to π.

$\mu(\theta, f)$ monotonically increases as the beamwidth increases. This can be explained as that under the transmission-group based scheduling a larger beamwidth leads to an increase in the transmission opportunity and therefore the maximum achievable throughput increases. A careful observation of the Fig. 4-10a tells that a too high packet redundancy may have a negative effect on the achievable throughput. It is an expected result since Lemma 13 indicates the existence of an optimal f that can achieve the optimal achievable throughput $\mu^*(\theta)$ for a given beamwidth θ. Fig. 4-10b shows how the maximum achievable throughput varies with θ for networks of $n = \{64, 120, 240\}$. It is interesting to see that the $\mu(\theta, f)$ of a larger network is less sensitive to the variation of the beamwidth. This is because that as the node density increases, the transmission opportunity for each node is reduced and therefore the advantage from the increase of beamwidth for each flow is attenuated.

Optimal Achievable Throughput

For the general setting of $\Delta = 0.2$, $m = \sqrt{n}$, we summarize in Fig. 4-11 that for $\theta = \{\pi/9, \pi/6, \pi/4 \text{ and } \pi/2\}$ how the optimal achievable throughput $\mu^*(\theta)$ and the corresponding setting of f vary as the number of users n increases. The Fig. 4-11a shows clearly that for the settings of θ here, the optimal achievable throughput $\mu^*(\theta)$ vanishes quickly at first and more slowly as the network size increases. This can be intuitively interpreted as follows. As n increases, the coverage area of each transmitter scales as $O(\frac{1}{n})$ and so does the probability that a node is able to receive packets from its source or relay nodes, which determines the growth rate of $\mu^*(\theta)$. It is interesting to see that the optimal achievable throughput in the network with a larger antenna beam is more sensitive to the variation of network size. This is for the reason that a larger beam amplifies the performance gain resulting from the decrease of the network size. The results in Fig. 4-11b show that for a given θ, the corresponding optimal setting of f is an increasing piecewise function of n. This phenomenon might be explained as that in a larger network, the opportunity for a source node to deliver packets to its destination is less than that in a smaller network, and therefore more redundant copies for each packet are necessary to achieve the optimal performance.

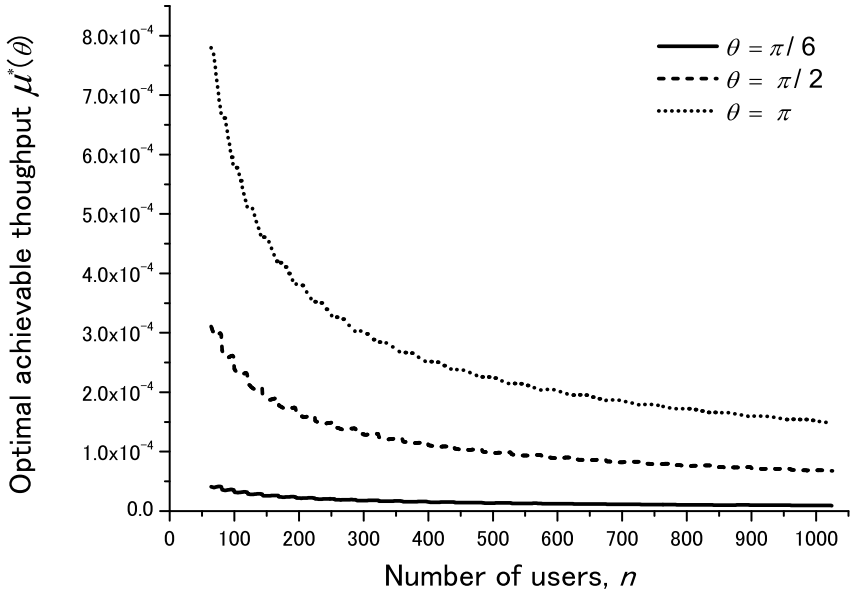

(a) The optimal achievable throughput $\mu^*(\theta)$ vs. n

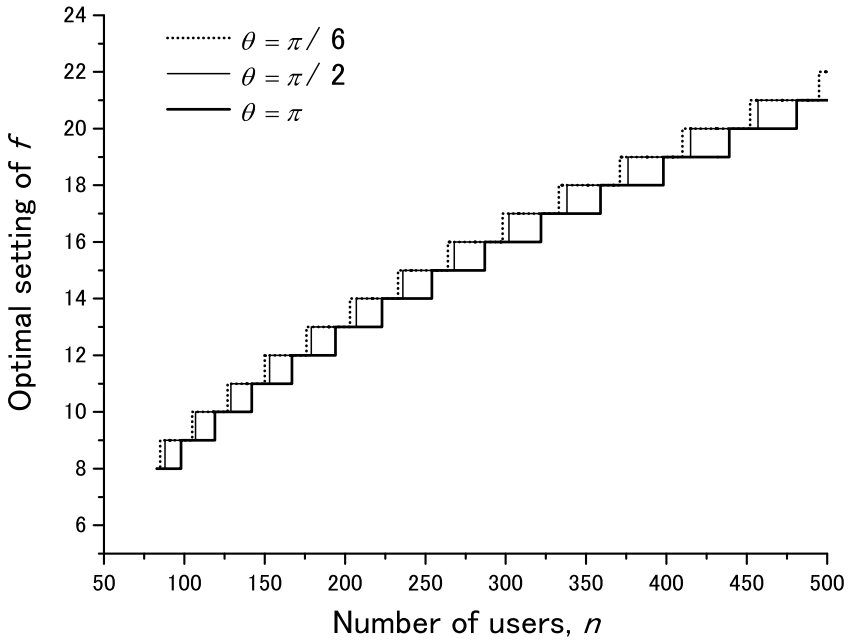

(b) The optimal setting of f vs. n

Figure 4-11: The optimal achievable throughput $\mu^*(\theta)$ and the corresponding setting of f when n increases.

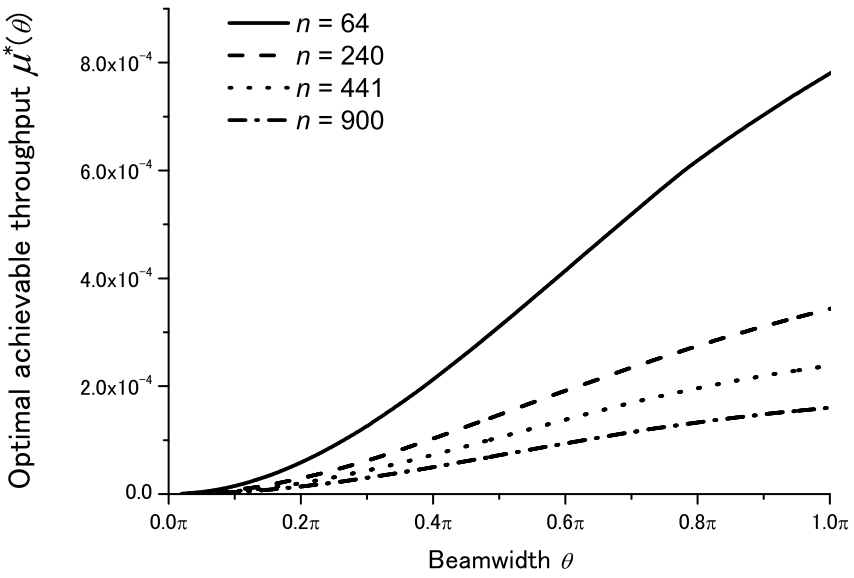

Figure 4-12: The optimal achievable throughput $\mu^*(\theta)$ vs. antenna beamwidth θ

We also see from the figure that for each network size n, the optimal setting of f with a larger antenna beam (e.x., $\theta = \pi$) is slightly less than that with a smaller one (e.x., $\theta = \pi/2$). This can be interpreted as follows. A large antenna beam will lead to a higher probability that a node is able to transmit to its destination, thus resulting in a reduction in the optimal f.

To further explore how the optimal achievable throughput is affected by the antenna beamwidth, we summarize in Fig. 4-12 how the $\mu^*(\theta)$ varies with θ for networks of $n = \{64, 240, 441, 900\}$. The figure shows clearly that the optimal achievable throughput monotonically increases as the antenna beamwidth increases, for the same reason of that in Fig. 4-10. We plot the optimal achievable throughput as a function of the transmission power for $\theta = \{\pi/6, \pi/4, \pi/2\}$ in Fig. 4-13. It is interesting to see that, for each network scenario here, as the $v(2\pi)$ increases the $\mu^*(\theta)$ always increases first and then decreases, and increases again until reaching a constant when the transmission range of a node can cover the whole network. The reason for this phenomenon is as follows. The increase on the transmission power can lead a larger transmission area, whose impact on the throughput is two-folds: on one hand, it increases the

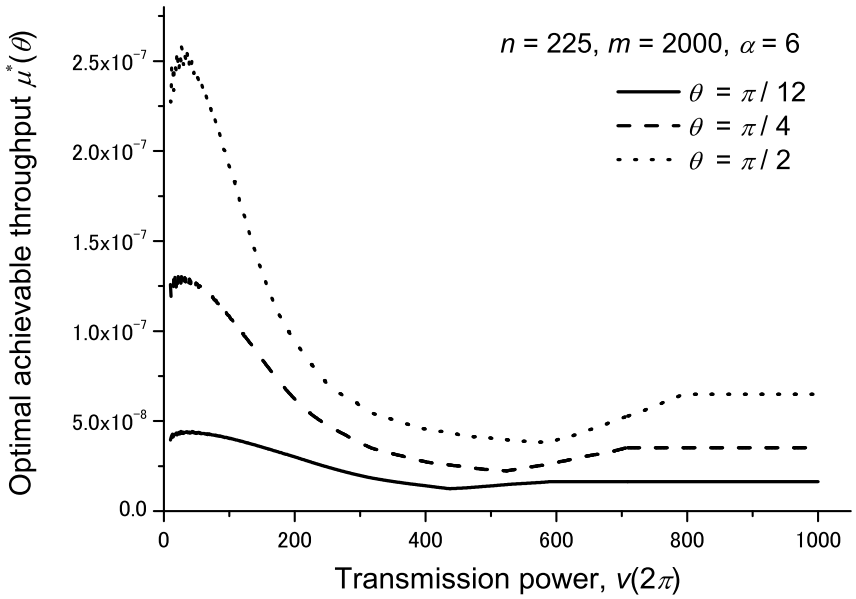

Figure 4-13: The optimal achievable throughput $\mu^*(\theta)$ vs. transmission power $v(2\pi)$ with different θ.

probability that a node could receive packets from its source or relay nodes; on the other hand, it decreases the number of concurrent transmissions. As illustrated in the figure, the former positive effect dominates when the $v(2\pi)$ is small, when the $v(2\pi)$ increases, the latter negative one becomes the dominate one. This result indicates that a local transmission strategy may achieve the optimal performance in terms of throughput in the considered network scenario here.

4.6 Summary

In this chapter, we studied the exact achievable throughput in a cell-partitioned MANET in which every node is equipped with a directional antenna of beamwidth θ for both transmission. We derived the theoretical models for such networks that enable the achievable throughput to be analyzed. Based on the theoretical models, we further explore the throughput optimization problem in such a network. Numerical studies are also conducted to demonstrate the efficiency of the proposed new

theoretical models in capturing the behaviors of achievable throughput. Noticed that the results in this chapter indicate that for a cell-partitioned MAENT with directional antennas its maximum achievable throughput is less than its omnidirectional counterpart based on this simple transmission scheduling scheme considered in this chapter.

Chapter 5

Conclusion and Future Directions

5.1 Conclusion

In this thesis, we studied the exact throughput capacity for three typical MANETs models: a sparse MANET with Poisson meeting process, a continuous MANET with ALOHA MAC protocol and a cell-partitioned MANET with group-based scheduling and directional antennas. For the considered MANETs, we developed theoretical results on their exact throughput capacity and also conducted simulation to validate the efficiency of the developed theoretical models. It is expected the theoretical results developed in this thesis will be helpful for exploring the exact throughput capacities in other MANET scenarios.

The result in Chapter 2 indicates that in the considered ICMNs, the throughput capacity is mainly determined by the pairwise meeting rate therein. A similar result was also reported in Chapter 3, where the throughput capacity is determined by the STP. The results of Chapters 2 and 3 also demonstrate that a constant throughput capacity is achievable for ICMN under random waypoint, random direction mobility models and A-MENNT under i.i.d mobility model, at a cost of average delay linearly increasing with the number of network nodes.

The results in Chapter 4 tell us that for the considered cell-partitioned MANET with directional antennas its maximum achievable throughput is less than its omnidirectional counterpart based on the group-based transmission scheduling scheme.

Therefore, it indicates that a carefully designed MAC protocol is required to get the benefits of using directional antennas in MANETs.

5.2 Future Directions

In this thesis, we studied the exact throughput capacity for three typical MANET models. The possible future works are as follows:

- Notice that the analysis developed in this thesis relied on some ideal assumptions, such as unlimited buffer space and constant data rate. Removing any of the these simplifications in the analysis will provide a more realistic model and can be a very interesting future direction.
- The exact throughput MANETs under other popular MAC protocols, like CSMA, remains an investigated area. How to develop theoretical tools to analyze the exact throughput capacity for MANETs under these more complicated MAC is also a good future direction.
- It is notable that the capacity achieving routing algorithm is of poor delay performance. Another promising direction is to design novel routing algorithm that makes a good balance between the throughput and delay performance.

Appendix A

Proofs

A.1 Proof of Lemma 7

A.1.1 Scenario of $0 < \Delta < 1$

Based on the discussion in Section 3.4.2, we know that the $\mathbb{E}\{\delta_{i,j}\}$ can be evaluated as

$$\mathbb{E}\{\delta_{i,j}\} = \underbrace{\int_{0}^{\frac{1}{3+\Delta}} \mathbb{E}\left\{\delta_{i,j} | d_{ij} = r\right\} f_{R_1}(r)\, \mathrm{d}r}_{(a)} + \underbrace{\int_{\frac{1}{3+\Delta}}^{\frac{\sqrt{2}}{2}} \mathbb{E}\left\{\delta_{i,j} | d_{ij} = r\right\} f_{R_1}(r)\, \mathrm{d}r}_{(b)},$$

The integration (a) can be analytically derived as follows. After some geometric

calculations, we have

$$\begin{aligned}
|\Omega_r^{(i)}| \quad &= \pi r^2, \\
|\Omega_{(1+\Delta)r}^{(j)}| &= \pi(1+\Delta)^2 r^2, \\
|\Omega_{r,\Delta}^{(i,j)}| \quad &= r^2(1+\Delta)^2 \arccos\left(\frac{1+\Delta}{2}\right) \\
&\quad + r^2 \arccos\left(1 - \frac{(1+\Delta)^2}{2}\right) \\
&\quad - r^2(1+\Delta)\sqrt{1 - \frac{(1+\Delta)^2}{4}}.
\end{aligned} \tag{A.1}$$

Based on (A.1), (3.24) and (3.23), the term $\mathbb{E}\{\delta_{i,j}|d_{ij} = r\}$ in integration (a) can be evaluated as

$$\mathbb{E}\{\delta_{i,j}|d_{ij} = r\} = \left(1 - q \cdot \frac{\pi(1+\Delta)^2 r^2 - |\Omega_{r,\Delta}^{(i,j)}|}{1 - \pi r^2}\right)^{n-2}. \tag{A.2}$$

Based on (A.2) and Lemma 6, the integration (a) can be evaluated as

$$\begin{aligned}
&\int_0^{\frac{1}{3+\Delta}} \mathbb{E}\left\{\delta_{i,j}|d_{ij} = r\right\} f_{R_1}(r)\,\mathrm{d}r \\
&= 2\pi(n-1)\int_0^{\frac{1}{3+\Delta}} r\left(1 - (\pi + q \cdot \Psi(\Delta))r^2\right)^{n-2}\,\mathrm{d}r \\
&= \frac{\pi}{\pi + q \cdot \Psi(\Delta)}\left(1 - (\pi + q \cdot \Psi(\Delta))r^2\right)^{n-1}\Big|_{\frac{1}{3+\Delta}}^{0} \\
&= \frac{\pi}{\pi + q \cdot \Psi(\Delta)} - \underbrace{\frac{\pi}{\pi + q \cdot \Psi(\Delta)}\left(1 - \frac{\pi + q \cdot \Psi(\Delta)}{(3+\Delta)^2}\right)^{n-1}}_{(c)},
\end{aligned} \tag{A.3}$$

where $\Psi(\Delta)$ is defined in (3.28).

As discussed in Section 3.4.2, the evaluation of integration (b) is quite cumbersome. However, we notice that the term $\mathbb{E}\left\{\delta_{i,j}|d_{ij} = r\right\}$ is monotonically decreasing. From the second mean value theorem for integration, we know that there exists a $\xi \in$

$(\frac{1}{3+\Delta}, \frac{\sqrt{2}}{2}]$ such that

$$
\begin{aligned}
0 \leq & \int_{\frac{1}{3+\Delta}}^{\frac{\sqrt{2}}{2}} \mathbb{E}\left\{\delta_{i,j} | d_{ij} = r\right\} f_{R_1}(r)\,\mathrm{d}r \\
&= \mathbb{E}\left\{\delta_{i,j} | d_{ij} = \frac{1}{3+\Delta}\right\} \int_{\frac{1}{3+\Delta}}^{\xi} f_{R_1}(r)\,\mathrm{d}r \\
&= \mathbb{E}\left\{\delta_{i,j} | d_{ij} = \frac{1}{3+\Delta}\right\} \left(F_{R_1}(\xi) - F_{R_1}\left(\frac{1}{3+\Delta}\right)\right) \\
&\leq \mathbb{E}\left\{\delta_{i,j} | d_{ij} = \frac{1}{3+\Delta}\right\} \left(1 - F_{R_1}\left(\frac{1}{3+\Delta}\right)\right) \\
&= \underbrace{\left(1 - q \cdot \frac{\Psi(\Delta)}{(3+\Delta)^2 - \pi}\right)^{n-2} \left(1 - \frac{\pi}{(3+\Delta)^2}\right)^{n-1}}_{(d)}.
\end{aligned}
\tag{A.4}
$$

Since both the (c) and (d) exponentially vanish with n, terms (c) and (b) can be neglected in the evaluation of $\mathbb{E}\{\delta_{i,j}\}$ without introducing a significant approximation error.

Combining the above results with (3.21), P_{S} can be approximated as follows.

Let $\widehat{P}_{\mathrm{S}} = \frac{\pi q(1-q)}{\pi + q \cdot \Psi(\Delta)}$, we have

$$
\begin{aligned}
P_{\mathrm{S}} - \widehat{P}_{\mathrm{S}} &\leq q(1-q)\left[(d) - (c)\right] \\
&= q(1-q)\left[\left(1 - q \cdot \frac{\Psi(\Delta)}{(3+\Delta)^2 - \pi}\right)^{n-2}\right. \\
&\cdot \left(1 - \frac{\pi}{(3+\Delta)^2}\right)^{n-1} - \frac{\pi}{\pi + q \cdot \Psi(\Delta)} \\
&\cdot \left.\left(1 - \frac{\pi + q \cdot \Psi(\Delta)}{(3+\Delta)^2}\right)^{n-1}\right] \\
&= \epsilon^{+}
\end{aligned}
\tag{A.5}
$$

and

$$\begin{aligned} P_{\mathrm{S}} - \widehat{P}_{\mathrm{S}} &= q(1-q)\left[\int_{\frac{1}{3+\Delta}}^{\frac{\sqrt{2}}{2}} \mathbb{E}\left\{\delta_{i,j} | d_{ij} = r\right\} f_{R_1}(r)\,\mathrm{d}r - (c)\right] \\ &\geq -\frac{\pi q(1-q)}{\pi + q\cdot\Psi(\Delta)}\left(1 - \frac{\pi + q\cdot\Psi(\Delta)}{(3+\Delta)^2}\right)^{n-1} \\ &= \epsilon^{-}, \end{aligned} \tag{A.6}$$

which complete the proof for the scenario of $0 < \Delta < 1$.

A.1.2 Scenario of $\Delta \geq 1$

Under this scenario the $\mathbb{E}\{\delta_{i,j}\}$ can be evaluated as

$$\begin{aligned} \mathbb{E}\{\delta_{i,j}\} = &\int_{0}^{\frac{1}{2+2\Delta}} \mathbb{E}\left\{\delta_{i,j} | d_{ij} = r\right\} f_{R_1}(r)\,\mathrm{d}r \\ &+ \int_{\frac{1}{2+2\Delta}}^{\frac{\sqrt{2}}{2}} \mathbb{E}\left\{\delta_{i,j} | d_{ij} = r\right\} f_{R_1}(r)\,\mathrm{d}r. \end{aligned}$$

In the first integration, the term $\mathbb{E}\{\delta_{i,j}|d_{ij} = r\}$ can be derived as

$$\mathbb{E}\{\delta_{i,j}|d_{ij} = r\} = \left(1 - q\cdot\frac{\pi(1+\Delta)^2 r^2 - \pi r^2}{1 - \pi r^2}\right)^{n-2}. \tag{A.7}$$

Hence,

$$\begin{aligned} &\int_{0}^{\frac{1}{2+2\Delta}} \mathbb{E}\left\{\delta_{i,j} | d_{ij} = r\right\} f_{R_1}(r)\,\mathrm{d}r \\ &= 2\pi(n-1)\int_{0}^{\frac{1}{2+2\Delta}} r\left(1 - (1 + 2\Delta q + \Delta^2 q)\pi r^2\right)^{n-2}\,\mathrm{d}r \\ &= \frac{1}{1 + 2\Delta q + \Delta^2 q}\left(1 - \left(1 - \frac{(1 + 2\Delta q + \Delta^2 q)\pi}{(2+2\Delta)^2}\right)^{n-1}\right). \end{aligned} \tag{A.8}$$

In the second integration, the evaluation of $\mathbb{E}\{\delta_{i,j}|d_{ij} = r\}$ is also quite cumber-

some. Following an argument similar to that of (A.4), we have

$$\begin{aligned}0\leq & \int_{\frac{1}{2+2\Delta}}^{\frac{\sqrt{2}}{2}} \mathbb{E}\left\{\delta_{i,j}|d_{ij}=r\right\} f_{R_1}(r)\,\mathrm{d}r \\ & \leq \mathbb{E}\left\{\delta_{i,j}|d_{ij}=\frac{1}{2+2\Delta}\right\}\left(1-F_{R_1}\left(\frac{1}{2+2\Delta}\right)\right) \\ & = \left(1-q\cdot\frac{\pi(1+\Delta)^2-\pi}{(2+2\Delta)^2-\pi}\right)^{n-2}\left(1-\frac{\pi}{(2+2\Delta)^2}\right)^{n-1}.\end{aligned} \tag{A.9}$$

Let $\widehat{P}_{\mathrm{S}}=\frac{q(1-q)}{1+2\Delta q+\Delta^2 q}$, we have $\epsilon^-\leq P_{\mathrm{S}}-\widehat{P}_{\mathrm{S}}\leq\epsilon^+$, where

$$\begin{aligned}\epsilon^+ = q(1-q)\Bigg[&\left(1-q\cdot\frac{\pi(1+\Delta)^2-\pi}{(2+2\Delta)^2-\pi}\right)^{n-2} \\ &\cdot\left(1-\frac{\pi}{(2+2\Delta)^2}\right)^{n-1}-\frac{1}{1+2\Delta q+\Delta^2 q} \\ &\cdot\left(1-\frac{(1+2\Delta q+\Delta^2 q)\pi}{(2+2\Delta)^2}\right)^{n-1}\Bigg]\end{aligned} \tag{A.10}$$

and

$$\epsilon^- = -\frac{q(1-q)}{1+2\Delta q+\Delta^2 q}\left(1-\frac{(1+2\Delta q+\Delta^2 q)\pi}{(2+2\Delta)^2}\right)^{n-1}. \tag{A.11}$$

A.2 Proof of Lemma 8

Notice that when $\Delta\geq 1$ the NRT scheme is equivalent to the NNT scheme, for the reason that the non-nearest neighbor transmissions can not be successfully received according to the protocol model in (3.1). Therefore, we only focus on the scenario of $0<\Delta<1$.

Without loss of generality, we focus on a node i in a time slot. We use R_k to denote the distance from node i to its k-th nearest neighbor, use B_i to denote the nearest silent node of node i, and use $B_i=k$ to indicate that the nearest silent node of i is its k-th nearest neighbor. The event that i can successfully conduct a transmission

in the time slot iff the following two events happen simultaneously. First, i decides to conduct a transmission. Second, the transmission from i to its nearest silent node B_i is successful under the protocol model of (3.1).

We use indicator function $\delta_{i,B_i} = 1$ to denote that the condition in (3.1) is true for the transmission from i to B_i ($\delta_{i,B_i} = 0$, otherwise). Since above two events are mutually independent, we can see that STP P_{S} under the NRT scheme is determined as

$$\begin{aligned} P_{\mathrm{S}} &= q \Pr\{\delta_{i,B(i)} = 1\} \\ &= q \mathbb{E}\{\delta_{i,B(i)}\}. \end{aligned} \tag{A.12}$$

Conditioning on $B_i = k$, we have

$$\mathbb{E}\{\delta_{i,B_i}\} = \sum_{k=1}^{n-1} \mathbb{E}\{\delta_{i,B_i} | B_i = k\} \cdot \Pr\{B_i = k\}, \tag{A.13}$$

where $\Pr\{B_i = k\} = q^{k-1}(1-q)$.

Further conditioning on $R_k = r$ and combining the result of Lemma 6, the $\mathbb{E}\{\delta_{i,B_i})\}$ can be evaluated as

$$\begin{aligned} \mathbb{E}\{\delta_{i,B_i})\} =& \sum_{k=1}^{n-1} \int_0^{\frac{1}{3+\Delta}} \mathbb{E}\{\delta_{i,k} | B_i = k, R_k = r\} \\ & \cdot \Pr\{B_i = k\} f_{R_k}(r)\, \mathrm{d}r \\ & + \sum_{k=1}^{n-1} \int_{\frac{1}{3+\Delta}}^{\frac{\sqrt{2}}{2}} \mathbb{E}\{\delta_{i,k} | B_i = k, R_k = r\} \\ & \cdot \Pr\{B_i = k\} f_{R_k}(r)\, \mathrm{d}r. \end{aligned} \tag{A.14}$$

The term $\mathbb{E}\{\delta_{i,k}|B_i = k, R_k = r\}$ in the first part of (A.14) can be determined as

$$\begin{aligned}
&\mathbb{E}\{\delta_{i,k}|B_i = k, R_k = r\} \\
&= \left(1 - \frac{|\Omega_{r,\Delta}^{(i,j)}|}{\pi r^2}\right)^{k-1} \sum_{t=0}^{n-k-1} \binom{n-k-1}{t} q^t (1-q)^{n-k-1-t} \\
&\left(1 - \frac{\pi(1+\Delta)^2 r^2 - |\Omega_{r,\Delta}^{(i,j)}|}{1-\pi r^2}\right)^t \\
&= \left(1 - \frac{|\Omega_{r,\Delta}^{(i,j)}|}{\pi r^2}\right)^{k-1} \left(1 - q \cdot \frac{\pi(1+\Delta)^2 r^2 - |\Omega_{r,\Delta}^{(i,j)}|}{1-\pi r^2}\right)^{n-1-k},
\end{aligned} \tag{A.15}$$

where $|\Omega_{r,\Delta}^{(i,j)}|$ is given in (A.1).

Hence, the first part of (A.14) can be determined as

$$\begin{aligned}
&\sum_{k=1}^{n-1} \int_0^{\frac{1}{3+\Delta}} \mathbb{E}\{\delta_{i,k}|B_i = k, R_k = r\} \Pr\{B_i = k\} f_{R_k}(r)\, \mathrm{d}r \\
&= (1-q) \int_0^{\frac{1}{3+\Delta}} 2\pi r \sum_{k=1}^{n-1} \frac{\Gamma(n)}{\Gamma(k)\Gamma(n-k)} (q[\pi r^2 - |\Omega_{r,\Delta}^{(i,j)}|])^{k-1} \\
&(1 - \pi r^2 - q[\pi(1+\Delta)^2 r^2 - |\Omega_{r,\Delta}^{(i,j)}|])^{n-k-1}\, \mathrm{d}r \\
&= (1-q) \int_0^{\frac{1}{3+\Delta}} 2\pi r (n-1)(1 - (1 + 2\Delta q + \Delta^2 q)\pi r^2)^{n-2}\, \mathrm{d}r \\
&= \frac{1-q}{1+2\Delta q + \Delta^2 q} \\
&- \frac{1-q}{1+2\Delta q + \Delta^2 q} \left(1 - \frac{(1+2\Delta q + \Delta^2 q)\pi}{(3+\Delta)^2}\right)^{n-1}.
\end{aligned} \tag{A.16}$$

Similar to the derivation of (A.4), the second part of (A.14) is bounded as

$$\begin{aligned}
&\sum_{k=1}^{n-1}\int_{\frac{1}{3+\Delta}}^{\frac{\sqrt{2}}{2}}\mathbb{E}\{\delta_{i,k}|B_i=k,R_k=r\}\Pr\{B_i=k\}f_{R_k}(r)\,\mathrm{d}r\\
&\le\sum_{k=1}^{n-1}\mathbb{E}\{\delta_{i,k}|B_i=k,R_k=\frac{1}{3+\Delta}\}\Pr\{B_i=k\}\\
&\cdot\left(1-F_{R_k}\left(\frac{1}{3+\Delta}\right)\right)\\
&\le\sum_{k=1}^{n-1}\mathbb{E}\left\{\delta_{i,k}|B_i=k,R_k=\frac{1}{3+\Delta}\right\}\Pr\{B_i=k\}\\
&=(1-q)\sum_{k=1}^{n-1}\left(q-q\cdot\frac{\Psi(\Delta)-(1+\Delta)^2}{\pi}\right)^{k-1}\\
&\cdot\left(1-q\cdot\frac{\Psi(\Delta)}{(3+\Delta)^2-\pi}\right)^{n-1-k}\\
&=(1-q)\frac{\left(1-q\cdot\frac{\Psi(\Delta)}{(3+\Delta)^2-\pi}\right)^{n-1}-\left(q-q\cdot\frac{\Psi(\Delta)-(1+\Delta)^2}{\pi}\right)^{n-1}}{1-q\left(1+\frac{\Psi(\Delta)}{(3+\Delta)^2-\pi}-\frac{\Psi(\Delta)-(1+\Delta)^2}{\pi}\right)}.
\end{aligned}\tag{A.17}$$

Let $\widehat{P}_{\mathrm{S}}=\frac{q(1-q)}{1+2\Delta q+\Delta^2 q}$, we have $\epsilon^-\le P_{\mathrm{S}}-\widehat{P}_{\mathrm{S}}\le\epsilon^+$, where

$$\begin{aligned}
\epsilon^+=&\frac{q(1-q)}{1-q\left(1+\frac{\Psi(\Delta)}{(3+\Delta)^2-\pi}-\frac{\Psi(\Delta)-(1+\Delta)^2}{\pi}\right)}\left[(1-q\right.\\
&\left.\cdot\frac{\Psi(\Delta)}{(3+\Delta)^2-\pi}\right)^{n-1}-\left(q-q\cdot\frac{\Psi(\Delta)-(1+\Delta)^2}{\pi}\right)^{n-1}\Bigg]\\
&-\frac{q(1-q)}{1+2\Delta q+\Delta^2 q}\left(1-\frac{(1+2\Delta q+\Delta^2 q)\pi}{(3+\Delta)^2}\right)^{n-1}
\end{aligned}\tag{A.18}$$

and

$$\epsilon^-=-\frac{q(1-q)}{1+2\Delta q+\Delta^2 q}\left(1-\frac{(1+2\Delta q+\Delta^2 q)\pi}{(3+\Delta)^2}\right)^{n-1}.\tag{A.19}$$

A.3 Proof of lemma 9

For a given node T that transmits in some time slot, let $\mathbb{T}$ be the set of nodes that simultaneously transmit with T. When the transmission is omnidirectional, according to the power propagation model (4.2), the SNR at distance $r(2\pi)$ is

$$\frac{P_t C \left(r(2\pi)\right)^{-\alpha}}{\sum_{K\in\mathbb{T},K\neq T} P_t C d_K^{-\alpha}} = \beta, \tag{A.20}$$

where β is the threshold, the antenna gain factors are equal to 1 in omnidirectional mode and d_K represents the distance between K and the receiver of T.

Under the same transmission power, if each transmitter conducts a directional transmission with beamwidth θ, then we have that a node $K \in \mathbb{T}, K \neq T$ can interfere the receiver with probability $\theta/2\pi$, since each transmitter randomly and uniformly selects beamforming direction. If we assume the same distance between the receiver and any other interfering transmitter, to the achieve the same SNR threshold β, the SNR at distance $r(\theta)$ satisfies:

$$\frac{P_t C G(\theta) \left(r(\theta)\right)^{-\alpha}}{\frac{\theta}{2\pi}\sum_{K\in\mathbb{T},K\neq T} P_t C G(\theta) d_K^{-\alpha}} = \beta \tag{A.21}$$

Where $G(\theta)$ is the directional antenna gain with beamwidth θ. Combining (A.20) and (A.21) and with some basic operations, the result follows.

A.4 Proof of Lemma 10

For a given time slot and a tagged flow, the source S conducts a source-to-destination transmission iff the following events happen simultaneously: (1) S is in an active cell; (2) S is selected as the transmitter; (3) D is either in the same cell or in one of the $w-1$ adjacent cells and is beamformed by S.

Consider an active cell, the S can conduct a source-to-destination transmission with D only under the following two mutually exclusive cases: (1) D is in the active

cell with S; (2) D is in one of the $w-1$ adjacent cells.

Furthermore, in either of the above cases, given that k nodes other than S and D are in the active cell, then we have

$$p_1(\theta) = \frac{\theta}{2\pi a^2}\left\{\sum_{k=0}^{n-2}\binom{n-2}{k}\left(\frac{1}{m^2}\right)^{k+1}\left(\frac{m^2-1}{m^2}\right)^{n-2-k}\frac{1}{k+2} + \sum_{k=0}^{n-2}\binom{n-2}{k}\left(\frac{1}{m^2}\right)^{k+1}\left(\frac{m^2-1}{m^2}\right)^{n-2-k}\frac{w-1}{k+1}\right\} \tag{A.22}$$

Similarly, the S conducts a source-to-relay transmission or a relay-to-destination one only under the following events: (1) S is in an active cell; (2) S is selected as the transmitter; (3) D is neither in the cell and is beamformed by S nor in one of the $w-1$ adjacent cells and is beamformed by S; (4) there is at least one node other than S and D either in the cell or in one of the $w-1$ adjacent cells and is beamformed by S.

By assuming there are k nodes other than S and D in the active cell, we have

$$
\begin{aligned}
p_2(\theta) = \frac{1}{a^2}\Bigg\{ & \frac{1}{m^2}\left(\frac{2\pi-\theta}{2\pi}\right)\sum_{k=0}^{n-1}\binom{n-2}{k}\left(\frac{1}{m^2}\right)^k\frac{1}{k+2} \\
& \left[\sum_{t=1}^{k}\binom{k}{t}\left(\frac{\theta}{2\pi}\right)^t\left(\frac{2\pi-\theta}{2\pi}\right)^{k-t}\left(\frac{m^2-1}{m^2}\right)^{n-2-k}\right. \\
& + \left(\frac{2\pi-\theta}{2\pi}\right)^k\sum_{t=1}^{n-2-k}\binom{n-2-k}{t}\left(\frac{\theta(w-1)}{2\pi m^2}\right)^t \\
& \left.\left(\frac{2\pi m^2-2\pi-\theta(w-1)}{2\pi m^2}\right)^{n-2-k-t}\right] \\
& + \left(\frac{2\pi m^2-2\pi-\theta(w-1)}{2\pi m^2}\right)\sum_{k=0}^{n-2}\binom{n-2}{k}\left(\frac{1}{m^2}\right)^k\frac{1}{k+1} \\
& \left[\sum_{t=1}^{k}\binom{k}{t}\left(\frac{\theta}{2\pi}\right)^t\left(\frac{2\pi-\theta}{2\pi}\right)^{k-t}\left(\frac{m^2-1}{m^2}\right)^{n-2-k}\right. \\
& + \left(\frac{2\pi m^2-2\pi-\theta(w-1)}{2\pi m^2}\right)^k\sum_{t=1}^{n-2-k}\binom{n-2-k}{t}\left(\frac{\theta(w-1)}{2\pi m^2}\right)^t \\
& \left.\left.\left(\frac{2\pi m^2-2\pi-\theta(w-1)}{2\pi m^2}\right)^{n-2-k-t}\right]\right\}
\end{aligned}
\tag{A.23}
$$

The results can be derived from (A.22) and (A.23) with basic algebraic operations, respectively.

A.5 Proof of Lemma 11

At first, we notice that in the current time slot all the relay nodes can be divided into two mutually exclusive sets: one consists of all the relay nodes who has a copy of P (denoted by $\mathbb{R}$) and the other consists of the one who doesn't (denoted by $\mathbb{V}$). Furthermore, we note that the number of nodes in $\mathbb{R}$ is $j-1$ and the number of nodes in $\mathbb{V}$ is $n-j-1$.

The proof to $P_r(\theta, j)$ and $P_d(\theta, j)$ is similar to that in [70, 71], we only provide the proof of $P_s(\theta, j)$ here. To derive $P_s(\theta, j)$, we should notice that the corresponding event happens iff the S delivers a new copy of P to one relay node of $\mathbb{V}$ and at the

same time the D receives P from one relay node of $\mathbb{R}$. As a result, given a node $V \in \mathbb{V}$ and a node $R \in \mathbb{R}$, if we denote the event that a source-to-relay transmission from S to V and a relay-to-destination transmission from R to D happen simultaneously in the next time slot by $(S \to V, R \to D)$, then we have:

$$P_s(\theta, j) = (j-1)(n-j-1)p(S \to V, R \to D) \tag{A.24}$$

Furthermore, given a particular pair (V, R), the event $(S \to V, R \to D)$ happens iff the following events happen simultaneously:

(1) S and R are in two different active cells; (2) S and R are selected as transmitters, respectively; (3) V and D are selected as the receiver of the S and the receiver of the R, respectively; (4) S chooses to conduct a source-to-relay transmission and R chooses to conduct a relay-to-destination transmission.

Notice that to make the D be selected as the transmitter of the R, the destination node of the R (denoted by $D(R)$) shouldn't be a candidate for the transmission from R. Therefore, we further divide the event $(S \to V, R \to D)$ into two cases based on whether $D(R)$ is one of S and V or not. For $D(R) \neq S$ and $D(R) \neq V$, D can be selected as the receiver of the R only under the following subevents: $D(R)$ is not a one hop neighbor of R or it is a one hop neighbor of R but it is not beamformed by R. To sum up, for the former case, we have:

$$
\begin{aligned}
&p\left(S \to V, R \to D \middle| D\left(R\right) \neq S \text{ and } D\left(R\right) \neq V\right) \\
&= \frac{m^2 - a^2}{4m^2a^4} \sum_{k=0}^{n-5} \binom{n-5}{k} \sum_{i=0}^{k} \binom{k}{i} \left(\frac{1}{m^2}\right)^i \left(\frac{w-1}{m^2}\right)^{k-i} \\
&\cdot \left[\frac{1}{m^2} \left(\frac{1}{i+2} + \frac{8}{i+1}\right) \sum_{u=0}^{k} \binom{k}{u} \frac{1}{u+1} \left(\frac{\theta}{2\pi}\right)^{u+1} \right. \\
&\cdot \left(1 - \frac{\theta}{2\pi}\right)^{k-u} \sum_{t=0}^{n-4-k} \binom{n-4-k}{t} \sum_{j=0}^{t} \binom{t}{j} \left(\frac{1}{m^2}\right)^{j+1} \\
&\cdot \left(\frac{w-1}{m^2}\right)^{t-j} \left(\frac{1}{j+2} + \frac{8}{j+1}\right) \sum_{v=0}^{t} \binom{t}{v} \frac{1}{v+1} \left(\frac{\theta}{2\pi}\right)^{v+1} \\
&\cdot \left(1 - \frac{\theta}{2\pi}\right)^{t-v} \left(\frac{m^2 - 2w}{m^2}\right)^{n-4-k-t} + \frac{1}{m^4} \left(\frac{1}{i+3}\right. \\
&\left. + \frac{16}{i+2} + \frac{64}{i+1}\right) \sum_{u=0}^{k} \binom{k}{u} \frac{1}{u+1} \left(\frac{\theta}{2\pi}\right)^{u+1} \\
&\cdot \left(1 - \frac{\theta}{2\pi}\right)^{k-u+1} \sum_{t=0}^{n-5-k} \binom{n-5-k}{t} \sum_{j=0}^{t} \binom{t}{j} \\
&\cdot \left(\frac{1}{m^2}\right)^{j+1} \left(\frac{w-1}{m^2}\right)^{t-j} \left(\frac{1}{j+2} + \frac{8}{j+1}\right) \sum_{v=0}^{t} \binom{t}{v} \frac{1}{v+1} \\
&\left. \cdot \left(\frac{\theta}{2\pi}\right)^{v+1} \left(1 - \frac{\theta}{2\pi}\right)^{t-v} \left(\frac{m^2 - 2w}{m^2}\right)^{n-5-k-t} \right]
\end{aligned}
\tag{A.25}
$$

Similarly, for the case $D(R) = S$ or V, we have

$$
\begin{aligned}
& p\left(S \to V, R \to D \middle| D(R) = S \text{ or } V\right) \\
& = \frac{m^2 - a^2}{4m^2a^4} \sum_{k=0}^{n-4} \binom{n-4}{k} \sum_{i=0}^{k} \binom{k}{i} \left(\frac{1}{m^2}\right)^{i+1} \left(\frac{w-1}{m^2}\right)^{k-i} \\
& \cdot \left(\frac{1}{i+2} + \frac{8}{i+1}\right) \sum_{u=0}^{k} \binom{k}{u} \frac{1}{u+1} \left(\frac{\theta}{2\pi}\right)^{u+1} \\
& \cdot \left(1 - \frac{\theta}{2\pi}\right)^{k-u} \sum_{t=0}^{n-4-k} \binom{n-4-k}{t} \sum_{j=0}^{t} \binom{t}{j} \left(\frac{1}{m^2}\right)^{j+1} \\
& \cdot \left(\frac{w-1}{m^2}\right)^{t-j} \left(\frac{1}{j+2} + \frac{8}{j+1}\right) \sum_{v=0}^{t} \binom{t}{v} \frac{1}{v+1} \left(\frac{\theta}{2\pi}\right)^{v+1} \\
& \cdot \left(1 - \frac{\theta}{2\pi}\right)^{t-v} \left(\frac{m^2 - 2w}{m^2}\right)^{n-4-k-t}
\end{aligned}
\tag{A.26}
$$

Notice that

$$p(D(R) \neq S \text{ and } D(R) \neq V) = \frac{n-4}{n-2} \tag{A.27}$$

$$p(D(R) = S \text{ or } V) = \frac{2}{n-2} \tag{A.28}$$

$$\begin{aligned}
&\sum_{i=0}^{k} \binom{k}{i} \left(\frac{1}{m^2}\right)^{i+1} \left(\frac{w-1}{m^2}\right)^{k-i} \left(\frac{1}{i+2} + \frac{8}{i+1}\right) \\
&= \sum_{i=0}^{k} \binom{k+1}{i+1} \left(\frac{1}{m^2}\right)^{i+1} \left(\frac{w-1}{m^2}\right)^{k-i} \frac{1}{i+2} \\
&- \sum_{i=0}^{k} \binom{k}{i+1} \left(\frac{1}{m^2}\right)^{i+1} \left(\frac{w-1}{m^2}\right)^{k-i} \frac{1}{i+2} \\
&+ \sum_{i=0}^{k} \binom{k}{i} \left(\frac{1}{m^2}\right)^{i+1} \left(\frac{w-1}{m^2}\right)^{k-i} \frac{8}{i+1} \\
&= \frac{9\left(\frac{w}{m^2}\right)^{k+1} - 8\left(\frac{w-1}{m^2}\right)^{k+1}}{k+2}
\end{aligned} \tag{A.29}$$

$$\begin{aligned}
&\sum_{u=0}^{k} \binom{k}{u} \left(\frac{\theta}{\pi}\right)^{u+1} \left(1 - \frac{\theta}{2\pi}\right)^{k-u} \frac{1}{u+1} \\
&= \frac{1}{k+1}\left[1 - \left(1 - \frac{\theta}{2\pi}\right)^{k+1}\right]
\end{aligned} \tag{A.30}$$

$$\begin{aligned}
&\sum_{i=0}^{k} \binom{k}{i} \left(\frac{1}{m^2}\right)^{i+2} \left(\frac{w-1}{m^2}\right)^{k-i} \left(\frac{1}{i+3} + \frac{16}{i+2} + \frac{64}{i+1}\right) \\
&= \frac{9\left(\frac{w}{m^2}\right)^{k+2} - 8\left(\frac{w-1}{m^2}\right)^{k+2}}{(k+3)}
\end{aligned} \tag{A.31}$$

$$\begin{aligned}
&\sum_{u=0}^{k} \binom{k}{u} \left(\frac{\theta}{2\pi}\right)^{u+1} \left(\frac{2\pi-\theta}{2\pi}\right)^{k-u+1} \frac{1}{u+1} \\
&= \left(1 - \frac{\theta}{2\pi}\right) \cdot \frac{1}{k+1}\left[1 - \left(1 - \frac{\theta}{2\pi}\right)^{k+1}\right]
\end{aligned} \tag{A.32}$$

The (4.11) follows by combining (A.24)-(A.32).

A.6 Proofs of Lemma 12, 13 and Theorem 6

The proofs of Lemma 12, 13 and Theorem 6 are similar to those in [70, 71], please refer to them for details.

Bibliography

[1] Piyush Gupta and P. R. Kumar. The capacity of wireless networks. *IEEE Trans. Inf. Theory*, 46(2):388–404, March 2000. doi: 10.1109/18.825799.

[2] Matthias Grossglauser and David N. C. Tse. Mobility increases the capacity of ad hoc wireless networks. *IEEE/ACM Trans. Netw.*, 10(4):477–486, August 2002. doi: 10.1109/TNET.2002.801403.

[3] Michael J. Neely and Eytan Modiano. Capacity and delay tradeoffs for ad-hoc mobile networks. *IEEE Trans. Inf. Theory*, 51(6):1917–1937, June 2005.

[4] Steven Weber and Jeffrey G Andrews. Transmission capacity of wireless networks. *arXiv preprint arXiv:1201.0662*, 2012.

[5] Andrew M. Hunter, Jeffrey G. Andrews, and Steven Weber. Transmission capacity of ad hoc networks with spatial diversity. *IEEE Trans. Wireless Commun.*, 7(12):5058 – 5071, December 2008.

[6] R. Groenevelt, P. Nain, and G. Koole. The message delay in mobile ad hoc networks. *Performance Evaluation*, 62(1-4):210–228, October 2005.

[7] Stavros Toumpis and Andrea J Goldsmith. Large wireless networks under fading, mobility, and delay constraints. In *Proc. IEEE INFOCOM*, 2004.

[8] Y. Xu and W. Wang. The speed of information propagation in large wireless networks. In *Proc. IEEE INFOCOM*, pages 16–20. IEEE, 2008.

[9] Y. Xu and W. Wang. The limit of information propagation speed in large-scale multihop wireless networks. *IEEE/ACM Trans. Netw.*, 19(1):209–222, 2011.

[10] P. Jacquet, B. Mans, and G. Rodolakis. Information propagation speed in mobile and delay tolerant networks. *IEEE Trans. Inf. Theory*, 56(10):5001, October 2010.

[11] C. Han and Y. Yang. Understanding the information propagation speed in multihop cognitive radio networks. *IEEE Trans. Mobile Comput.*, pp(99):1, April 2012.

[12] P. Jacquet, B. Mans, and G. Rodolakis. Information propagation speed in delay tolerant networks: Analytic upper bounds. In *Proc. IEEE ISIT*, pages 6–10. IEEE, 2008.

[13] E. Baccelli, P. Jacquet, B. Mans, and G. Rodolakis. Highway vehicular delay tolerant networks: information propagation speed properties. *IEEE Trans. Inf. Theory*, 58(3):1743–1756, March 2012.

[14] Andrea Goldsmith, Michelle Effros, Ralf Koetter, Muriel Médard, Asu Ozdaglar, and Lizhong Zheng. Beyond shannon: the quest for fundamental performance limits of wireless ad hoc networks. *IEEE Commun. Mag.*, 49(5):195–205, May 2011.

[15] Jeffrey Andrews, Sanjay Shakkottai, Robert Heath, Nihar Jindal, Martin Haenggi, Randy Berry, Dongning Guo, Michael Neely, Steven Weber, Syed Jafar, and Aylin Yener. Rethinking information theory for mobile ad hoc networks. *IEEE Commun. Mag.*, 46(12):94–101, December 2008.

[16] Abbas El Gamal, James Mammen, Balaji Prabhakar, and Devavrat Shah. Optimal throughput-delay scaling in wireless networks-part i: The fluid model. *IEEE Trans. Inf. Theory*, 52(6):2568–2592, June 2006.

[17] Abbas El Gamal, James Mammen, Balaji Prabhakar, and Devavrat Shah. Optimal throughput–delay scaling in wireless networkspart ii: Constant-size packets. *IEEE Trans. Inf. Theory*, 52(11):5111– 5116, November 2006.

[18] James Mammen and Devavrat Shah. Throughput and delay in random wireless networks with restricted mobility. *IEEE Trans. Inf. Theory*, 53(3):1108–1116, March 2007.

[19] Pan Li, Yuguang Fang, Jie Li, and Xiaoxia Huang. Smooth trade-offs between throughput and delay in mobile ad hoc networks. *IEEE Trans. Mobile Comput.*, 11(3):427–438, March 2012.

[20] Abbas El Gamal, James Mammen, Balaji Prabhakar, and Devavrat Shah. Throughput-delay trade-off in wireless networks. In *Proc. IEEE INFOCOM*, 2004.

[21] Xiaojun Lin, Gaurav Sharma, Ravi R. Mazumdar, and Ness B. Shroff. Degenerate delay-capacity tradeoffs in ad-hoc networks with brownian mobility. *IEEE/ACM Trans. Netw.*, 14(SI):2777–2784, June 2006. ISSN 1063-6692. doi: http://dx.doi.org/10.1109/TIT.2006.874544.

[22] Gaurav Sharma, Ravi Mazumdar, and Ness B. Shroff. Delay and Capacity Trade-Offs in Mobile Ad Hoc Networks: A Global Perspective. *IEEE/ACM Trans. Netw.*, 15(5):981–992, October 2007.

[23] Delia Ciullo, Valentina Martina, Michele Garetto, and Emilio Leonardi. Impact of correlated mobility on delay-throughput performance in mobile ad hoc networks. *IEEE/ACM Trans. Netw.*, 19(6):1745–1758, December 2011.

[24] R. Urgaonkar and M.J. Neely. Network capacity region and minimum energy function for a delay-tolerant mobile ad hoc network. *IEEE/ACM Trans. Netw.*, 19(4):1137–1150, 2011.

[25] Juntao Gao, Jiajia Liu, Xiaohong Jiang, Osamu Takahashi, and Norio Shiratori. Throughput Capacity of MANETs with Group-Based Scheduling and General Transmission Range. *IEICE Trans. Commun.*, E96-B(7):1791–1802, June 2013. In press.

[26] Yin Chen, Yulong Shen, Xiaohong Jiang, and Jie Li. Throughput capacity of aloha manets. In *Proc. IEEE ICCC*, 2013.

[27] Zhensheng Zhang. Routing in intermittently connected mobile ad hoc networks and delay tolerant networks: overview and challenges. *Communications Surveys & Tutorials, IEEE*, 8(1):24–37, First Quarter 2006.

[28] Ramanan Subramanian and Faramarz Fekri. Analysis of multiple-unicast throughput in finite-buffer delay-tolerant networks. In *Proc. IEEE ISIT*, 2009.

[29] Ramanan Subramanian, Badri N Vellambi, and Faramarz Fekri. A generalized framework for throughput analysis in sparse mobile networks. In *Proc. IEEE WiOpt*, 2009.

[30] Ramanan Subramanian and Faramarz Fekri. Queueing models for the performance of multihop routing in a intermittently-connected mobile network. In *Proc. IEEE ICC*, 2012.

[31] Robin Groenevelt. *Stochastic models in mobile ad hoc networks.* PhD thesis, University of Nice, Sophia Antipolis, France, 2005.

[32] X. Zhang, G. Neglia, J. Kurose, and D. Towsley. Performance modeling of epidemic routing. *Computer Networks*, 51(10):2867–2891, July 2007.

[33] Ahmad Al Hanbali, Philippe Nain, and Eitan Altman. Performance of ad hoc networks with two-hop relay routing and limited packet lifetime (extended version). *Performance Evaluation*, 65(6):463–483, June 2008.

[34] Thrasyvoulos Spyropoulos, Konstantinos Psounis, and Cauligi S Raghavendra. Efficient routing in intermittently connected mobile networks: The single-copy case. *IEEE/ACM Trans. Netw.*, 16(1):63–76, February 2008.

[35] Thrasyvoulos Spyropoulos, Konstantinos Psounis, and Cauligi S Raghavendra. Efficient routing in intermittently connected mobile networks: the multiple-copy case. *IEEE/ACM Trans. Netw.*, 16(1):77–90, February 2008.

[36] Michael James Neely. *Dynamic power allocation and routing for satellite and wireless networks with time varying channels.* PhD thesis, Massachusetts Institute of Technology, 2003.

[37] Paul J Burke. The output of a queuing system. *Oper. Res.*, 4(6):699–704, December 1956.

[38] Christian Bettstetter, Christian Wagner, et al. The spatial node distribution of the random waypoint mobility model. In *Proc. WMAN*, 2002.

[39] Philippe Nain, Don Towsley, Benyuan Liu, and Zhen Liu. Properties of random direction models. In *Proc. IEEE INFOCOM*, 2005.

[40] S. Srinivasa and M. Haenggi. Distance Distributions in Finite Uniformly Random Networks: Theory and Applications. *IEEE Trans. Veh. Technol.*, 59(2):940–949, February 2010. Available at `http://www.nd.edu/~mhaenggi/pubs/tvt10.pdf`.

[41] F. Baccelli, B. Blaszczyszyn, and P. Muhlethaler. An aloha protocol for multihop mobile wireless networks. *IEEE Trans. Inf. Theory*, 52(2):421–436, February 2006.

[42] Dietrich Stoyan, Wilfrid S Kendall, Joseph Mecke, and DG Kendall. *Stochastic geometry and its applications*. Wiley Chichester, 1995.

[43] M. Haenggi, J.G. Andrews, F. Baccelli, O. Dousse, and M. Franceschetti. Stochastic geometry and random graphs for the analysis and design of wireless networks. *IEEE J. Sel. Areas Commun.*, 27(7):1029–1046, September 2009.

[44] F. Baccelli, P. Miihlethaler, and B. Blaszczyszyn. Stochastic analysis of spatial and opportunistic aloha. *IEEE J. Sel. Areas Commun.*, 27(7):1105–1119, September 2009.

[45] R. K. Ganti and M. Haenggi. Spatial and Temporal Correlation of the Interference in ALOHA Ad Hoc Networks. *IEEE Commun. Lett.*, 13(9):631–633, September 2009. Available at `http://www.nd.edu/~mhaenggi/pubs/commletter09.pdf`.

[46] Z. Gong and M. Haenggi. Interference and Outage in Mobile Random Networks: Expectation, Distribution, and Correlation. *IEEE Trans. Mobile Comput.*, 2012. Accepted. Available at `http://www.nd.edu/~mhaenggi/pubs/tmc13.pdf`.

[47] P. Jacquet, B. Mans, P. Muhlethaler, and G. Rodolakis. Opportunistic routing in wireless ad hoc networks: Upper bounds for the packet propagation speed. *IEEE J. Sel. Areas Commun.*, 27(7):1192–1202, September 2009.

[48] R. K. Ganti and M. Haenggi. Bounds on Information Propagation Delay in Interference-Limited ALOHA Networks. In *Proc. IEEE WiOpt*, Seoul, Korea, June 2009. Available at `http://www.nd.edu/~mhaenggi/pubs/spaswin09.pdf`.

[49] X. Zhang and M. Haenggi. Random Power Control in Poisson Networks. *IEEE Trans. Commun.*, 60(9):2602–2611, September 2012.

[50] François Baccelli and B Baszczyszyn. A new phase transitions for local delays in MANETs. In *Proc. IEEE INFOCOM*, pages 1–9. IEEE, 2010.

[51] M. Haenggi. The Local Delay in Poisson Networks. *IEEE Trans. Inf. Theory*, 59(3):1788–1802, March 2013.

[52] Zhenhua Gong and Martin Haenggi. The local delay in mobile poisson networks. *IEEE Trans. Wireless Commun.*, 2013. submitted.

[53] Wei-jen Hsu, Thrasyvoulos Spyropoulos, Konstantinos Psounis, and Ahmed Helmy. Modeling time-variant user mobility in wireless mobile networks. In *Proc. IEEE INFOCOM*, pages 758–766. IEEE, 2007.

[54] Michele Garetto, Paolo Giaccone, and Emilio Leonardi. Capacity scaling in ad hoc networks with heterogeneous mobile nodes: The subcritical regime. *IEEE/ACM Trans. Netw.*, 17(6):1888–1901, December 2009.

[55] Hans Daduna. *Queueing Networks with Discrete Time Scale: Explicit Expressions for the Steady State Behavior of Discrete Time Stochastic Networks*, volume 2046. Springer Verlag, 2001.

[56] Frank WJ Olver, Daniel W Lozier, Ronald F Boisvert, and Charles W Clark. *NIST handbook of mathematical functions*. Cambridge University Press, 2010.

[57] Yin Chen. A C++ simulator for the ALOHA MANET. URL `http://www.researchgate.net/profile/Yin_Chen5/`.

[58] Ram Ramanathan. On the performance of ad hoc networks with beamforming antennas. In *Proc. ACM MobiHoc*, 2001.

[59] X. Liu, A. Sheth, M. Kaminsky, K. Papagiannaki, S. Seshan, and P. Steenkiste. DIRC: increasing indoor wireless capacity using directional antennas. In *Proc. ACM SIGCOMM*, 2009.

[60] Akis Spyropoulos and Cauligi S. Raghavendra. Asympotic capacity bounds for ad-hoc networks revisited: the directional and smart antenna cases. In *Proc. IEEE GLOBLECOM*, 2003.

[61] Akis Spyropoulos and Cauligi S. Raghavendra. Capacity bounds for ad-hoc networks using directional antennas. In *Proc. IEEE ICC*, 2003.

[62] Su Yi, Yong Pei, and Shivkumar Kalyanaraman. On the capacity improvement of ad hoc wireless networks using directional antennas. In *Proc. ACM MobiHoc*, pages 108–116, 2003. doi: 10.1145/778415.778429.

[63] Su Yi, Yong Pei, Shivkumar Kalyanaraman, and Babak Azimi-Sadjadi. How is the capacity of ad hoc networks improved with directional antennas? *Wireless Networks*, 13(5):635–648, October 2007. ISSN 1022-0038.

[64] Pan Li, Chi Zhang, and Yuguang Fang. The capacity of wireless ad hoc networks using directional antennas. *IEEE Trans. Mobile Comput.*, 10(10):1374–1387, October 2011. doi: 10.1109/TMC.2010.243.

[65] Christina Peraki and Sergio D. Servetto. On the maximum stable throughput problem in random networks with directional antennas. In *Proc. ACM MobiHoc*, 2003. ISBN 1-58113-684-6. doi: http://doi.acm.org/10.1145/778415.778426.

[66] Hong-Ning Dai, Kam-Wing Ng, Raymond Chi-Wing Wong, and Min-You Wu. On the capacity of multi-channel wireless networks using directional antennas. In *Proc. IEEE INFOCOM*, pages 628–636, 2008.

[67] Guanglin Zhang, Youyun Xu, Xinbing Wang, and Mohsen Guizani. Capacity of hybrid wireless networks with directional antenna and delay constraint. *IEEE Trans. Commun.*, 58(7):2097–2106, July 2010. ISSN 0090-6778.

[68] Guanglin Zhang, Youyun Xu, and Xinbing Wan. Multicast capacity for hybrid MANETs with directional antenna and delay constraint. In *Proc. IEEE GLOBLECOM*, 2011.

[69] Guanglin Zhang, Youyun Xu, Xinbing Wang, Xiaohua Tian, Xiaoying Gan, Hui Yu, and Liang Qian. Multicast capacity for VANETs with directional antenna and delay constraint. *IEEE J. Sel. Areas Commun.*, 2012. to appear.

[70] Jiajia Liu, Xiaohong Jiang, H. Nishiyama, and N. Kato. Delay and capacity in ad hoc mobile networks with f-cast relay algorithms. *IEEE Trans. Wireless Commun.*, 10(8):2738–2751, August 2011. doi: 10.1109/TWC.2011.062111.101976.

[71] Jiajia Liu, Xiaohong Jiang, Hiroki Nishiyama, and Nei Kato. Exact throughput capacity under power control in mobile ad hoc networks. In *Proc. IEEE INFOCOM*, 2012.

[72] Chi-Kin Chau, Richard J. Gibbens, and Don Towsley. Impact of directional transmission in large-scale multi-hop wireless ad hoc networks. In *Proc. IEEE INFOCOM*, 2012.

[73] Constantine A. Balanis. *ANTENNA THEORY ANALYSIS AND DESIGN*. John Wiley & Sons, Inc., Hoboken, New Jersey, 2005.

[74] Jue Wang, Linghe Kong, and Min-You Wu. Capacity of wireless ad hoc networks using practical directional antennas. In *Proc. IEEE WCNC*, 2010. doi: 10.1109/WCNC.2010.5506381.

[75] L. Ying, S. Yang, and R. Srikant. Optimal delay–throughput tradeoffs in mobile ad hoc networks. *IEEE Trans. Inf. Theory*, 54(9):4119–4143, September 2008.

[76] Shan Zhou and Lei Ying. On delay constrained multicast capacity of large-scale mobile ad-hoc networks. In *Proc. IEEE INFOCOM*, 2010.

[77] Theodore S. Rappaport. *Wireless Communications: Principles and Practice (2nd Edition)*. Prentice Hall, January 2002. ISBN 9780130422323.

[78] C.K. Chau, M. Chen, and S.C. Liew. Capacity of large-scale csma wireless networks. *IEEE/ACM Trans. Netw.*, 19(3):893–906, June 2011.

[79] P. Li, C. Zhang, and Y. Fang. Asymptotic connectivity in wireless ad hoc networks using directional antennas. *IEEE/ACM Trans. Netw.*, 17(4):1106–1117, August 2009.

[80] Pan Li, Yuguang Fang, and Jie Li. Throughput, delay, and mobility in wireless ad hoc networks. In *Proc. IEEE INFOCOM*, 2010. URL `http://dl.acm.org/citation.cfm?id=1833515.1833718`.

[81] C. Zhang, Y. Fang, and X. Zhu. Throughput-delay tradeoffs in large-scale MANETs with network coding. In *Proc. IEEE INFOCOM*, 2009.

[82] S.R. Kulkarni and P. Viswanath. A deterministic approach to throughput scaling in wireless networks. *IEEE Trans. Inf. Theory*, 50(6):1041–1049, June 2004.

[83] Piyush Gupta and P. R. Kumar. Critical power for asymptotic connectivity in wireless networks. *Stochastic Analysis, Control, Optimization and Applications: A Volume in Honor of W.H. Fleming*, pages 547–566, 1998.

THIS PAGE INTENTIONALLY LEFT BLANK

Pulications

Jounal Articles

[1] Yin Chen, Jiajia Liu, Xiaohong Jiang, and Osamu Takahashi. Throughput analysis in mobile ad hoc networks with directional antennas, *Ad Hoc Networks*, 11(3): 1122–1135, MAY 2013.

[2] Yin Chen, Yulong Shen, Xiaohong Jiang, and Jie Li. On Exact Throughput Capacity in ALOHA Mobile Ad Hoc Networks. *IEEE/ACM Trans. Netw.*, *Submitted*, 2013.

[3] Yin Chen, Yulong Shen, Jinxiao Zhu and Xiaohong Jiang. Capacity and Delay-Throughput Tradeoff in ICMNs with Poisson Meeting Process. *Ad Hoc Networks*, *Submitted*, 2013.

Conference Papers

[4] Yin Chen, Jiajia Liu, Xiaohong Jiang, Osamu Takahashi, and Norio Shiratori. Exact throughput capacity in MANETs with directional antenna and transmission power constraint. In *Proc. APCC*, 2012.

[5] Yin Chen, Jiajia Liu, Xiaohong Jiang, Osamu Takahashi, and Norio Shiratori. Asymptotic Upper Bound on the Packet Propagation Speed in WANETs with Directional Antennas. In *Proc. IEEE ICCC*, 2013.

[6] Yin Chen, Yulong Shen, Xiaohong Jiang, and Jie Li. Throughput Capacity of ALOHA MANETs. In *Proc. IEEE ICCC*, 2013.